

Regulation of the homeoprotein Hesx1 via Mad2l2 and the anaphase promoting complex

Doctoral Thesis

In partial fulfillment of the requirements
for the degree “Doctor rerum naturalium (Dr. rer. nat.)”
in the Molecular Biology Program
at the Georg-August University Göttingen,
Faculty of Biology

submitted by

Sven Pilarski

born in

Wolfsburg, Germany

Göttingen, March 2008

AFFIDAVIT

Here I declare that my doctoral thesis entitled “**Regulation of the homeoprotein Hesx1 via Mad2l2 and the anaphase promoting complex**” has been written independently with no other sources and aids than quoted.

.....

Sven Pilarski, Göttingen, March 2008

To my family

TABLE OF CONTENTS

ACKNOWLEDGEMENTS	1
ABSTRACT	2
LIST OF FIGURES	3
LIST OF TABLES	4
ABBREVIATIONS AND NOMENCLATURE	5
INTRODUCTION	6
Role of Hesx1 during early embryonic and pituitary development	6
The ubiquitin ligase Cdh1-APC and its inhibitor Mad2l2	15
Polymerase ζ: Function of Mad2l2 and Rev3 in DNA damage repair	20
Aims of this study	25
RESULTS	26
Hesx1 interacts with Mad2l2 and the APC recognition subunit Cdh1	26
<i>Hesx1</i>, <i>Mad2l2</i> and <i>Cdh1</i> have overlapping expression domains	28
Mad2l2 prevents DNA binding of Hesx1	30
The E3 ubiquitin ligase Cdh1-APC polyubiquitinates Hesx1	32
Generation of Mad2l2 deficient mice	34
Use of Recombineering to create the conditional knockout targeting vector	35
Gene targeting in ES-cells and Cre mediated deletion of <i>Mad2l2</i> in mice	38
Phenotypic analysis of Mad2l2 knockout mice	41
Variable viability and growth retardation in <i>Mad2l2</i> deficient embryos	41
<i>Mad2l2</i> targeted MEF's show decelerated proliferation.....	43
<i>Mad2l2</i> deficient MEF's show an altered cell cycle phase distribution.....	44
Accumulation of γ -H2AX in <i>Mad2l2</i> deficient MEF's	46
Pituitary gland displays impaired cell differentiation	47
DISCUSSION	50
Hesx1 regulation through Mad2l2 and Cdh1-APC	50
Mad2l2 prevents Hesx1 from DNA binding	50
The Cdh1-APC complex controls Hesx1 stability.....	52
Phenotypical analysis of <i>Mad2l2</i> deficiency	54
Infertility, reduced viability and size in <i>Mad2l2</i> deficient embryos	54
Proliferation and DNA damage in <i>Mad2l2</i> deficient MEF's	56
<i>Mad2l2</i> deficiency impairs pituitary cell lineage differentiation	58

SUMMARY AND CONCLUSIONS	61
MATERIAL AND METHODS	63
Isolation, analysis and manipulation of nucleic acids	63
Total RNA isolation from eukaryotic cells or mouse embryos.....	63
Genomic DNA extraction from mammalian cells or mouse tissues	63
Plasmid DNA isolation from <i>E. coli</i>	63
P1-derived artificial chromosome (PAC) isolation from <i>E. coli</i>	64
Standard and Genomic polymerase chain reaction (PCR)	64
Reverse transcriptase – polymerase chain reaction (RT-PCR)	65
Purification of PCR products	65
PCR-Primers.....	65
DNA electrophoresis and purification from agarose gel.....	67
Quantification of nucleic acids	67
Restriction digest of DNA	67
Dephosphorylation of DNA fragments.....	68
DNA ligation	68
Sequencing	70
Dig-labeled antisense RNA probe preparation	70
Preparation of random radioactively labeled DNA probes.....	70
Purification of labeled nucleic acids.....	71
Phenol extraction and ethanol precipitation of DNA	71
Northern blot analysis.....	71
Southern blot analysis.....	72
Transformation of <i>E. coli</i>	73
Bacterial strains.....	73
Preparation of electrocompetent <i>E. coli</i>	73
Preparation of <i>E. coli</i> competent for heat shock transformation.....	74
Transformation of <i>E. coli</i> by electroporation	74
Transformation of <i>E. coli</i> by heat shock.....	74
Cryopreservation of <i>E. coli</i>	75
Yeast Two-Hybrid Assay	75
Transformation of yeast.....	75
Characterization of transformants.....	76

X-Gal assay	76
Long term storage of yeast	77
Purification and analysis of proteins	77
Expression and purification of GST-fused recombinant proteins.....	77
Thrombin cleavage of GST-fused recombinant proteins	78
Quantification of protein concentrations	78
<i>In vitro</i> transcription/translation	79
SDS-polyacrylamide gel electrophoresis of proteins (SDS-PAGE).....	79
Western blot analysis.....	80
Antibodies	81
Analysis of protein-protein interactions.....	82
GST Pull-down assay.....	82
Peptide array analysis	82
Co-immunoprecipitation	83
<i>In vivo</i> ubiquitination assay.....	84
MeOH/CHCl ₃ precipitation	85
Analysis of protein-DNA associations.....	85
Electrophoretic mobility shift assay (EMSA)	85
Generation of the <i>Mad212</i> conditional knockout vector via recombineering.....	86
Construction of retrieval and targeting vectors.....	89
Transformation of PAC or plasmid DNA into recombinogenic strains	89
Retrieving and targeting.....	90
Excision of the Neo cassette	90
Gene targeting in mouse ES cells and production of chimeras	91
Isolation and analysis of embryos and mice	91
Dissection and fixation of mouse embryos.....	91
Bouin's fixation of postnatal mouse heads.....	92
Paraffin embedding and sectioning	92
Hematoxylin and Eosin staining (H&E staining).....	93
<i>Whole mount in situ</i> -hybridization.....	93
Immunohistochemistry	94
Cell culture.....	95
Cell lines	95

Revival, subculture and cryopreservation of cells	95
Cell transfection	96
Preparation of primary mouse embryonic fibroblasts (MEF's)	97
Measurement of cell proliferation rates.....	97
Giemsa staining	97
Immunohistochemistry	98
TUNEL assay	99
FACS analysis of mouse embryonic fibroblasts.....	99
BIBLIOGRAPHY	101
CURRICULUM VITAE	114

ACKNOWLEDGEMENTS

I would like to thank my supervisor *Prof. Dr. Michael Kessel* for giving me the opportunity to work in his laboratory on this interesting project. His continuous support, guidance and the many helpful discussions are the cornerstones of this work and have added value to my scientific and personal development.

I am thankful to *Prof. Dr. Tomas Pieler* and *Prof. Dr. Herbert Jäckle*, the members of my thesis committee. The thesis committee meetings are a central feature of the graduate program “Molecular Biology” and the additional advice, guidance and critical comments I received during these meetings were very helpful. In addition, I would like to thank *Dr. Steffen Burkhardt* and the coordination office of the “Molecular Biology” program for their helpfulness and untiring dedication.

Furthermore, I am grateful to the members of the Department Molecular Cell Biology for their continuous support. My special thanks go to *Dr. Anastassia Stoykova*, *Prof. Dr. Ahmed Mansouri* and *Dr. Kamal Chowdhury* for helpful discussions and advice, to *Dr. Stephen Blanke*, *Martina Daniel*, *Dr. Gundula Griesel*, *Sharif Mashur* and *Dr. Tran Cong Tuoc* for all their help, technical advice and scientific as well as non-scientific discussions. I would like to thank *Dr. Ulrike Teichmann* and *Daniela Wollradt* for their help and advice concerning the mice. Moreover, I am grateful to *Prof. Dr. Detlef Doenecke*, *Krisitina Haenecke* and *Dr. Nicole Happel* for their help with the FACS analysis.

My thanks also go to all my current and former lab mates of the Kessel-lab. I am very thankful to *Naisana Seyed Asli*, *Alexander Klimke*, *Dr. Lingfei Luo*, *Dr. Mara Pitulescu*, *Petra Rus*, *Yvonne Uerlings* and *Dr. Lars Wittler* for all their help, discussions and just for sharing good and bad times. They really created a pleasant lab atmosphere, which made the whole work fun!

I would like to thank *Oliver Arendt*, *Stefan Klose* and *Dr. Pia Schmidt* for patiently listening to problems, discussions, “taking a day off” and proofreading parts of the present thesis.

I am grateful to my non-scientific advisory board, my parents *Elke* and *Hartmut* and my brother *Björn Pilarski* for all their continuous support and advice. Finally, I would like to thank *Claudia Hennecke* for all her patience, help and just for being there and sharing a great time together.

ABSTRACT

Understanding the functional significance of the coordinate expression and interaction of homeobox transcription factors remains a critical question in developmental biology. *Hesx1* is a *paired*-like homeodomain transcription factor, which is required for normal forebrain and pituitary gland formation. *Hesx1* deficient mice display variable degrees of forebrain and pituitary gland defects. A comparable phenotype in humans is septo optical dysplasia (SOD) and humans harboring mutations in *HESX1* were observed to display some form of SOD.

This study has identified so far unknown *Hesx1* interaction partners. As an interesting binding partner *Mad2l2* was found to bind *Hesx1*. *Mad2l2* is involved in DNA damage repair as a component of the polymerase ζ as well as in cell cycle regulation by inhibiting the anaphase promoting complex (APC). The interaction with *Hesx1* resulted in a diminished ability of *Hesx1* to bind to target DNA. Furthermore, *Cdh1*, the substrate recognition subunit of the APC, was found to bind *Hesx1*. The *Cdh1*-APC complex is an E3 ubiquitin ligase that targets proteins for proteolysis via the 26S proteasome. Indeed, *Hesx1* could be identified as a target of the *Cdh1*-APC complex and was polyubiquitinated and subsequently degraded.

To study the consequence of *Mad2l2* inactivation in mice, knockout animals were produced. These animals and mouse embryonic fibroblasts (MEF's) displayed DNA damage as well as a pituitary gland phenotype, indicating that *Mad2l2* is a crucial factor during embryonic development. It was previously shown, that precise spatially and temporally expression of *Hesx1* is crucial for proper pituitary gland development. Interactions of *Mad2l2* and *Cdh1* with *Hesx1* suggest that these factors are responsible for regulation and timed degradation of *Hesx1* in the developing anterior pituitary gland.

Therefore, the present study has extended the regulative network in which *Hesx1* is embedded and identified novel mechanisms of *Hesx1* regulation, involving binding to *Mad2l2* and ubiquitination via the *Cdh1*-APC complex.

LIST OF FIGURES

Figure 1. <i>Hesx1</i> expression during pituitary organogenesis.	7
Figure 2. Signaling molecules, selected transcription factors and hormones during pituitary development.	11
Figure 3. Cdh1-APC substrate ubiquitination in the presence of Mad2l2.	18
Figure 4. DNA lesion bypass by <i>S. cerevisiae</i> Rev1-polymerase ζ at a stalled replication fork.	22
Figure 5. Mad2l2 and Cdh1 interact with Hesx1.	27
Figure 6. <i>Hesx1</i> expression pattern during mouse development.	28
Figure 7. Mad2l2 and Cdh1 expression overlaps with Hesx1.	29
Figure 8. Mad2l2 binds to the N-terminal part of the homeodomain of Hesx1.	31
Figure 9. Mad2l2 disturbs the ability of Hesx1 to bind DNA.	32
Figure 10. Hesx1 is subject to <i>in vivo</i> ubiquitination.	33
Figure 11. Search results for Mad2l2 in the Ensembl database.	35
Figure 12. Construction and functional analysis of the Mad2l2 conditional knockout vector.	38
Figure 13. Targeting of the Mad2l2 genomic locus with the cko construct in ES cells.	39
Figure 14. Generation of Mad2l2 knockout mice.	40
Figure 15. Genotypic analysis of progeny from <i>Mad2l2</i> ^{+/-} intercrosses reveals embryonic lethality of <i>Mad2l2</i> ^{-/-} mice.	41
Figure 16. Mad2l2 deficient mice are reduced in size and weight.	42
Figure 17. Growth curve of <i>Mad2l2</i> ^{-/-} newborns and wild-type littermates.	43
Figure 18. Influence of <i>Mad2l2</i> deficiency on plating efficiency and proliferation rate of MEF's.	44
Figure 19. FACS analysis of <i>Mad2l2</i> deficient MEF's.	45
Figure 20. Elevation of γ -H2AX expression levels in Mad2l2 deficient MEF's.	46
Figure 21. <i>Mad2l2</i> deficient mice display a morphologically normal pituitary.	47
Figure 22. Expression of TSH in the developing pituitary gland.	48
Figure 23. GH expression in the developing anterior pituitary gland.	49
Figure 24. The N-terminal arm of paired homeodomains is involved in DNA binding.	51
Figure 25. Possible model of Hesx1 ubiquitination during anterior pituitary gland development.	53
Figure 26. DNA lesion bypass by polymerase ζ might be disturbed in <i>Mad2l2</i> ^{-/-} mice.	58
Figure 27. Delayed somatotrope differentiation in <i>Mad2l2</i> deficient mice.	60
Figure 28. Standard curve for the determination of protein concentrations.	79
Figure 29. Generation of the Mad2l2 conditional knockout vector via recombineering.	88

LIST OF TABLES

Table 1. Pituitary phenotypes due to Hesx1 misexpression and mutations.....	14
Table 2. Standard thermocycling program for PCR.....	65
Table 3. Standard thermocycling program for RT-PCR.....	65
Table 4. List of PCR-primers.....	67
Table 5. Concentration of agarose used for separating DNA of different sizes.....	67
Table 6. List of plasmids.....	69
Table 7. Bacterial strains used in this study.	73
Table 8. SDS-polyacrylamide gel preparation.	80
Table 9. List of antibodies.....	81
Table 10. Cell lines used in this study.....	95

ABBREVIATIONS AND NOMENCLATURE

3AT	3-Amino-1,2,4-Triazole	LB	Luria Bertani medium
ACTH	adrenocorticotropin	LH	Luteinizing hormone
α GSU	α -glycoprotein subunit	LiAc	Lithium acetate
APS	Ammonium persulphate	<i>loxP</i>	DNA recognition site for Cre
BBR	Boehringer Blocking Reagent	MEF	Mouse embryonic fibroblasts
bHLH	Basic helix-loop-helix	<i>neo</i>	neomycin
bp	Base pairs	OD	Optical density
BSA	Bovine serum albumin	o/n	Overnight
cDNA	complementary DNA	P	Postnatal
cko	Conditional knockout	PAC	P1-derived artificial chromosome
CMV	Cytomegalovirus	PBS	Phosphat buffered saline
CPHD	Combined pituitary hormone deficiency	PFA	Paraformaldehyd
cpm	Counts per minute	PMSF	Phenylmethanesulphonylfluoride
Cre	Cre recombinase	POMC	proopiomelanocortin
DMF	N,N-dimethyl formamide	PRL	Prolactin
DNA	Deoxyribonucleic acid	RNA	Ribonucleic acid
dpc	Days post coitum	RNAi	RNA interference
DTT	Dithiothreitol	RNase	Ribonuclease
<i>E. coli</i>	<i>Escherichia coli</i>	rpm	Revolutions per minute
EDTA	Ethylenedinitrilotetraacetic acid	SC-	Synthetic complete medium
ES cell	Embryonic stem cell	medium	lacking a specific amino acid
FACS	Fluorescence-activated cell sorting	SDS	Sodium dodecyl sulfate
FCS	Inactivated fetal calf serum	SOD	Septo optical dysplasia
Flpe	Flp recombinase	TBE	Tris-borate buffer
FRT	DNA recognition site for Flpe	TBS	Tris bufferd saline
FSH	Follicle-stimulating hormone	TEMED	Tetramethylethylendiamin
g	gravity	TK	Thymidine kinase
GH	Growth hormone	TSH	Thyroid-stimulating hormone
<i>HIS3</i>	Imidazoleglycerol-phosphate dehydratase	U	Units
IGHD	Isolated growth hormone deficiency	V	Volt
kb	Kilo base pairs	X-Gal	5-bromo-5-chloro-3-indolyl(-D-galactoside)
<i>lacZ</i>	β -galactosidase	YPDG	yeast-rich glycerol medium containing 0.1% glucose

INTRODUCTION

The development from a single cell, the fertilized egg, into a multicellular organism, whether fly, frog, chicken, mouse or human, implies a sophisticated coordination of growth and differentiation. Each cell needs to maintain the integrity of its genome; inconsistencies or changes might induce cell death or have dramatic effects on the development of the entire organism. Cell proliferation has to be coordinated with cell cycle exit and differentiation. The spatial and temporal expression and interaction of transcription factors finally initiates the specialization of cell types to allow the proper formation of the embryo and its organs. These processes are most likely to involve genes capable of coordinating and crosslinking more than just one operation at any point in time.

Role of *Hesx1* during early embryonic and pituitary development

The murine transcription factor *Hesx1* (also referred to as Rpx; Hermes et al., 1996; Thomas et al., 1995; Thomas and Rathjen, 1992) and its homologue the *Xenopus laevis* *Xanf* gene (Zarasky et al., 1992) belong to the anterior neural fold (*Anf*) gene family (Kazanskaya et al., 1997). It is a class of *paired*-like homeobox genes that is probably unique to vertebrates since there are no orthologues found e.g. in *Drosophila melanogaster* and *Caenorhabditis elegans* genomes.

Expression of Hesx1 in mice

The murine *Hesx1* transcript was initially identified in embryonic stem (ES) cells where it is down-regulated upon ES cell differentiation (Thomas et al., 1995; Thomas and Rathjen, 1992). During development, *Hesx1* transcripts can be first detected before the onset of gastrulation in the anterior visceral endoderm. During primitive streak elongation the expression remains in this small patch of cells, but soon afterwards (7.5 days past coitum (dpc)) transcripts can be detected in the prospective neuroectoderm adjacent to the endoderm *Hesx1* expressing cells. This expression domain intensifies and spreads laterally during the formation of the cranial neural folds (8 dpc). In 8.5 dpc embryos, *Hesx1* expression gets restricted to the neuroectoderm of the prospective prosencephalon and a small region of anterior foregut endoderm. At 9-9.5 dpc, transcripts are limited to the ventral diencephalon and a thickened layer of oral ectoderm. Subsequently, *Hesx1* is

expressed only in the oral ectoderm cells that will give rise to Rathke's pouch, the primordium of the anterior and intermediate lobe of the pituitary gland (Hermesz et al., 1996; Thomas and Beddington, 1996).

The expression level of *Hesx1* remains high throughout these oral ectodermal cells that subsequently invaginate and eventually detach to form the definitive pouch structure (Figure 1. e9.5-12). With the onset of pituitary gland cell differentiation around 12.5 dpc, *Hesx1* expression is down-regulated in a progressive ventral to dorsal direction (Figure 1. e12-14.5), resembling the spatial and temporal appearance of differentiated pituitary cell types (Japon et al., 1994; Simmons et al., 1990). *Hesx1* transcripts become undetectable around 15 dpc (Dasen et al., 2001; Hermesz et al., 1996).

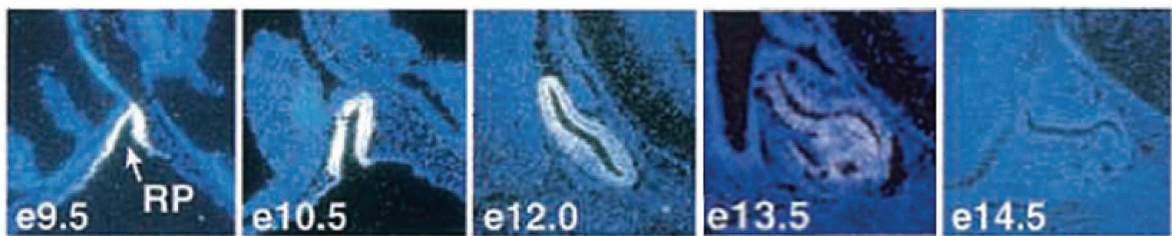


Figure 1. *Hesx1* expression during pituitary organogenesis.

Hesx1 expression in Rathke's pouch (RP) at mouse embryonic stage (e) 9.5-14.5. Transcripts are found in a patch of cells from the oral ectoderm that invaginate and form Rathke's pouch. *Hesx1* is strongly expressed in the developing Rathke's pouch and subsequently gets down-regulated in a ventral to dorsal pattern (modified from Dasen et al., 2001).

Similar expression pattern of *Hesx1* in the anterior neuroectoderm and the developing pituitary gland are described in other vertebrates e.g. in *Xenopus laevis* (Zaraisky et al., 1995) and *Gallus gallus* (Knoetgen et al., 1999). However, an exception might be the human *HESX1* gene which is not transcriptionally silenced during adult life in normal pituitaries nor in pituitary adenomas (Mantovani et al., 2006).

In mice, this dynamic and complex expression pattern is regulated by at least two functional independent genomic elements. The early expression of *Hesx1* is controlled by a highly conserved 5' *cis*-regulatory element while a 3' regulatory sequence drives the expression in Rathke's pouch (Chou et al., 2006; Hermesz et al., 2003; Spieler et al., 2004). The 5' element is bound by LIM-homeodomain-containing proteins, Otx2 and Pax6 which seem to be key molecules in regulating early *Hesx1* expression (Chou et al., 2006; Spieler et al., 2004). Moreover, it contains conserved *paired*-like homeodomain sites which are

bound by Prop1/ β -catenin to repress *Hesx1* transcription (Olson et al., 2006). The 3' element is bound by Pitx2 and GATA transcription factors (Chou et al., 2006). In *Xenopus laevis* it has been shown that the 5' regulatory element (Eroshkin et al., 2002) is bound by X-nkx-5.1, FoxA4a and Xvent2. These factors define the posterior border of the *Xanf* expression by inhibiting its transcription (Bayramov et al., 2004; Martynova et al., 2004). Since the 5' regulatory region is highly conserved, murine orthologues of X-nkx-5.1, FoxA4a and Xvent2 might play a similar role in *Hesx1* regulation in mice.

Hesx1 and its function

The size of the Hesx1 proteins varies from 161 (*Danio rerio*) to 187 amino acids (*Xenopus laevis*; Figure 8. C). The homeodomains reveal an identity of over 75% if compared to each other and is less than 55% compared to other known classes (Kazanskaya et al., 1997). In addition to the homeodomain, all *Hesx1* homologues contain two conserved motifs which are located at the N-terminus of the protein. The engrailed homology domain (eh1) was originally characterized in the *Drosophila* repressor engrailed but has also been found in other homeoprotein classes including goosecoid, Nkx, and msh (Smith and Jaynes, 1996) and a sequence similar to the WPRW motif found in several basic helix-loop-helix (bHLH) proteins (Paroush et al., 1994). Both of these motifs are linked to the Groucho class of corepressors (Jimenez et al., 1997; Tolkunova et al., 1998) and indeed Hesx1 was shown to bind to the Groucho-like TLE1 corepressor. This interaction occurs at the eh1 domain and is sufficient for the repressive action of Hesx1. In addition, the homeodomain can recruit the N-CoR/mSin3/HDAC(1/2) and Brg-1 complexes to mediate repression (Dasen et al., 2001). These interactions are not mutually exclusive and might strengthen the repressive potential of Hesx1. Furthermore, the DNA methyltransferase 1 (DNMT1) was identified as a Hesx1 binding protein. This interaction led to the idea that Hesx1 might permanently silence target genes by CpG methylation (Sajedi et al., 2007). Several other studies contributed evidence that Hesx1 acts *in vivo* and *in vitro* as a transcriptional repressor (Brickman et al., 2001; Carvalho et al., 2003; Ermakova et al., 1999; Ermakova et al., 2007; Quirk and Brown, 2002; Susa et al., 2007). More recently it was found that the eh1 domain of Xanf binds in addition to the LIM-domain protein Zyxin which might inhibit the transcriptional repressor function. This interaction might add another level of regulation to the repressive function of Xanf (Martynova et al., 2008).

The previously described dynamic spatially and temporal restricted expression of *Hesx1* in the anterior visceral endoderm, the neuroectoderm and finally Rathke's pouch was shown to be crucial for proper rostral development in mice. *Hesx1* deficient mice display reduction of the anterior forebrain, defects in the dorsal forebrain commissural structures, eye abnormalities and pituitary gland dysplasia to a variable degree (Dattani et al., 1998; Martinez-Barbera et al., 2000). This phenotype is comparable to the human congenital disorder septo-optic dysplasia (SOD). Several mutations in the eh1 domain and the homeodomain of the human *Hesx1* orthologue could be linked to familial cases of SOD and hypopituitarism (Brickman et al., 2001; Carvalho et al., 2003; Cohen et al., 2003; Dattani et al., 1998; Sobrier et al., 2006; Sobrier et al., 2005).

Recent studies showed that the absence of *Hesx1* in mice leads to a posterior transformation of the anterior forebrain (Andoniadou et al., 2007). These findings were in line with data from *Xenopus*, where downregulation of *Xanf* leads to an anterior shift of genes involved in posterior forebrain regulation (Ermakova et al., 2007). Even though overexpression of *Xanf* results in an expansion of the rostral forebrain in *Xenopus* (Ermakova et al., 1999), this effect could not be observed in mice (Andoniadou et al., 2007).

Taken together, previous research has revealed an important role of *Hesx1* as a transcriptional repressor during early anterior forebrain and pituitary development in vertebrates.

Anterior pituitary development and consequences of Hesx1 misregulation

The pituitary gland is a crucial component of the endocrine system. It is composed of two anatomically and functionally distinct structures: the posterior lobe or the neurohypophysis and the non-neural adenohypophysis, including the anterior and intermediate lobe.

The posterior lobe is composed of terminal axons of the hypothalamic magnocellular neurons. These neurons synthesize peptide hormones oxytocin and vasopressin, which are transported down to the axonal terminals of the posterior lobe. From the posterior lobe they are released into the blood circulation, where they target the uterus, the mammary glands and the kidney tubules respectively.

The anterior pituitary gland regulates a great variety of processes, including growth, metabolism, reproduction, lactation and the body's response to stress by means of secreting specific hormones. Secretion of hormones from distinct endocrine cell types is regulated by the hypothalamus and positive/negative feedback loops from the peripheral organs. The anterior lobe consists of five different endocrine cell types.

(1) Somatotropes secrete growth hormone (GH) that regulates linear growth and metabolism by targeting the liver, kidney and most other tissues.

(2) Lactotropes synthesize prolactin (PRL) which targets the mammary gland and controls milk production in females.

(3) Thyrotropes produce thyroid-stimulating hormone (TSH) and affect the thyroid.

(4) Corticotropes secrete adrenocorticotrophic hormone (ACTH), a proteolytic product of proopiomelanocortin (POMC), which stimulates the production and secretion of glucocorticoids by the adrenal cortex.

(5) Gonadotropes synthesize luteinizing hormone (LH) and follicle-stimulating hormone (FSH) which stimulate the gonads to initiate sexual maturation and maintain reproductive function.

FSH, LH and TSH are glycoproteins consisting of a common α -subunit (α GSU), and a specific β -subunit (FSH β , LH β , and TSH β ; (Rizzoti and Lovell-Badge, 2005; Scully and Rosenfeld, 2002; Zhu et al., 2007; Zhu et al., 2005)).

Development of the anterior pituitary gland is highly conserved in vertebrates. The anterior pituitary anlage is localized in the midline portion of the anterior neural ridge, rostral to the region of the neural plate that is destined to give rise to the hypothalamus and the posterior lobe of the pituitary (Couly and Le Douarin, 1988; Eagleson and Harris, 1990; Gleiberman et al., 1999). Due to growth of the forebrain, the cells of the midline anterior neural ridge are displaced and become a layer of thickened cells in the oral ectoderm. The formation of Rathke's pouch, the primordium of the anterior pituitary gland, from these cells is induced by the infundibulum at around 8.5 dpc (Gleiberman et al., 1999). The infundibulum, an evagination of the ventral diencephalon that will subsequently give rise to the posterior lobe, is in direct contact with Rathke's pouch and

acts as a key organizing center for the patterning and commitment. This initial phase of proliferation and determination involves the combinatorial and opposing activity of signaling molecules like BMPs, Wnts, FGFs, Shh, Notchs and EGF (reviewed in Scully and Rosenfeld, 2002; Zhu et al., 2007). These transient signaling gradients induce the differential expression of specific transcription factors which subsequently lead to the precise spatial and temporal differentiation of hormone secreting cell types (Figure 2.; Japon et al., 1994; Simmons et al., 1990).

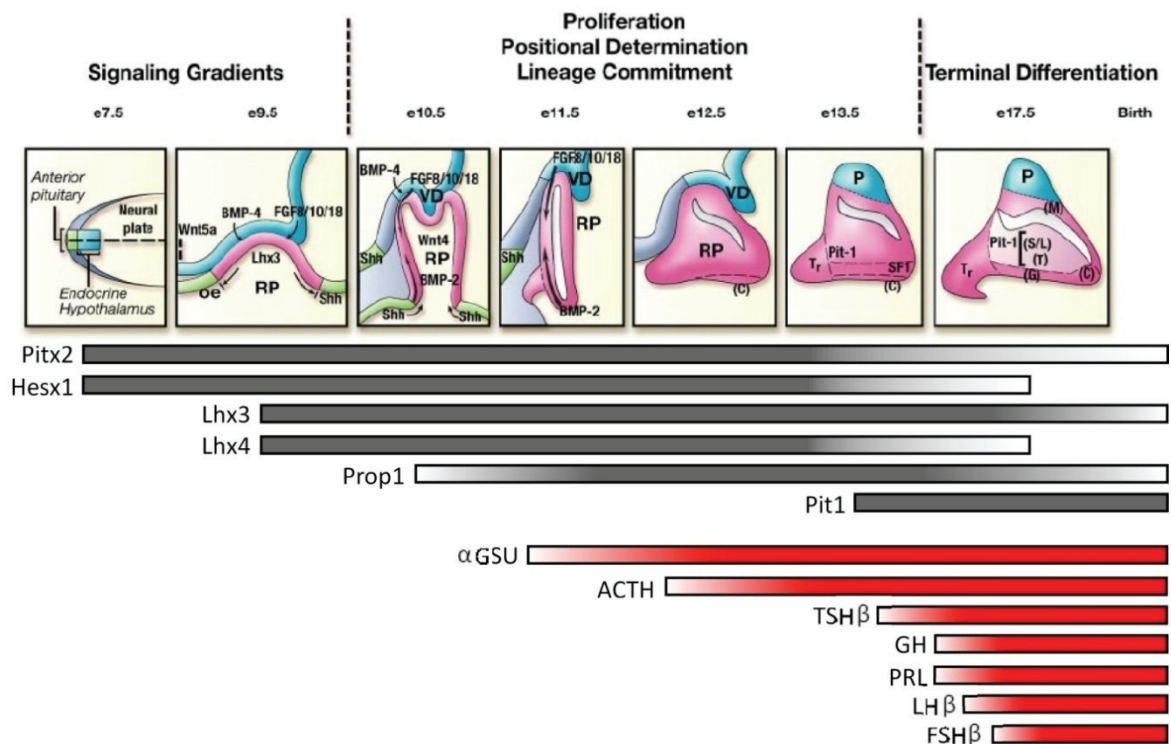


Figure 2. Signaling molecules, selected transcription factors and hormones during pituitary development.

The midline anterior neural ridge gives rise to Rathke's pouch (RP) and subsequently to the anterior pituitary gland. Adjacent to this field is the prospective endocrine hypothalamus located. The ventral diencephalon (VD) expresses BMP4, FGF8/10/18 and Wnt5a and directly contacts the oral ectoderm that is induced to form Rathke's pouch. Shh is expressed throughout the entire oral ectoderm with the exception of Rathke's pouch. The opposing dorsal BMP4/FGF and ventral BMP2/Shh signals during development provide proliferative as well as positional cues by regulating the appearance of several transcription factors (grey bars). This combinatorial expression of transcription factors leads finally to the differentiation of the pituitary cell lineages, corticotropes (C), rostral tip thyrotropes (T_r), thyrotropes (T), somatotropes (S), lactotropes (L) and gonadotropes (G). The approximate expression of the hormones is indicated (red bars). The dorsal region of the anterior pituitary becomes the intermediate lobe populated by melanotropes (M) and the invaginating ventral diencephalon gives rise to the posterior lobe of the pituitary gland (modified from Zhu et al., 2007).

Some transcription factors that are directly or indirectly involved in *Hesx1* regulation and activity are described below and are displayed in Figure 2., an in-depth review with detailed description of signaling molecules and transcription factors was recently published by Zhu et al. (Zhu et al., 2007).

The bicoid-related *Pitx1/2* transcription factors are expressed together with *Hesx1* in the anterior neural plate. They regulate cell proliferation, survival and differentiation. *Pitx1*^{-/-} mice display mild pituitary defects with a decrease of FSH β , LH β , and TSH β expression but an increase of POMC expressing cells (Szeto et al., 1999). *Pitx2* deficiency does not allow a pituitary development past pouch formation with only a few cells producing POMC. These phenotypes were shown to be due to a decrease in proliferation and an increase in apoptosis (Kioussi et al., 2002; Suh et al., 2002). Together, *Pitx1* and 2 are essential for the induction of *Lhx3* (Charles et al., 2005).

The LIM-homeodomain proteins *Lhx3* and *Lhx4* are expressed in the developing pouch from 9.5 dpc on. Whereas *Lhx3* is expressed in the anterior and intermediate lobe during development and throughout adulthood, *Lhx4* remains restricted to the anterior lobe and is down-regulated at around 15.5 dpc. *Lhx3* deficient mice form a definitive Rathke's pouch but in this case the pouch fails to develop any further from this initial induction. The pouch is not able to maintain *Hesx1* expression and to induce *Pit1*. Endocrine cell types of the anterior and intermediate lobe are completely absent with the exception of some corticotropes (Sheng et al., 1996). The anterior lobe of *Lhx4*^{-/-} mice is hypoblastic due to increased cell death during development. Numbers of somatotropes, corticotropes, thyrotropes and gonadotropes are significantly reduced (Raetzman et al., 2002).

Prop1 (Prophet of *Pit1*) is a *paired*-like homeodomain transcription factor that is expressed in the developing pituitary gland in a reciprocal but overlapping fashion with *Hesx1*. The first transcripts can be found around 10.5 dpc with a peak at 12.5 dpc, and the expression attenuates from 14.5 dpc on. Both *Prop1* and *Hesx1* can bind as homo- or hetero dimers to a well-described palindromic site (Sornson et al., 1996; Wilson et al., 1993). *Prop1* acts as a transcriptional repressor for *Hesx1* and as an activator for *Pit1* (Olson et al., 2006; Sornson et al., 1996). *Hesx1* prevents *Prop1* from initiating the program required for Pit-1 and gonadotrope lineage differentiation (Dasen et al., 2001). A

homozygous mutation in the homeodomain of *Prop1* in the *Ames dwarf* mice (Sornson et al., 1996) and a target deletion of *Prop1* (Nasonkin et al., 2004) display an absence in *Pit1* dependent cell types (somatotropes, lactotropes and thyrotropes) and a delay in the differentiation of gonadotropes. Interestingly, the *Ames dwarf* mice display a prolonged expression of *Hesx1* (Sornson et al., 1996). Premature expression of *Prop1* under the control of the *Pitx1* promoter leads to an absence of the anterior pituitary gland with no induction of *Lhx3* (Dasen et al., 2001). In addition, continuous expression of *Prop1* under the control of the α *GSU* regulatory element leads to a delay in terminal differentiation of gonadotropes, resulting in transient hypogonadism and hypothyroidism (Cushman et al., 2001).

Pit1 is a POU domain containing transcription factor that is initially expressed in the anterior lobe from 13.5 dpc on and continues in somatotropes, lactotropes and thyrotropes throughout adult life. In mouse mutant models, *Pit1* has been shown to be essential for the differentiation of these cell types (Camper et al., 1990; Li et al., 1990). Transcriptional regulation of *GH*, *PRL*, *TSH β* and *Pit1* itself is *Pit1*-dependent (Andersen and Rosenfeld, 2001).

Hesx1 and its co-repressor *TLE1* have a spatial and temporal overlapping expression pattern in the developing Rathke's pouch with a slightly longer expression of *TLE1* (Dasen et al., 2001).

Targeted deletion of *Hesx1* results in a phenotype similar to SOD (Dattani et al., 1998). The pituitary gland of *Hesx1* deficient mice displays a variable phenotype. In approximately 5% of the mice an initial thickening of the oral ectoderm and *Lhx3* induction is observed but the pituitary gland is lacking at 18.5 dpc. Yet, the majority of the *Hesx1*^{-/-} mice display multiple oral ectoderm invaginations and overproliferation of all endocrine pituitary cell types. The expression domains of *Lhx3* and *Prop1* are increased within Rathke's pouch and *FGF8* and *FGF10* domains are expanded rostrally (Dasen et al., 2001; Dattani et al., 1998; Martinez-Barbera et al., 2000). Misexpression of *Hesx1* under the control of either the *Pitx1* or the α *GSU* promoter to maintain expression during later stages of development displayed a modest reduction of some anterior lobe cell lineages. In contrast, co-expression of *TLE1* under the *Pitx1* regulating element results in a near to complete absence of all ventral pituitary gland cell types resembling the *Prop1* mutant

phenotype (Gage et al., 1996; Sornson et al., 1996). All *Prop1/Pit1* dependent cell lineages as well as gonadotropes are absent while the expression of *Prop1* appears to be normal. This phenotype does not occur by the co-expression of *TLE1* and a *Hesx1* variant with a mutated eh1 domain that prevents TLE1 binding of Hesx1 (Dasen et al., 2001).

Mutation	Molecular phenotype	Effect on pituitary gland	References
Mouse mutants			
<i>Hesx1</i> knockout	Loss of <i>Hesx1</i> ; Increase of <i>Lhx1</i> and <i>Prop1</i> ; Rostral extension of <i>FGF8/10</i>	Absence of the pituitary gland or multiple oral ectoderm invaginations and cellular overproliferation	(Dattani et al., 1998)
<i>Pitx1</i> - or α GSU-promoter driving <i>Hesx1</i>	Prolonged <i>Hesx1</i> expression	Modest reduction of some pituitary cell lineages	(Dasen et al., 2001)
<i>Pitx1</i> -promoter driving <i>Hesx1/TLE1</i>	Prolonged <i>Hesx1/TLE1</i> expression	Near complete absence of all ventral pituitary gland cell types	(Dasen et al., 2001)
<i>Pitx1</i> -promoter driving <i>Hesx1_{eh1 mut}/TLE1</i>	Prolonged <i>Hesx1_{eh1 mut}/TLE1</i> expression	No pituitary gland defects	(Dasen et al., 2001)
<i>Prop1</i> mutants	Prolonged <i>Hesx1</i> expression	Absence of somatotropes, lactotropes and thyrotropes; Delay gonadotropes	(Sornson et al., 1996)
Human mutations			
<i>HESX1</i> mutations in the homeodomain	Absence, decrease or increase in DNA binding ability	IGHD, CPHD and SOD	(reviewed in Dattani, 2005; Zhu et al., 2005)
<i>HESX1</i> mutations in the eh1 domain	Impaired TLE1 recruitment	CPHD	(Carvalho et al., 2003)

Table 1. Pituitary phenotypes due to Hesx1 misexpression and mutations.

To date several *Hesx1* mutations in humans were found to be involved in SOD and hypopituitarism. These mutations were found to be spread across all four exons and lead to an absence (Sobrier et al., 2006; Tajima et al., 2003), decrease (Dattani et al., 1998; Thomas et al., 2001), or increase (Cohen et al., 2003) of the DNA binding ability. In one case, the eh1 domain of Hesx1 contained a missense mutation leading to an impaired ability to recruit TLE1 (Carvalho et al., 2003). The patients displayed isolated GH

deficiency (IGHD) or combined pituitary hormone deficiency (CPHD) together with various degrees of extrapituitary SOD phenotypes. The mutations were found in the homozygous as well as the heterozygous state. Interestingly, heterozygous mutation in humans result in a milder phenotype as it is observed in 1% *Hesx1*^{+/-} mice (Dattani et al., 1998).

In summary, these data suggest that the tightly regulated expression of signaling molecules and transcription factors in a correct temporal and spatial order is vital for the proper development of the anterior pituitary gland. Disruptions of the normal transcriptional patterns and levels have a tremendous influence on the developing gland and the subsequent differentiation of the endocrine cell lineages of the pituitary. *Hesx1* showed to be a critical homeodomain transcription factor involved in early pituitary gland development. Moreover, spatial and temporal distinct downregulation of *Hesx1* during later development is necessary to allow ventral pituitary cell lineage differentiation (see as well Table 1.).

The ubiquitin ligase Cdh1-APC and its inhibitor Mad2I2

The spatial and temporal control of *Hesx1* at the transcriptional level is crucial for normal anterior pituitary gland development. Besides control at the transcriptional level and alternative RNA splicing, the precise tuning of protein activity and abundance can be achieved by post-translational modifications (PTMs). PTMs allow cells to respond instantly to cues received from their environment, such as growth factors, cell-cycle checkpoints, nutrient status and DNA damage. They include methylation, acetylation, phosphorylation, hydroxylation, sumoylation and ubiquitination. These modifications expand the properties of the protein, including alteration of its function, modulation of protein-interaction domains and half-life (reviewed in Seet et al., 2006; Yang, 2005).

Among these PTMs ubiquitination plays a key role in the regulation of both protein function and levels. Monoubiquitination of the e.g. proliferating cell nuclear antigen (PCNA), a polymerase processivity factor that forms a sliding clamp around DNA, is a response to DNA damage and stabilizes the interactions with translesion synthesis polymerases to bypass DNA lesions (Andersen et al., 2008; Hoege et al., 2002; Kannouche et al., 2004; Stelter and Ulrich, 2003). At the same time, polyubiquitination of substrates with chains of at least four ubiquitins is a well characterized signal which renders proteins

susceptible to degradation via the 26S proteasome (Thrower et al., 2000). Ubiquitination of target proteins is a result of the sequential activity of three classes of enzymes. The ubiquitin activating enzyme (E1) forms a thioester linkage between its active site cysteine and the carboxyl-terminal glycine of ubiquitin. This activated ubiquitin on E1 is then transferred to the ubiquitin conjugating enzyme (E2) by transesterification. Finally, the ubiquitin protein ligase (E3) binds to the ubiquitin-charged E2 and a target protein and enables the formation of an isopeptide linkage between the carboxyl-terminal glycine of the ubiquitin and the ϵ -amino-group of a lysine residue of the substrate or an already attached ubiquitin (reviewed in Hershko and Ciechanover, 1998; Pickart, 2001). Substrate specificity is mediated mainly through the E3 ligase and there are several hundreds of predicted E3 ligases based on the so far known E3 motifs, including HECT, RING, U-box and PHD/LAP finger domains (reviewed in Fang and Weissman, 2004).

The anaphase promoting complex

The anaphase promoting complex/cyclosome (APC/C; APC) is a RING-type E3 ligase that has essential functions in and outside of the eukaryotic cell cycle. The APC consists of at least 12 subunits with APC11, the RING finger protein and APC2, a Cul1-related scaffold protein, being the catalytic core of the complex.

Still, this complex can only ubiquitinate substrates by interacting with a E2 enzyme and a co-activator (among them; Cdc20 or Cdh1; (reviewed in Peters, 2006)). Substrate specificity is largely achieved by the co-activators which target proteins with distinct recognition motifs. Both Cdc20 and Cdh1 recognize substrates with a destruction or D-box (RXXLXXXXN/D/E) motif in its sequence (Fang et al., 1998; Glotzer et al., 1991), in addition Cdh1 targets proteins primarily containing a KEN-box (KENXXXXN/D), A-box (QRVL), O-box (LXXXXN) or CRY-box (CRYXPS) motif (Araki et al., 2005; Littlepage and Ruderman, 2002; Pflieger and Kirschner, 2000; Reis et al., 2006).

Initially, the APC complex was identified as an ubiquitin ligase specific for cell cycle control, more recently it was found that the APC complex adopted new roles in postmitotic differentiated cells. In both cases proteins containing a recognition motif are targeted for polyubiquitination and subsequent degradation (reviewed in Kim and Bonni, 2007; Peters, 2002).

APC regulation and cell cycle control

The APC plays a central role in the rapid, coordinated and oscillating degradation of specific cell cycle proteins required for an appropriate cell cycle progression. It is involved in regulating mitosis and the G1 phase by targeting cyclins for degradation and coordinating sister-chromatid separation (reviewed in Thornton and Toczyski, 2006). Activation of the APC in early mitosis is achieved by binding of Cdc20. The co-activator Cdc20 has already been synthesized during S and G2 phase, but an association with the APC requires the preceded phosphorylation of several APC subunits (Kraft et al., 2003; Rudner and Murray, 2000). Cdc20-APC mediates the degradation of cyclins as well as securin, permitting sister chromatid separation and disassembly of the mitotic spindle. Cdh1 that was phosphorylated during the S and G2 phases by different cyclin-dependent kinases (Cdks) is dephosphorylated upon the deactivation of these Cdks and subsequent associates with the APC complex. The assembly of Cdh1-APC renders Cdc20 as a substrate of the APC which is degraded between mitosis and G1/S phase (Prinz et al., 1998). Cdh1-APC activity during late mitosis and G1 phase targets cyclins thereby keeping Cdk activity levels low which prevents a premature entry into S phase and allows loading of the pre-replication complexes onto the origin of replication (Diffley, 2004). In addition, Cdh1-APC targets the substrate adaptor subunit of the E3 ligase SCF. SCF controls the G1-S transition by targeting Cdk inhibitors (Bashir et al., 2004; Wei et al., 2004). The stimulation of G1-S transition occurs finally by at least two mechanisms. On the one hand, an APC specific E2 enzyme is targeted by Cdh1-APC, therefore initiating its own deactivation and in addition the early mitotic inhibitor (Emi1) is expressed at the G1-S transition. Emi1 is able to inhibit preformed Cdc20-APC and Cdh1-APC complexes (Hsu et al., 2002; Reimann et al., 2001). Besides the Emi1 inhibition and the opposing phosphorylation on Cdc20-APC and Cdh1-APC that is required for a coordinated progression through M and G1 phase, several other APC inhibitors are known (Peters, 2006; Thornton and Toczyski, 2006). Among them are Mad1, Mad2 and BubR1 as components of the mitotic checkpoint complex. This complex is part of the spindle assembly checkpoint that inhibits Cdc20-APC function as a response to unattached kinetochores delaying subsequently the degradation of cyclin B and securin (Li et al., 1997; Sudakin et al., 2001).

A homolog of Mad2 is the Mad212 protein, also referred to as MAD2B and Rev7. The human MAD2L2 shares 23% identity and 54% similarity with MAD2. The murine Mad212 protein consists of 211 amino acids that shows high degree of identity among vertebrates (about 94%) but only 23% identity and 53% similarity when compared to *Saccharomyces cerevisiae* Rev7 (Cahill et al., 1999; Lawrence et al., 1985; Murakumo et al., 2000). The protein consists basically of one domain (amino acids 13-183), the HORMA domain. This domain has been suggested to be involved in protein-protein interaction as well as in recognizing chromatin status (Aravind and Koonin, 1998).

Mad212 is able to inhibit ubiquitination through Cdh1-APC and to a lesser extent by Cdc20-APC. This inhibition does not prevent substrate binding to Cdc20 and Cdh1 but it prevents substrate release (Figure 3.). Interestingly, preformed Cdc20-APC and Cdh1-APC complexes are not inhibited by Mad212 (Chen and Fang, 2001; Pflieger et al., 2001).

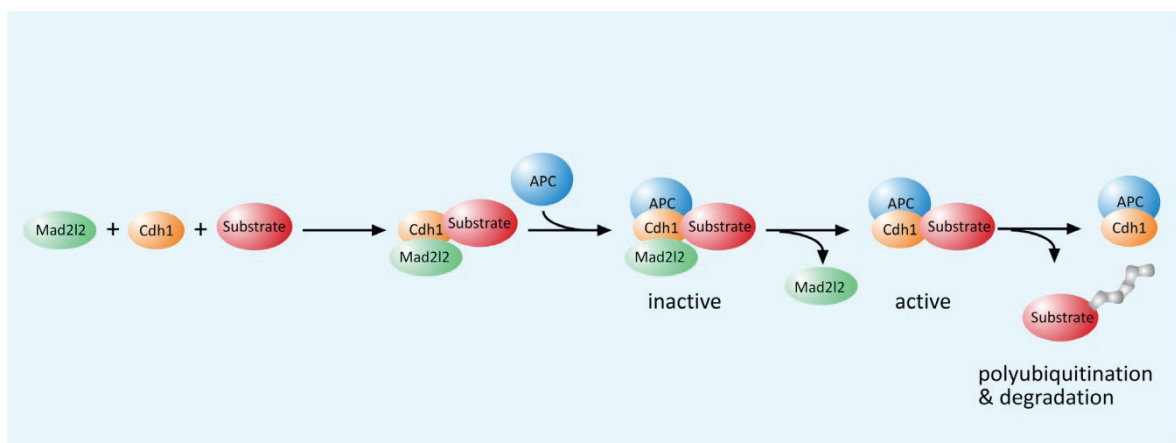


Figure 3. Cdh1-APC substrate ubiquitination in the presence of Mad212.

Mad212 binds to the co-activator Cdh1 which does not prevent the targeting of substrates but leads to an inactive complex. Polyubiquitination and subsequent degradation of the substrate through the 26S proteasome is mediated only in the absence of Mad212.

The role of the inhibitory effect of Mad212 on Cdc20/Cdh1-APC in cell cycle control is still not clear; it seems not to be associated with the spindle assembly checkpoint even though the human MAD2L2 interacts with MAD2 but not with MAD1 alone or in a complex with MAD2 (Chen and Fang, 2001; Murakumo et al., 2000; Pflieger and Kirschner, 2000). Mad212 gain and loss of function experiments concerning its function in cell cycle regulation are ambiguous. Overexpression in *Xenopus laevis* embryos results in a gastrulation arrest after mid blastula transition with cells displaying large nuclei or arrested late in nuclear division (Pflieger et al., 2001). In cell culture systems,

overexpression of the human MAD2L2 does not lead to alterations of the cell cycle (Murakumo et al., 2000). Knockdown or deletion of Mad2L2 in HeLa or chicken DT40 cells led to retarded growth kinetics (Iwai et al., 2007; McNally et al., 2008; Okada et al., 2005). In contrast, downregulation of Mad2L2 by shRNA in human nasopharyngeal carcinoma cells has no effect on proliferation rate and mitotic exit (Cheung et al., 2006). These differing observations may reflect differences due to the model-systems and due to the distinct RNAi constructs that were used and might affect the extent of Mad2L2 knockdown. Moreover, these different, but not necessarily conflicting observations may reflect the difficulties in identifying changes in the complex regulatory processes. To interpret these results, a function of Mad2L2 as part of the translesion polymerase ζ needs consideration (see next chapter).

Overall, the intricate functions of the APC complex and its co-activators in cell cycle control require a precise and tight regulation of its activity. This regulation is achieved by phosphorylation, interaction with regulatory proteins and ubiquitination. Mad2L2 was shown to be one of them.

Patterning during embryonic development

Mutations in the APC or its activator Cdc20 in *Saccharomyces cerevisiae*, *Drosophila melanogaster* and *Caenorhabditis elegans* resulted in cells arrested at the metaphase to anaphase transition (Furuta et al., 2000; Golden et al., 2000; Irniger et al., 1995; Sigrist and Lehner, 1997). In mice deficient for the subunits *Apc2* and *Apc10* embryos are lethal early in development (Pravtcheva and Wise, 1996; Wirth et al., 2004). Interestingly, Cdh1 and core subunits of the APC are expressed in differentiated adult mouse tissues, whereas Cdc20 and Cdk1 are not, suggesting that Cdh1-APC is not restricted to proliferating cells. In fact, postmitotic neurons express functional Cdh1-APC (Gieffers et al., 1999). Knockdown experiments of Cdh1 by RNAi in rodent postmitotic neurons revealed a function of the Cdh1-APC complex in axon growth and patterning (Konishi et al., 2004). SnoN, a transcriptional co-repressor involved in TGF- β -Smad2 signaling, was found to be a target of Cdh1-APC. The ubiquitination of SnoN by Cdh1-APC in these postmitotic neurons and subsequent axonal morphogenesis is regulated by TGF- β -Smad2 signaling (Stegmuller et al., 2008; Stegmuller et al., 2006). Furthermore Id2 (inhibitor of DNA binding 2) was identified as a substrate of Cdh1-APC. Id2 is a transcriptional

regulator that among others enhances cell proliferation probably by inhibiting bHLH transcription factors. Stabilization of Id2 by mutating the D-box revealed a similar phenotype in cerebellar granule neurons as earlier described by Konishi et al. (Lasorella et al., 2006). Studies in *Drosophila* and *C. elegans* have revealed additional functions of Cdh1-APC in the nervous system. A loss-of-function mutant for APC2 in *Drosophila* revealed an increase of neuromuscular junction size (van Roessel et al., 2004). In *C. elegans* it was furthermore found that Cdh1-APC is involved in regulating the abundance of glutamate receptors (Juo and Kaplan, 2004).

Besides these functions in the nervous system, Cdh1-APC has also been identified to play a crucial role in lens differentiation. Upon TGF- β signaling SnoN is targeted by Cdh1-APC for degradation (see also Stegmuller et al., 2008) resulting in a cell cycle arrest followed by terminal lens cell differentiation (Wu et al., 2007). This finding fits with observations from quiescent hepatocytes, where a deletion of APC2 leads to a re-entry into the cell cycle and a subsequent arrest in a mitotic-like state (Wirth et al., 2004). In addition to Id2, two other proteins involved in cell cycle regulation and differentiation were found to be targeted for degradation by the APC. The homeoproteins Six1 and HOXC10 displayed a cell cycle dependent degradation mediated by the APC complex (Christensen et al., 2006; Gabellini et al., 2003).

In conclusion, these studies clearly identify a role of the Cdh1-APC complex and its function as an E3 ligase besides cell cycle regulation. One important function is apparently the mediation of the G1 phase cell cycle arrest and subsequent terminal differentiation of cell lineages. This is achieved amongst other things by targeting different substrates for ubiquitination, including factors involved in transcriptional regulation.

Polymerase ζ : Function of Mad212 and Rev3 in DNA damage repair

Cells need to deal with thousands of DNA lesions per cell cycle. DNA lesions are created by the influence of environmental agents, like UV-irradiation or chemicals and by endogenous damage. Endogenous damage is mediated through metabolic byproducts including reactive oxygen species, spontaneous depurination, and DNA single- and double-strand breaks from deoxyribose oxidation or replication fork collapse. Approximately 5000 DNA single-strand lesions are generated per nucleus during a single

cell cycle (Vilenchik and Knudson, 2003). Most of these lesions are repaired by essentially error-free mechanisms, including nucleotide excision repair, base excision repair or mismatch repair. However, about 1% of these single-strand lesions remain unrepaired and give rise to double-strand breaks (Vilenchik and Knudson, 2003). An early response to double-strand breaks is the phosphorylation of H2AX on Ser 139 (γ -H2AX; Rogakou et al., 1998), leading finally in the homologous recombination or non-homologous end-joining pathway (reviewed in Li and Heyer, 2008; Weterings and Chen, 2008). To prevent unrepaired non-coding lesions from stalling DNA replication which may cause a collapse of the replication fork and a subsequent double-strand break, cells have translesion synthesis (TLS) polymerases (polymerase η , ι , κ , ζ and Rev1). These polymerases incorporate a nucleotide opposite a lesion with low fidelity and are able to extend DNA from mismatch primer templates. In other words, these polymerases enable DNA replication to be continued but at the expense of a high probability of generating mutations (reviewed in Lehmann, 2006). The “polymerase switch” from the replicative polymerase to a TLS polymerase is achieved by mono-ubiquitination of PCNA (reviewed in Andersen et al., 2008; Hoege et al., 2002).

Polymerase ζ

Mad212 as an inhibitor of the Cdh1-APC complex has been already earlier found in *Saccharomyces cerevisiae* to be involved in TLS as a subunit of polymerase ζ (Lawrence et al., 1985). Polymerase ζ consists of two subunits, the catalytic polymerase subunit Rev3, a B-family type polymerase with low fidelity and no 3' to 5' exonuclease activity (reviewed in McCulloch and Kunkel, 2008), and the accessory subunit Mad212 which enhances the catalytic activity up to 20 to 30 folds (Nelson et al., 1996). In *S. cerevisiae*, polymerase ζ interacts with Rev1 and mono-ubiquitinated PCNA at stalled replication forks. Rev1 displays a dCMP transferase activity and seems to be an important scaffold protein which associates as well with other TLS polymerases. Polymerase ζ in concert with Rev1 is able to extend DNA from mismatched primer-templates and AP (apurinic and apyrimidinic) sites but only at the expense of creating mutations (Figure 4.). In fact, studies in *S. cerevisiae* showed that Rev1 and polymerase ζ are responsible for most of the spontaneous and damage-induced mutations created by DNA damaging agents (reviewed in Murakumo, 2002). In addition, polymerase ζ has been shown to be involved in

recombinational repair of double-strand breaks by a not yet defined mechanism (Holbeck and Strathern, 1997; Rattray et al., 2002).

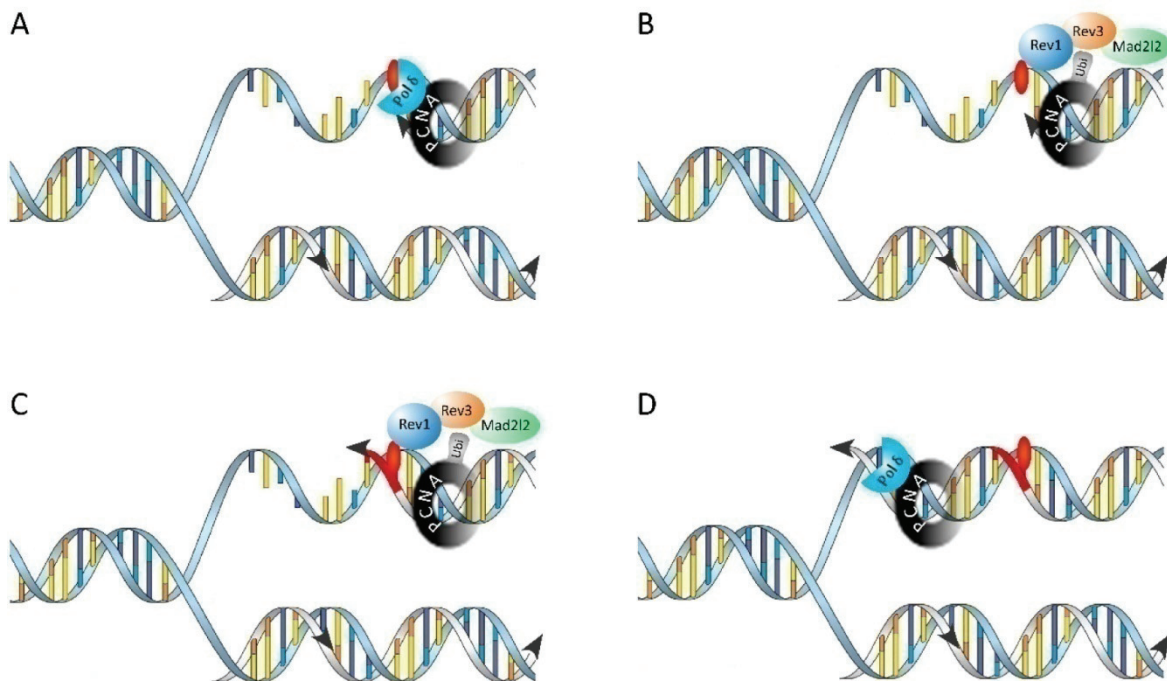


Figure 4. DNA lesion bypass by *S. cerevisiae* Rev1-polymerase ζ at a stalled replication fork.

(A) DNA replication polymerase δ is unable to bypass the non-coding lesion (red) and is stalled. (B) The stalled replication fork induces the mono-ubiquitination (Ubi, grey) of PCNA by the ubiquitin E2-E3 complex Rad6-Rad18. Mono-ubiquitination of PCNA causes the “polymerase switch” from polymerase δ to TLS polymerases, including Rev1-polymerase ζ . (C) Rev1-polymerase ζ inserts a nucleotide opposite the non-coding lesion and extends several nucleotides. (D) Deubiquitination of PCNA enables that the high fidelity replication is continued (after Gan et al., 2008).

REV3L is widely expressed in several different human tissues and cell lines (Kawamura et al., 2001; Lin et al., 1999). During mouse development expression of *Rev3l* starts around 7.5 dpc within the somites followed by an expression in mesoderm derived tissues. The expression becomes more ubiquitously during further development and is later on highest in brain, ovaries and testes (Van Sloun et al., 1999; Wittschieben et al., 2000). *Mad2l2* displays quite a similar expression pattern. In *Xenopus laevis* transcripts can be found from stage 1 on, and later during development it shows a ubiquitous expression across the different tissues with a strong domain in reproductive tissues (van den Hurk et al., 2004). In human tissues transcripts can be found also across all different tissues analyzed so far with a particularly high expression in testes (Murakumo et al., 2000; Nelson et al., 1999; Ying and Wold, 2003). Interaction of REV1, REV3L and Mad2l2 found

in *S. cerevisiae* could be confirmed in the human orthologues apart from the REV1-REV3L interaction (Masuda et al., 2003; Murakumo et al., 2001; Murakumo et al., 2000).

Recently it was found that Mad2I2 might also be involved in the integration of the cellular DNA damage response at the transcriptional level. The JNK MAP kinase cascade is activated by several stress signals including DNA damage (reviewed in Kyriakis and Avruch, 2001). The transcription factor Elk-1 is one of the targets that are activated through phosphorylation by the JNK MAP kinase cascade upon DNA damage. Mad2I2 was found to bind Elk-1 and enhances its phosphorylation and subsequent activation, which finally promotes the expression of target genes (Zhang et al., 2007).

Polymerase ζ deficiency

Several approaches have been used to study the consequences of *Rev* gene deficiency. Knockdown experiments of Rev3 in human and mice fibroblasts using RNA interference show a reduced UV radiation-induced mutagenesis rate but neither significant change in sensitivity to UV radiation nor cell viability was observed (Diaz et al., 2001; Li et al., 2002). In contrast, Rev3L showed to be indispensable during mouse development. Three independently generated knockout mice strains display embryonic lethality between 8.5 dpc and 12.5 dpc. Embryos that survive until mid-gestation are disorganized with significantly reduced cell density (Bemark et al., 2000; Esposito et al., 2000; Wittschieben et al., 2000). Generation of *Rev3L*^{-/-} mouse embryonic fibroblasts was unsuccessful; the cells entered a quiescent state with cell death occurring over weeks (Wittschieben et al., 2006; Zander and Bemark, 2004). The discrepancy in the results from the anti-sense RNA knockdown and the genetic ablation of Rev3L might be due to the fact that a low level of Rev3L is sufficient for cell survival. However, *Rev3L*^{-/-}, *p53*^{-/-} mouse embryonic fibroblasts are viable. These cells reveal a slower growth rate, sensitivity towards genotoxic agents, accumulate in the G2/M phase with a decrease in S phase cells and display striking chromosomal instability (Wittschieben et al., 2006; Zander and Bemark, 2004). Chicken DT40 cells lacking either Rev3 or Mad2I2 display a decreased viability and growth kinetics. These cells are more sensitive towards genotoxic agents and show an increase in chromosomal aberrations but an elevated level of sister chromatid exchange, a marker for homologous recombination in post-replication repair (Okada et al., 2005). *Mad2I2* knockdown experiments in nasopharyngeal carcinoma cells and human fibroblasts display

as well more sensitivity towards genotoxic agents with a decreased rate of mutagenesis (Cheung et al., 2006; McNally et al., 2008). Moreover, nasopharyngeal carcinoma cells show an elevated level of γ -H2AX with an increase in chromosomal aberration but a reduced frequency of sister chromatid exchange (Cheung et al., 2006) and *MAD2L2* deficient fibroblasts display a slower progression through the S phase (McNally et al., 2008). Disruption of the *Drosophila melanogaster Rev3* orthologue leads to an increase of sensitivity towards UV radiation and alkylating agents but has no effect on the mutagenesis rate (Eeken et al., 2001). In *Arabidopsis thaliana Rev3* ablation is not lethal but root growth is sensitive to UV-B radiation and even in the absence of radiation root stem cells display an increased mortality (Curtis and Hays, 2007; Sakamoto et al., 2003). *AtMad2l2* disruption displays only a minor phenotype with an increased sensitivity to a DNA cross-linker agent and long-term UV-B radiation (Takahashi et al., 2005).

In summary, Rev3 and Mad2l2 as subunits of the polymerase ζ are required for TLS to prevent the accumulation of double-strand breaks induced by endogenous damage through metabolic side-products. This TLS is responsible for a major fraction of mutations in our genome but its function was shown to be crucial for survival and normal proliferation of cells and during vertebrate embryonic development.

Aims of this study

The homeodomain protein Hesx1 is involved in forebrain and anterior pituitary gland development. Spatially and temporally precise expression of this transcription factor has been shown to be crucial for normal anterior pituitary gland development. The regulation of differential gene expression can be accomplished at the level of gene transcription, RNA processing/translation and protein modification. In order to identify and understand the protein modification pathways and protein-protein interactions involved in the regulation of transcription factor function, the aim of this work was to gain further insight into the regulative network in which Hesx1 is embedded.

In a previous study a yeast two-hybrid screen was performed to identify proteins which bind to Hesx1 and might regulate its function during forebrain and pituitary organogenesis. Among others, Mad2l2 a so far unknown interaction partner of Hesx1 was identified (Pilarski, 2004). Since Mad2l2 was shown to be involved in regulating cell cycle progression and DNA damage repair probably coordinating both events, the observed interaction raised the question whether broader functionality of Mad2l2 towards transcriptional regulation could be found. Furthermore, the function of Mad2l2 in inhibiting the Cdh1-APC complex led to the suspicion that Hesx1 might be targeted for ubiquitination by this complex.

The aims of this work were therefore, to (1) verify the binding of Mad2l2 to Hesx1 and (2) to elucidate the biological function of this interaction on a biochemical level. Moreover, (3) the possibility of an ubiquitination of Hesx1 through the Cdh1-APC complex was addressed and (4) *Mad2l2* deficient mice were generated in order to gain further insight into the biological function of *Mad2l2*, both on cell cycle progression, and on DNA damage. The developing pituitary gland of these animals might provide an excellent model system to investigate the significance of the Mad2l2-Hesx1 interaction. The role of Hesx1 is well defined during anterior pituitary gland development and already minor changes in cell type differentiation can be monitored by the expression of different transcription factors and hormones.

RESULTS

Hesx1 interacts with Mad2l2 and the APC recognition subunit Cdh1

In order to verify the interactions of Hesx1 and the potential binding partners found in the 8.5 dpc mouse library screen (Pilarski, 2004) the full length open reading frames including a short linker sequence were cloned into the pPC86 vector. Therefore, the Hesx1 protein was fused to the GAL4 DNA-binding domain (*pDB-Leu-Hesx1*) and the potential interaction partners were fused to the GAL4 activation domain (*pPC86-X*). The interaction of two proteins, led to the reconstitution of an active GAL4 transcription factor. This functional transcription factor activated the expression of reporter genes, which were driven by promoters containing the GAL4 binding site. The reporters used in this assay were driven by different promoters to reduce the probability of false positives. The *pDBLeu-Hesx1* and candidate *pPC86* vectors were transformed into the MaV203 yeast strain and monitored for reporter gene activation. The induction of these reporters was assayed on SC-Leu-Trp-His 50 mM 3AT selection plates (HIS3 reporter) and by the X-Gal assay (lacZ reporter). Hesx1 was used as a positive control since it is known to homodimerize (Brickman et al., 2001; Dattani et al., 1998; Sornson et al., 1996). All four candidates verified the interaction and showed no self-activation activity. Mad2l2 and Map-1 displayed a strong to very strong interaction with Hesx1 whereas Traf4 and Importin13 showed a weak to moderately strong binding affinity to Hesx1 (Figure 5. A).

As Mad2l2 functions as a regulator of the cell cycle by inhibiting the Cdh1-APC complex (Chen and Fang, 2001; Pflieger et al., 2001) and displays regulatory function in DNA damage repair (Lawrence, 2002; Okada et al., 2005), it was chosen for further analysis as an interesting candidate that might link its functions to transcriptional control.

The Mad2l2-Hesx1 interaction found in the yeast two-hybrid assay was confirmed by *in vitro* pull-down experiments. Bacterial recombinant GST-Hesx1 and GST-Mad2l2 fusion proteins were produced and purified. These fusion proteins were tested for binding to Mad2l2 and Hesx1 that were synthesized by *in vitro* transcription/translation in the presence of L-[³⁵S] methionine. In these pull-down assays Mad2l2 bound weakly to GST-Hesx1 but not to GST alone and Hesx1 bound to GST-Mad2l2 but not to GST (Figure 5. B).

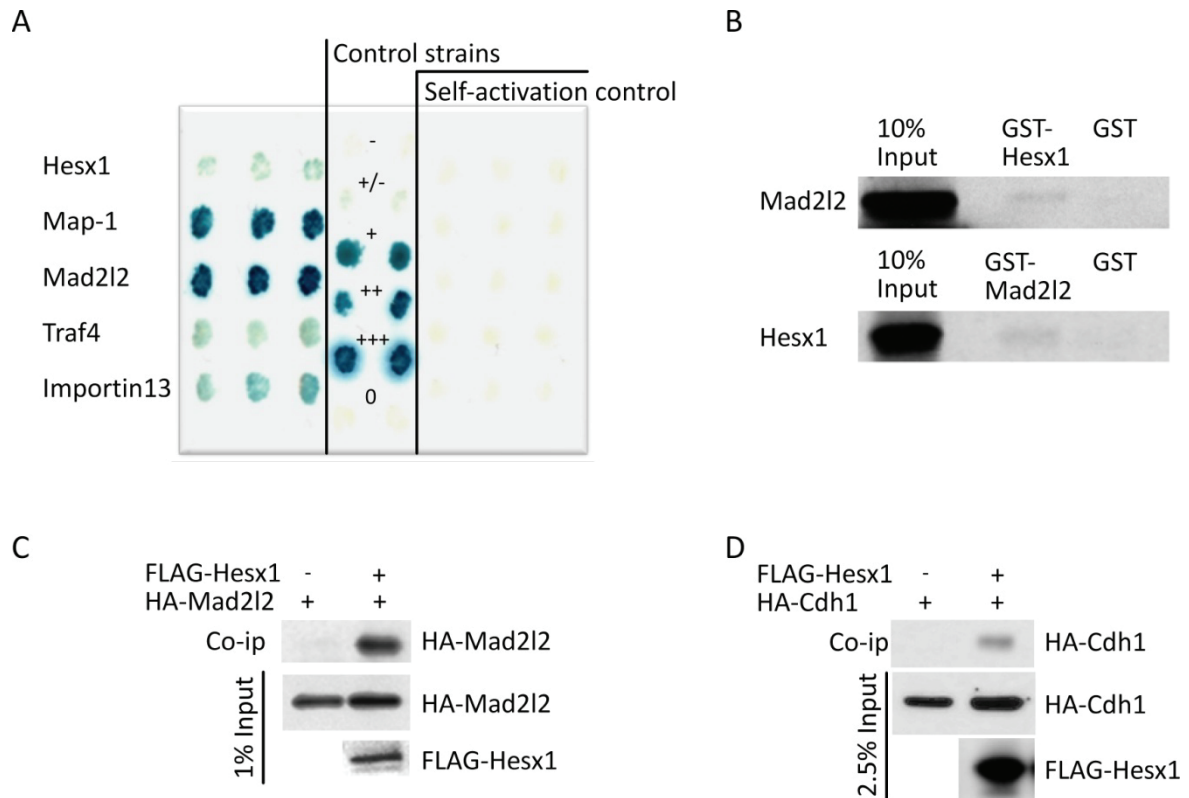


Figure 5. Mad2I2 and Cdh1 interact with Hesx1.

(A) The yeast two-hybrid assay with full orf of Map-1, Mad2I2, Traf4 and Importin13 confirmed the interaction found in the 8.5 dpc mouse library screen (Pilarski, 2004) as indicated by lacZ activity. Control strains: - = no interaction; +/- = weak; + = moderately strong; ++ = strong; +++ = very strong and 0 = Hesx1 self activation. (B) *In vitro* transcribed/translated Mad2I2 binds to a GST-Hesx1 fusion protein but not to GST alone and vice versa. (C) FLAG-Hesx1 specifically co-immunoprecipitates HA-Mad2I2 from COS-7 cell extracts. (B) FLAG-Hesx1 co-immunoprecipitates HA-Cdh1 from COS-7 cell extracts.

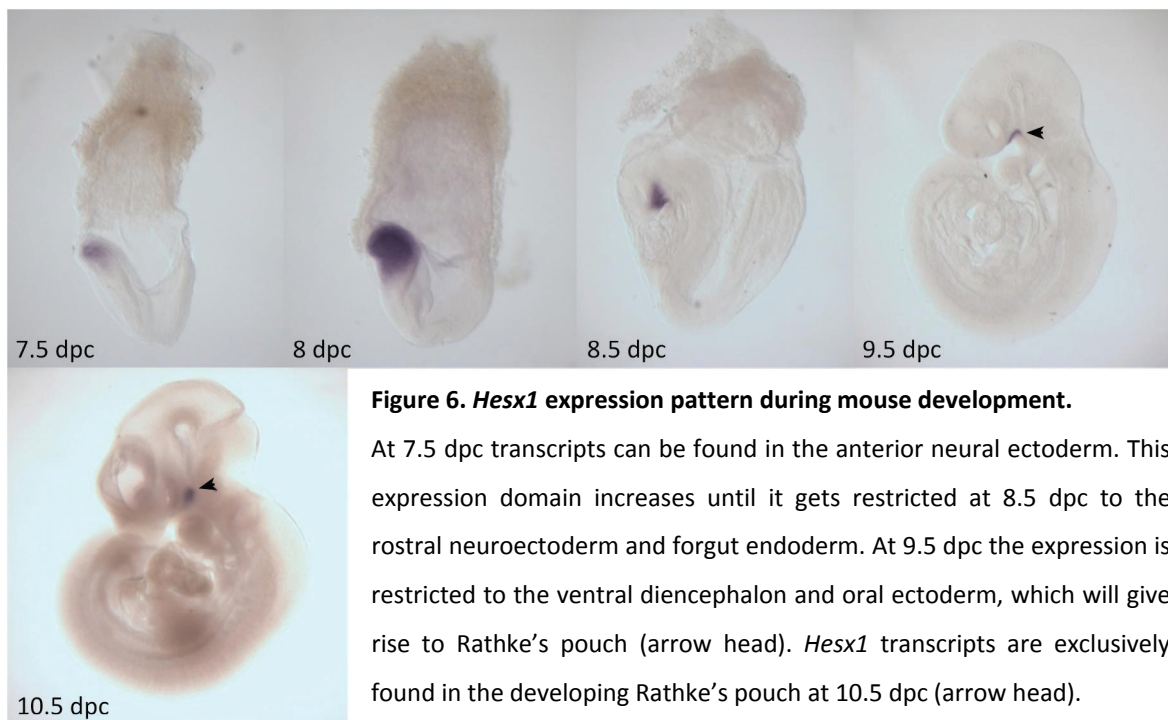
Since the interaction strength varied greatly between the yeast two-hybrid assay and the pull-down experiment the binding was validated in mammalian cells. Since no cell line expressing Hesx1 is available and Mad2I2 expression levels are relatively low, overexpression experiments were performed. Plasmids expressing N-terminal FLAG tagged Hesx1 (FLAG-Hesx1) and HA tagged Mad2I2 (HA-Mad2I2) were transiently transfected in COS-7 cells, and FLAG-Hesx1 was immunoprecipitated with an ANTI-FLAG resin. In analogy to the previously described experiments HA-Mad2I2 was co-immunoprecipitated. However, there was no binding to the negative control where only the FLAG backbone vector was co-transfected with HA-Mad2I2 (Figure 5. C). The interaction of Hesx1 and Mad2I2 raised the question if Hesx1 would bind to the APC substrate recognition subunit Cdh1 as well. Since Mad2I2 is binding and regulating Cdh1, this interaction would qualify Hesx1 as a potential target of the APC complex. After FLAG-

Hesx1 and *HA-Cdh1* co-transfection in COS-7 cells, FLAG-Hesx1 could specifically co-immunoprecipitate HA-Cdh1 (Figure 5. D).

Taken together, these results confirmed an interaction of Hesx1 with Mad2l2 *in vivo* and *in vitro*. Furthermore, Hesx1 bound to the APC substrate recognition subunit Cdh1 *in vivo*.

***Hesx1*, *Mad2l2* and *Cdh1* have overlapping expression domains**

The biological significance of Hesx1 interaction with Mad2l2 and Cdh1 would imply that these proteins have a spatial and temporal overlapping expression pattern. *Hesx1* displays a highly restricted expression pattern in the developing mouse, transcripts are found mainly in the anterior neural ectoderm and Rathke's pouch as confirmed by *whole mount in-situ* hybridization (Figure 6.; Hermes et al., 1996; Thomas and Beddington, 1996).



As described in the introduction, *Mad2l2* shows a ubiquitous expression pattern throughout human tissues and *Xenopus laevis* tissues and embryonic stages. *Whole mount in-situ* hybridization analysis of *Mad2l2* in mice gave no conclusive result (data not shown). *Cdh1* is expressed in a variety of mouse tissues and is not restricted to proliferating cells (see introduction).

To address the question whether *Mad2l2*, *Cdh1* and *Hesx1* have overlapping expression domains in mice a RT-PCR analysis was carried out. 8 dpc mouse embryos were isolated and separated in an anterior and posterior part. Subsequently, RNA was isolated from these tissues. RT-PCR analysis revealed that *Hesx1* was only expressed in the anterior part whereas *Mad2l2* and *Cdh1* were present in anterior as well as posterior tissues (Figure 7. A). Transient expression of FLAG-Hesx1 and HA-Mad2l2 followed by a double immunofluorescent staining with antibodies against the FLAG and HA epitop uncovered a co-localization in the nucleus of COS-7 cells (Figure 7. B). In addition northern blot analysis was performed to assess gene expression across several adult mouse tissues. The result confirmed the expected mRNA size of 1.2 kb and indicated a ubiquitous expression of *Mad2l2* with a slightly higher abundance in kidney, 14 dpc embryos and ovary and a very high level in testis (Figure 7. C).

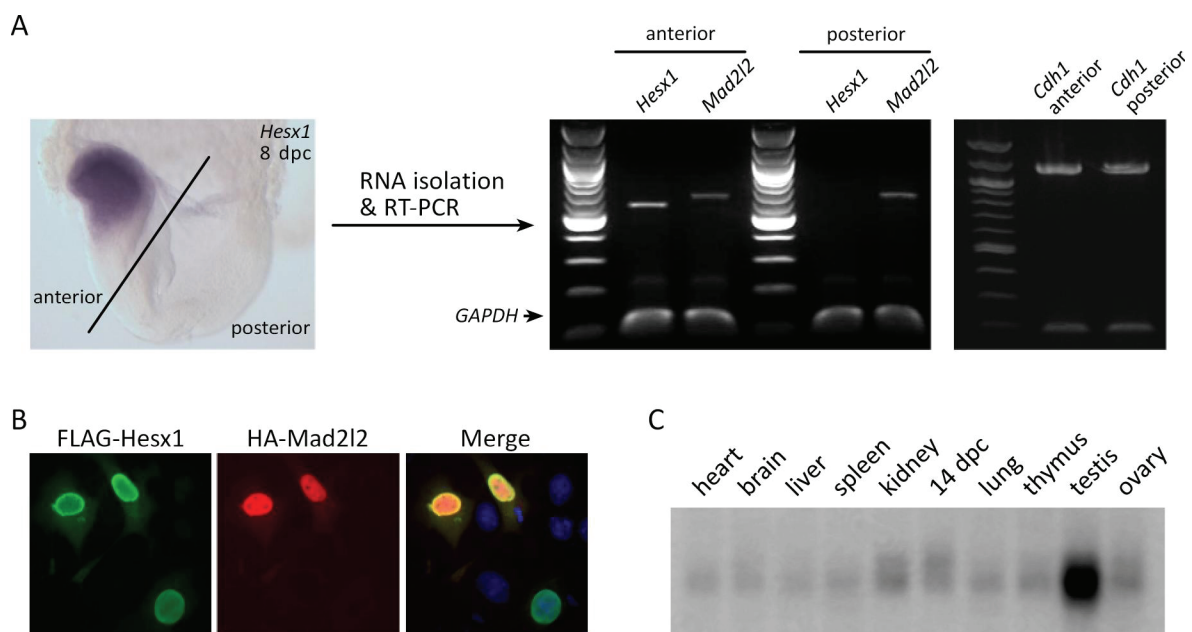


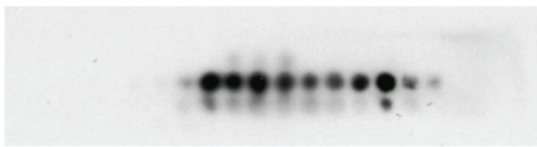
Figure 7. Mad2l2 and Cdh1 expression overlaps with Hesx1.

(A) RNA was isolated from the anterior and posterior part of an 8 dpc embryo. RT-PCR analysis revealed that *Hesx1* was only expressed in the anterior part whereas *Mad2l2* and *Cdh1* are expressed anterior as well as posterior. *GAPDH* served as a loading control. (B) Co-expression of FLAG-Hesx1 and HA-Mad2l2 in COS-7 cells display co-localization in the nucleus. (C) Northern blot analysis showed a ubiquitous presence of *Mad2l2* RNA in mice with a slight elevation in kidney, 14 dpc embryos and ovary and a strong expression in testis. The northern blot (Ambion FirstChoice Northern Blot) contained 2 μ g poly(A) RNA per lane.

Mad2I2 prevents DNA binding of Hesx1

To gain insight into the nature of the Mad2I2-Hesx1 interaction, the Hesx1 binding site of Mad2I2 was specified by a peptide array. The amino acid sequence of Hesx1 was spotted as 20meric peptides which were overlapping by 17 amino acids on a cellulose membrane. Recombinant Mad2I2 was shown to bind two elements at the amino-terminal part of the homeodomain (Figure 8. A, B).

A



27. RPEERAPKYENYFSASETRSLK
 28. ERAPKYENYFSASETRSLKR
 29. PKYENYFSASETRSLKRELS
 30. ENYFSASETRSLKRELSWYR
 31. FSASETRSLKRELSWYRGRR
 32. SETRSLKRELSWYRGRRPRT
 33. RSLKRELSWYRGRRPRTAFT
 34. KRELSWYRGRRPRTAFTQNQ
 35. LSWYRGRRPRTAFTQNQVEV
 36. YRGRRPRTAFTQNQVEVLEN
 37. RRPRTAFTQNQVEVLENVFR

B



C

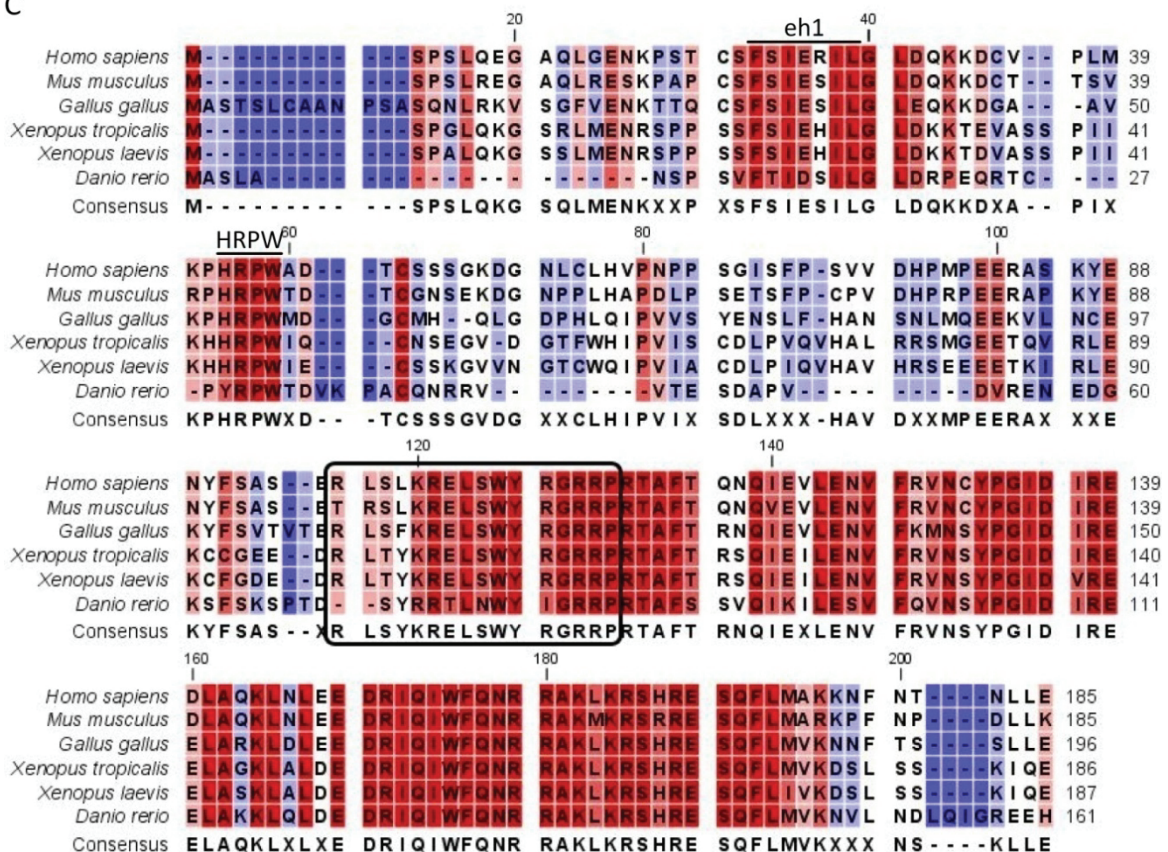


Figure 8. Mad2l2 binds to the N-terminal part of the homeodomain of Hesx1.

(A) Recombinant Mad2l2 binds to the Hesx1 peptide array. The bound peptides are listed and the core peptides are framed in green. (B) The Mad2l2 binding domain of Hesx1 is localized at the N-terminal part of the homeodomain (grey letters = start of the homeodomain). (C) Sequence alignment of Hesx1 in different species. The Mad2l2 binding domain of Hesx1 is highly conserved among the species (framed in black). The background color of the amino acids varies from blue (nonconserved residues) to red (conserved residues).

This region is highly conserved across species like only few other regions of the protein are; such as the engrailed homology domain, the HRPW region and the carboxy-terminal region of the homeodomain (Figure 8. C; (Kazanskaya et al., 1997)).

This finding lead to the idea, that binding of Mad2l2 in this region of Hesx1 might impair the interaction with the N-CoR complex or its DNA binding properties (Figure 9. A). To address the latter, electrophoretic mobility shift assays (EMSA) were performed. Hesx1 is known to bind to an oligonucleotide containing a palindromic PIII site (PrdQ) (Dattani et al., 1998; Sornson et al., 1996; Wilson et al., 1993). *In vitro* transcribed/translated Hesx1 was shown to bind to radioactive labeled double-stranded PrdQ-oligonucleotides which led to a prominent shift during electrophoresis, whereas the free oligonucleotides did not led to any shift (Figure 9. B, Lane 3 & 7). This shift was specific to Hesx1 binding as shown by the prominent super-shift when Hesx1 antibodies were added (Figure 9. B, Lane 1). Pre-incubation of Hesx1 with increasing amounts of recombinant Mad2l2 reduced the binding of Hesx1 to the oligonucleotide as indicated by the reduction of the shifted probe (Figure 9. B, Lane 4, 5, 6). Mad2l2 had no binding affinity to the PrdQ sequence (Figure 9. B, Lane 2). To determine the specificity of this effect, the same amount of recombinant GST protein was pre-incubated with Hesx1 but had almost no influence on the ability of Hesx1 to bind to the oligonucleotides (Figure 9. B, Lane 8). This demonstrates that Mad2l2 is able to prevent Hesx1 from binding to its target DNA.

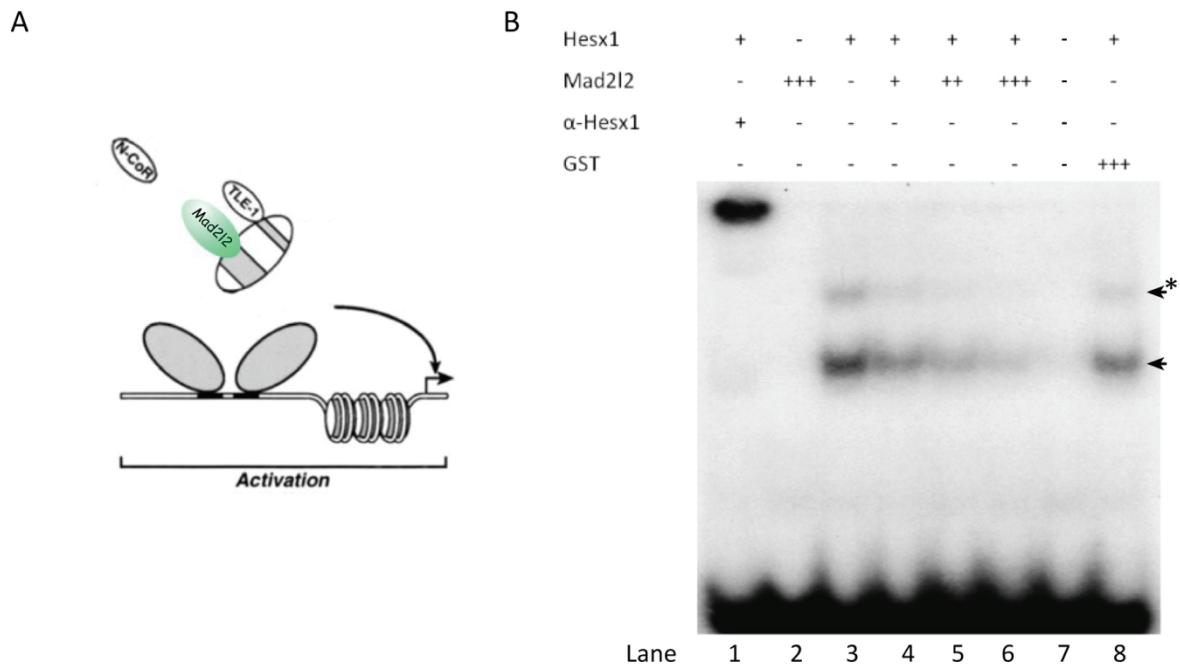


Figure 9. Mad212 disturbs the ability of Hesx1 to bind DNA.

(A) Mad212 might prevent Hesx1 from binding to its target DNA and subsequently disturb its repressive activity (modified from Dasen et al., 2001). (B) Increasing amounts of Mad212 interfere with the binding of Hesx1 to target DNA *in vitro*. Arrow heads indicate Hesx1 bound to the radioactive PrdQ-oligonucleotide as monomer and probably as homodimers (*).

The E3 ubiquitin ligase Cdh1-APC polyubiquitinates Hesx1

The interaction of the APC substrate recognition subunit Cdh1 and Hesx1 raised the question if Hesx1 might be targeted for ubiquitination through the formation of the complex. Several Cdh1 recognition sequences are known to be necessary for Cdh1-APC mediated ubiquitination. Sequence analysis of Hesx1 revealed an imperfect KEN box (Pfleger and Kirschner, 2000) and an imperfect D-box (Fang et al., 1998; Glotzer et al., 1991). The D-box and KEN-box sequence was conserved in the human as well as the mouse protein but not in other species (Figure 10. A & Figure 8. C). The presence of these motifs led to the assumption that Hesx1 is targeted by the Cdh1-APC complex and subsequently ubiquitinated. An initial co-immunoprecipitation experiment in COS-7 cells provided evidence that HA-Cdh1 binds to the conserved carboxy-terminal region of Hesx1 (FLAG-Hesx1 Δ eh1; amino acids 88-185) but not to the amino-terminal domain (FLAG-Hesx1 Δ HD; amino acids 1-86) (Figure 10. B).

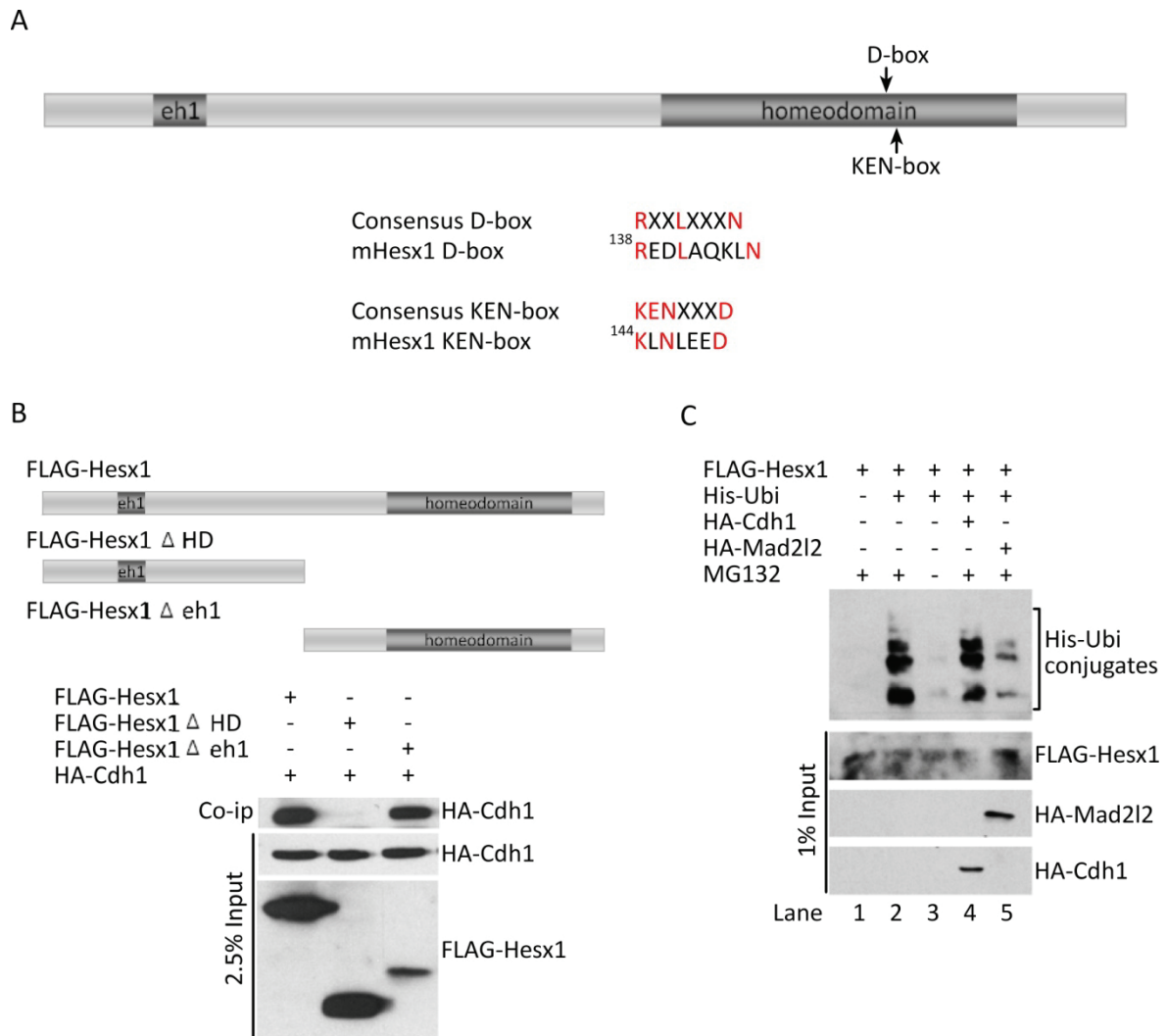


Figure 10. Hesx1 is subject to *in vivo* ubiquitination.

(A) The protein sequence of Hesx1 contains two imperfect destruction motifs. (B) In COS-7 cell extracts HA-Cdh1 co-immunoprecipitates specifically with FLAG-Hesx1 and the FLAG-Hesx1 Δ eh1 containing only the C-terminal homeodomain region. (C) FLAG-Hesx1 is ubiquitinated in NIH3T3 cells and the co-expression of HA-Mad2I2 attenuates this ubiquitination.

To assess whether Hesx1 is a substrate of the Cdh1-APC E3 ubiquitin ligase complex, FLAG-Hesx1 was used in an *in vivo* ubiquitination assay. In this assay, ubiquitin conjugates were purified using His tagged Ubiquitin (His-Ubi) and Ni-NTA Agarose. Substrate conjugation to ubiquitin was detected in the form of high molecular weight polyubiquitin conjugates. Transient overexpression of FLAG-Hesx1 and His-Ubi in NIH-3T3 cells revealed a large amount of polyubiquitinated Hesx1 in the presence of the 26S proteasome inhibitor MG132 (Figure 10. C, Lane 2). In the absence of MG132 only a small amount of polyubiquitinated Hesx1 could be purified (Figure 10. C, Lane 3). The additional co-transfection with HA-Cdh1 did not significantly increase the level of Hesx1 polyubiquitin

conjugates in the presence of MG132 (Figure 10. C, Lane 4.). In contrast, the co-transfection of HA-Mad212 strongly reduced the level of polyubiquitinated Hesx1 (Figure 10. C, Lane 5).

Hence, Hesx1 is subject to polyubiquitination which can be inhibited by Mad212, the inhibitor of the Cdh1-APC E3 ubiquitin ligase complex.

Generation of Mad212 deficient mice

In order to gain further insight into the biological function of Mad212 and its influence on developmental processes, gene targeting in ES cells was used to generate Mad212 deficient mice. Since a null mutation can result in early embryonic lethality which might be uninformative for the function of Mad212 at later stages of development or adulthood, a conditional knockout targeting construct was created. The design of the conditional targeting construct is based on the inducible Cre/*loxP* system. Cre is a site-specific DNA recombinase that recognizes a 34 bp site called *loxP* and catalyzes the DNA recombination between two *loxP* sites. The recombination leads to excision of the DNA between these sites (Sauer, 1998; Sauer and Henderson, 1989).

The genomic region of the murine *Mad212* is located on chromosome 4 at position 147514599 bp to 147519805 bp (NC_000070.5 Reference assembly (C57BL/6J)). The *Mad212* targeting vector was designed to flank the entire coding region by *loxP* sites to generate a null allele upon expression of Cre. The *loxP* sites were introduced 113 bp upstream of the first coding exon and 20 bp downstream of the last exon, finally deleting a region of 5330 bp. This strategy was chosen because the protein comprises several methionine (amino acid position: 1, 54, 160, 181, 192, 199) that could serve as a start codon leading to a truncated Mad212 protein. Especially the first three methionine residues, encoded in coding exon 1, 3 and 6 bear the risk of creating a dominant negative or active form of Mad212. At the time the targeting construct was designed only the Ensemble “common known protein coding” transcript was known (Figure 11., yellow annotation) meanwhile several other transcripts were annotated (Figure 11.). However, the targeting construct deletes the entire *Mad212* coding region.

To minimize the probability of deleting regulatory domains, introns and adjacent genomic regions were analyzed for highly conserved elements across different species using the

databases of the National Center for Biotechnology Information (NCBI, <http://www.ncbi.nih.org>) and Ensembl (<http://www.ensembl.org>). The first regulatory region predicted by cisRED/miRANDA was found 696 bp upstream of the first coding exon (Robertson et al., 2006). These elements were not disturbed nor deleted by the targeting construct.

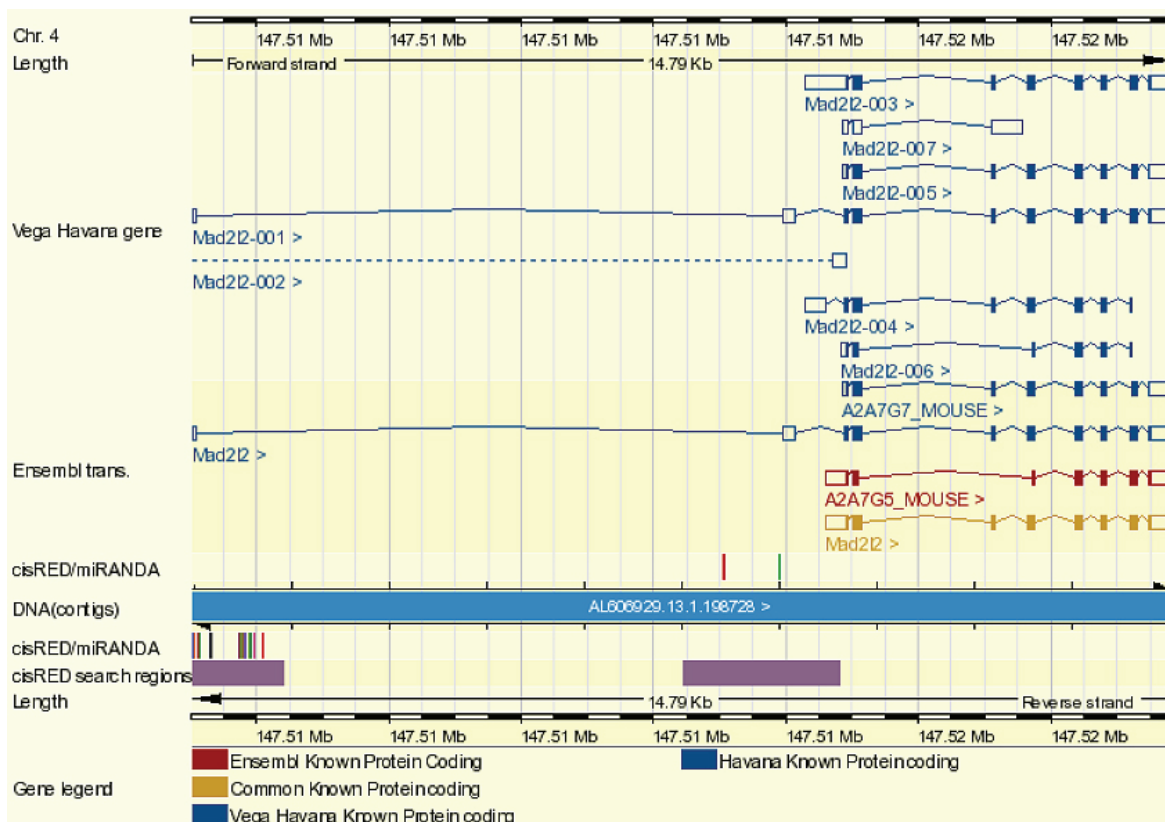


Figure 11. Search results for *Mad2l2* in the Ensembl database.

The annotations all relate to *Mad2l2* but there are differences in the structural details between VEGA (Vertebrate Genome Annotation Group) manual annotation, showing multiple transcripts and the computational predictions of Ensembl. cisRED/miRANDA are databases that provide information about regulatory modules and elements (Robertson et al., 2006). Filled boxes display coding exons whereas open boxes represent untranslated exons. Source: <http://www.ensembl.org>.

Use of Recombineering to create the conditional knockout targeting vector

To isolate *Mad2l2* genomic DNA the Mouse PAC (RPCI-21) library 711 (Strain: 129/SvevTACfBR) (RZPD; (Osoegawa et al., 2000)) was screened using a radioactive labeled probe of *Mad2l2* cDNA. Five PAC clones were identified and three of them used for subsequent analysis. All three clones contained the *Mad2l2* genomic region necessary for the generation of the targeting vector as it was identified by PCR analysis.

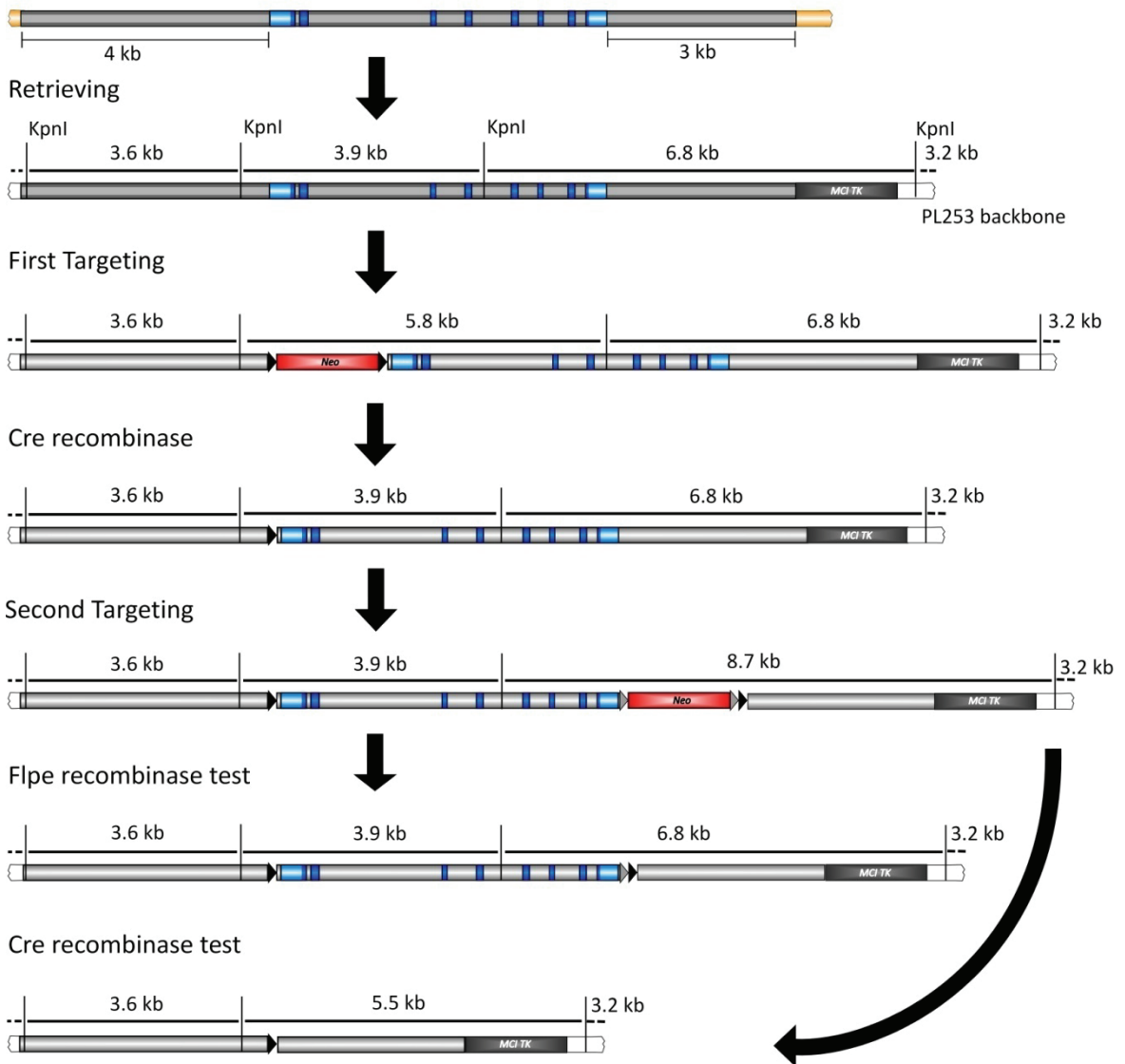
The targeting vector was created using a method described as recombineering or recombinogenic engineering (Liu et al., 2003; Muyrers et al., 2001; Warming et al., 2005). This method is based on homologous recombination via the gap repair mechanism mediated by the λ phage Red proteins in *E. coli*. The entire procedure is described in detail in the material and methods section (Figure 29.).

One of the positive PAC clones (RPCIP711B01141Q6) was used to subclone the targeting region including a 4 kb 5' homology and a 3 kb 3' homology arm via gap repair into the retrieval plasmid (Retrieving; Figure 12. A). The 5' and 3' homology arms are important to ensure correct targeting in ES cells by homologous recombination. For the negative selection process in ES cells, the retrieval plasmid contains a *Mc1*-driven Thymidine Kinase (*tk*) cassette. In a next step, the floxed *Neo* cassette was targeted 113 bp upstream of the first coding *Mad2l2* exon (First Targeting; Figure 12. A). Thereupon, the floxed *Neo* cassette was excised by the expression of Cre recombinase in *E. coli* leaving a single *loxP* site behind (Cre recombinase; Figure 12. A). Next, the positive selection cassette was targeted 20 bp down stream to the last *Mad2l2* coding exon. This cassette contains a *Neo* cassette flanked by two *frt* and a downstream *loxP* site. The expression of the neo gene is regulated by the prokaryotic *em7* and the eukaryotic *PgK* promoter for positive selection in the ES cells (Second Targeting; Figure 12. A).

To test the functionality of the *frt* sites in the conditional targeting vector, the plasmid was electrotransformed into *E. coli* expressing Flpe recombinase. The *Neo* cassette was excised leaving a single *frt* site behind. This step was performed to ensure that the positive selection cassette could be removed in the ES cells (Flpe recombinase test; Figure 12. A). This excision step might be necessary in case the eukaryotic promoter of the *Neo* cassette alone creates a phenotype in the conditional targeted mice. In the knockout situation it would be removed together with the *Mad2l2* coding region. In order to test the functionality of the *loxP* sites which would create the null allele, the targeting vector was electroporated into *E. coli* expressing the Cre recombinase. The genomic *Mad2l2* locus together with the *Neo* cassette was successfully removed (Cre recombinase test; Figure 12. A).

A

PAC



B

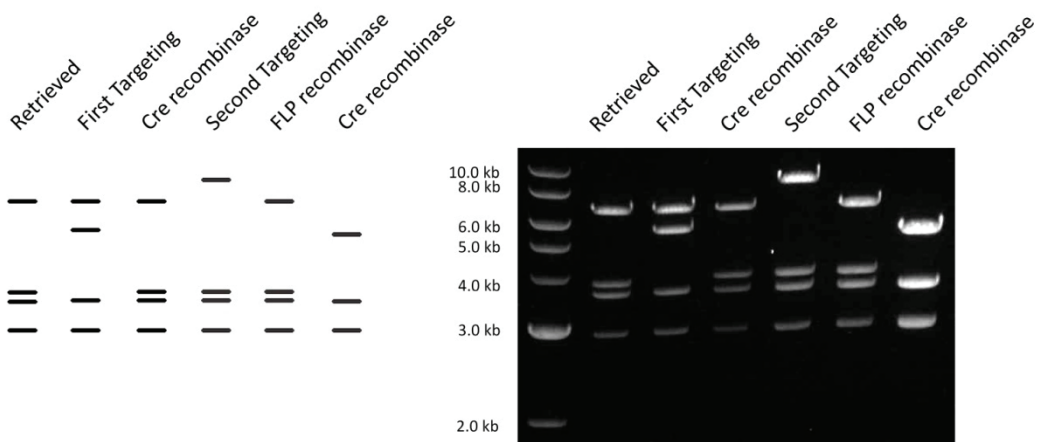


Figure 12. Construction and functional analysis of the Mad2l2 conditional knockout vector.

(A) Retrieving and targeting of the 12.2 kb genomic region containing the Mad2l2 coding exons. Targeting region is depicted in grey. Blue are Mad2l2 coding exons and light blue display untranslated regions. Black arrow heads are *loxP* sites and grey arrow heads are *frt* sites. The *Neo* cassette is depicted in red whereas the *tk* cassette is grey. (B) KpnI-digestion pattern of the plasmids at every stage of the targeting vector construction (left: expected pattern; right: actual pattern).

All the steps described above were monitored by restriction enzyme digestion. KpnI digestion gave a distinct pattern at every stage of the targeting vector construction (Figure 12. B). In addition each step was followed by sequencing of the targeted region to ensure that no additional mutations were inserted in the genomic *Mad2l2* locus. The final conditional knockout vector was also sequenced at all altered position, exonic regions and intron-exon boundaries to exclude any additional modifications.

Gene targeting in ES-cells and Cre mediated deletion of *Mad2l2* in mice

The linearized *Mad2l2* conditional knockout targeting vector was electroporated into the MPI-II ES cells and subsequently went through a positive/negative selection with G418 and ganciclovir (Ganc) respectively. Cells which underwent correct homologous recombination contained the *Neo* cassette and survived the exposure to G418. In addition, the ES cells lost the *tk* cassette and thus also survived the exposure to ganciclovir (Figure 13. A).

217 ES cell clones survived the positive/negative selection process and were analyzed by southern blotting. Genomic DNA was isolated from each clone and the correct insertion of the 5' *loxP* site was monitored by a BglI digestion and southern blotting with the 5' probe. A BglI restriction site was integrated upstream of the *loxP* site, creating a 9.5 kb band instead of the 14 kb band found in the wild-type situation (Figure 13. A & B). The integration of the *Neo* cassette with the flanking *frt* sites and the 3' *loxP* site was analyzed by southern blotting with the 3' probe following a DraI digestion. Correct insertion was marked by a 6.2 kb band due to the insertion of a DraI site 5' to the *Neo* cassette. The wild-type band was around 4.9 kb (Figure 13. A & B). Two clones (SP-34 and 106) were found to be positive for both, the 5' and 3' probe (Figure 13. B).

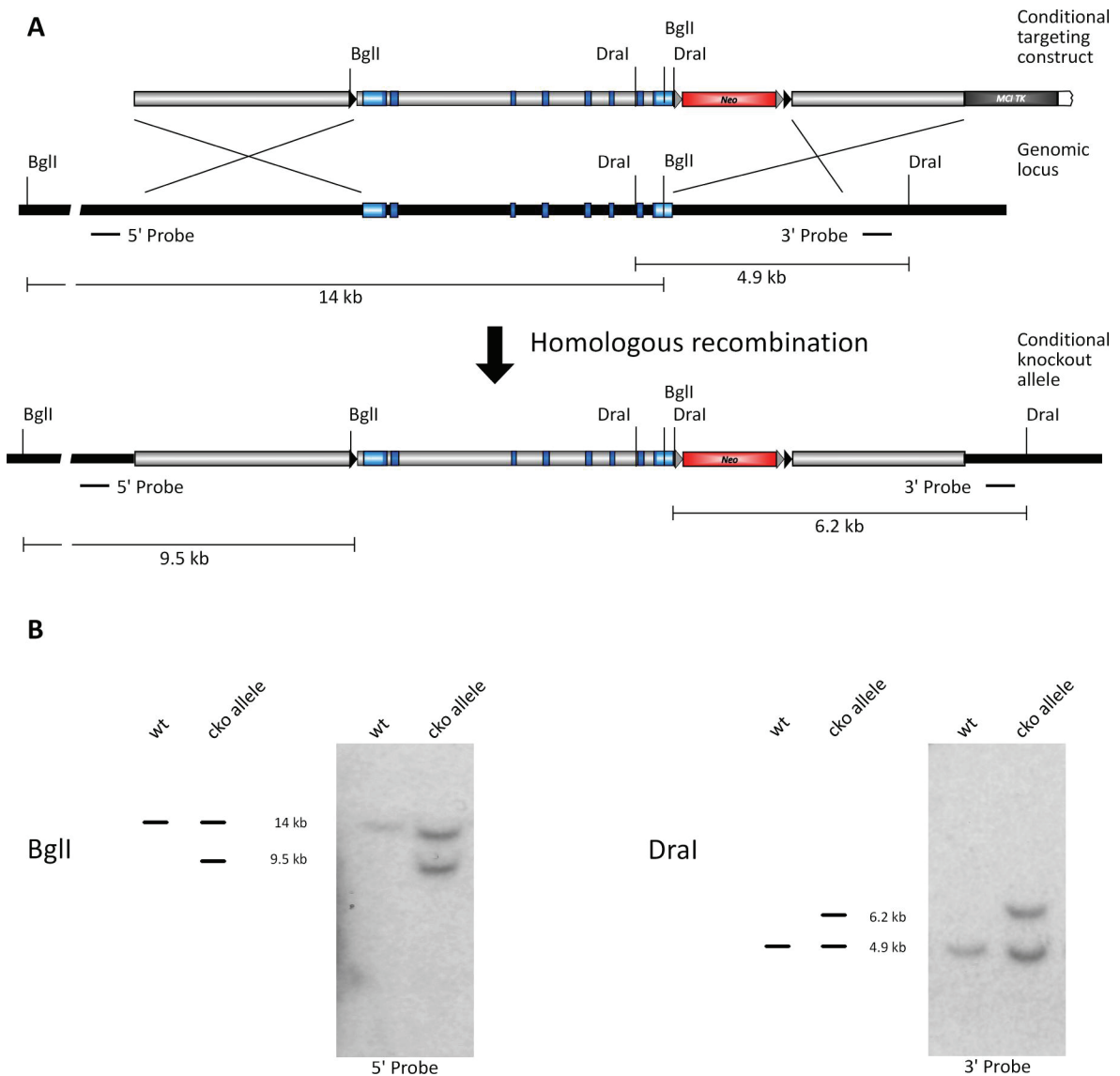


Figure 13. Targeting of the *Mad2l2* genomic locus with the cko construct in ES cells.

(A) Structure of the conditional targeting construct, *Mad2l2* genomic locus and targeted locus. (B) Confirmation of *Mad2l2* targeting by southern blot analysis of BglI (5' Probe) and DraI (3' Probe) digested ES cell DNA. Clone SP-34 is shown (left: expected pattern; right: actual pattern).

The two positive ES cell clones were used for the production of aggregation chimeras. The ES cells were aggregated with CD-1[®]/ICR morula-stage embryos and cultured to the blastocyst-stage. The aggregated blastocysts were transferred into the oviduct of pseudopregnant female recipient mice. Chimeric offspring could be easily detected on the basis of the coat color when the fur becomes visible at around 10 days after birth. MPI-II ES cells are derived from an agouti-pigmented substrain of the 129 strain whereas CD-1[®]/ICR mice are albino. Test breedings with CD-1[®]/ICR and chimeras, primarily with at least 50% ES derived coat color were done to identify germ-line transmission of the

transgenic MPI-II cells. Only ES cell clones from SP-34 gave germ-line transmission. Additional test breedings of mice heterozygous for the *Mad2l2* conditional knockout allele revealed, that homozygous mice are viable, fertile and without any obvious phenotype. This indicates that the targeted region is functional and does not disturb the genomic locus.

In order to generate *Mad2l2* deficient mice, SP-34 chimeric mice which gave germ-line transmission were crossed with CMV-Cre mice (CMV promoter driven Cre recombinase; (Schwenk et al., 1995)) to generate *Mad2l2*^{+/-} (heterozygous) offspring (Figure 14. A). Heterozygous *Mad2l2* mice were without pathological findings, viable and fertile. Matings of *Mad2l2*^{+/-} mice gave birth to wild-type, heterozygous as well as homozygous animals as determined by PCR-genotyping of tail DNA (Figure 14. A & B).

To confirm that *Mad2l2* deficient mice do not express the *Mad2l2* RNA and protein, primary mouse embryonic fibroblasts (MEF's) were prepared from 13.5 dpc embryos. RT-PCR analysis of total RNA extracts confirmed the loss of *Mad2l2* transcripts in the homozygous lines (Figure 14. B). Western blotting following whole protein extraction approved the loss of Mad2l2 protein in *Mad2l2*^{-/-} cells (Figure 14. D).

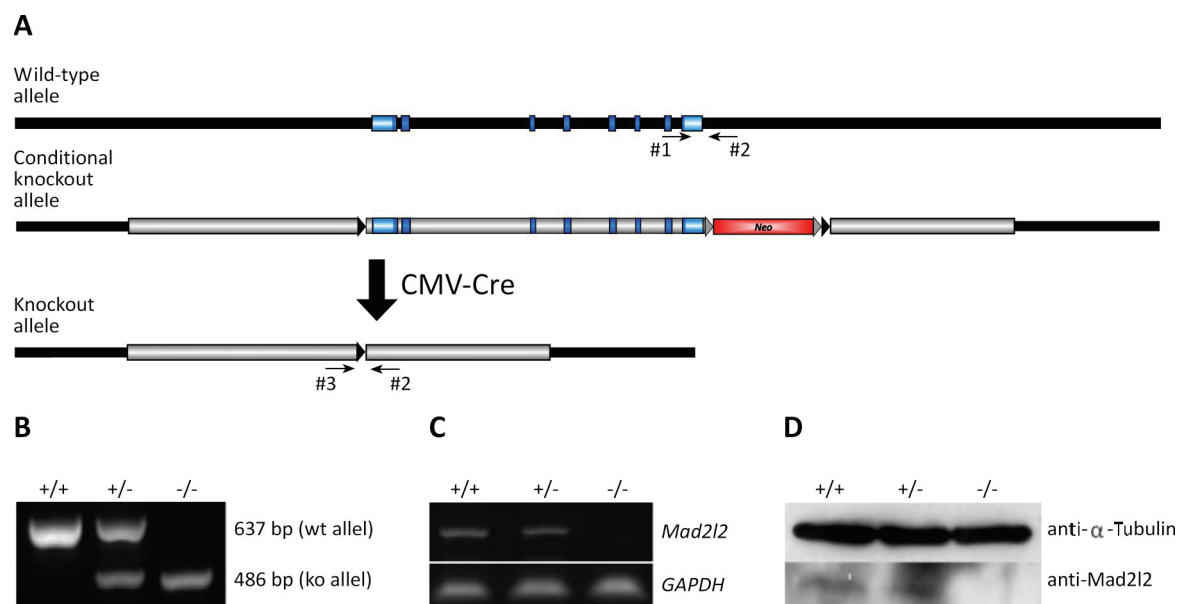


Figure 14. Generation of *Mad2l2* knockout mice.

(A) Heterozygous *Mad2l2* cko chimeric mice were crossed with CMV-Cre mice to obtain heterozygous *Mad2l2* ko mice. (B) PCR analysis of tail DNA using primers #1, #2 and #3. (C) RT-PCR of RNA obtained from MEF's. (D) Western blot analysis of full protein extracts generated from MEF's.

Phenotypic analysis of *Mad2l2* knockout mice

Variable viability and growth retardation in *Mad2l2* deficient embryos

Offspring of *Mad2l2*^{+/-} mice intercrosses diverged from the expected Mendelian frequency of 25% *Mad2l2*^{-/-} mice. Only 13% of the offspring were homozygous *Mad2l2* mutants, indicating intra-uterine lethality (Figure 15. A). To determine the time point of lethality several different stages were analyzed but did not give conclusive results so far. Most of the examined stages did not match the expected number of *Mad2l2* deficient animals according to the Mendelian rules (Figure 15. B). Even though the number of homozygous mutant embryos at 10.5 and 12.5 dpc was found to be higher, in general it was found to be significantly lower than anticipated.

A

stage (dpc)	litter	Number per genotype			Total
		+/+	+/-	-/-	
Mice born	15	29 (30%)	57 (59%)	13 (13%)	97
8.5	1	4	8	2	14
10.5	1	3	3	4	10
11.5	2	6	15	0	21
12.5	2	5	3	5	13
13.5	3	6	15	1	22
14.5	3	8	16	2	26
15.5	1	3	4	1	8
16.5	1	2	5	2	9
17.5	1	1	4	1	6

B

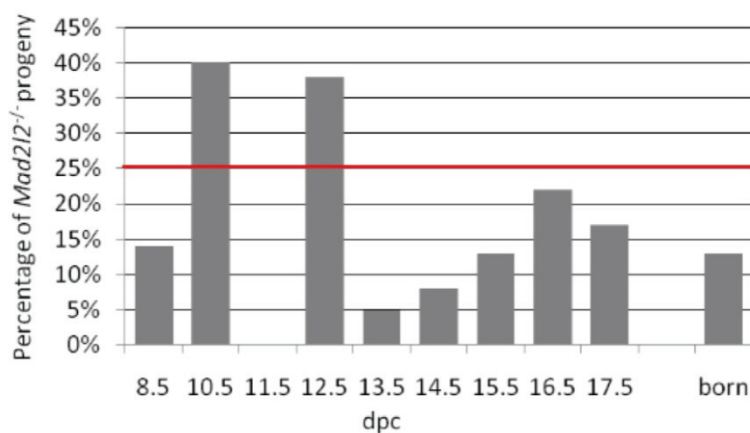


Figure 15. Genotypic analysis of progeny from *Mad2l2*^{+/-} intercrosses reveals embryonic lethality of *Mad2l2*^{-/-} mice.

(A) Total numbers of progenies. The number of *Mad2l2*^{-/-} offspring is reduced by 50%. (B) Percentage of *Mad2l2*^{-/-} embryos at different stages and progeny. Most stages do not reach the expected number of *Mad2l2* deficient embryos. The red line indicates the expected percentage according to the Mendelian rules.

Newborns, pups and adult *Mad2l2* deficient animals showed no obvious abnormal behavior, but were infertile. Matings of *Mad2l2*^{-/-} female and male animals among themselves as well as with heterozygous or C57BL/6 wild-type animals resulted in no offspring. To exclude a mating behavioral phenotype, the female animals were checked for vaginal plugs and were positive.

Mad2l2^{-/-} embryos, newborns and adult animals were morphologically normal but smaller than their heterozygous or wild-type littermates. Embryos and animals of each stage and age were proportional reduced in size (Figure 16).

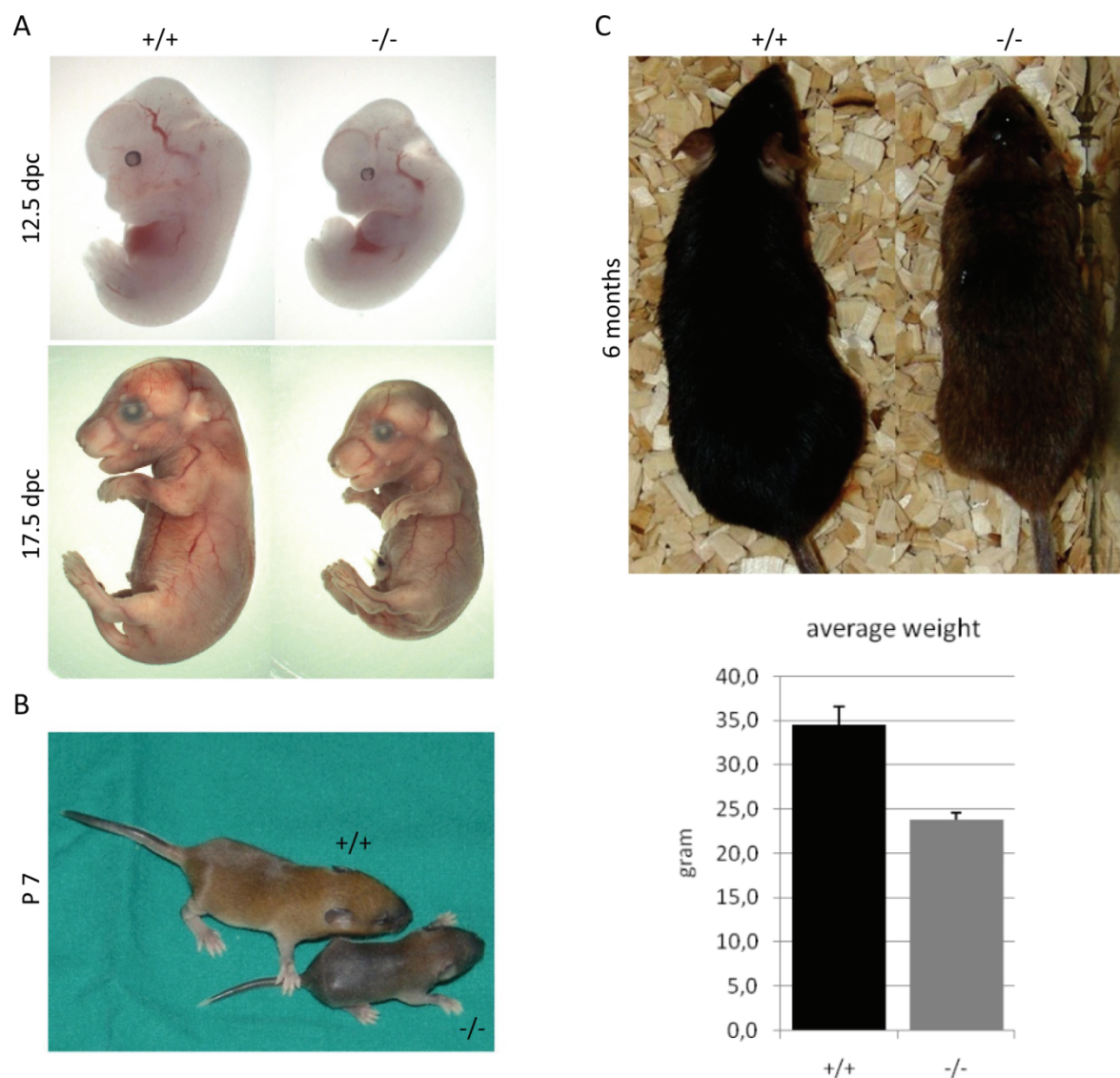


Figure 16. *Mad2l2* deficient mice are reduced in size and weight.

(A) Embryos lacking *Mad2l2* are smaller in comparison to their wild-type littermates. (B) Shortly after birth *Mad2l2*^{-/-} pups at P7 are reduced in size. (C) At six months of age the wild-type mice are still larger and approximately 1/3 heavier than their homozygous, transgenic littermates. Error bars indicate standard errors of the means.

During development and maturation *Mad212* deficient mice were not able to catch up with their wild-type littermates (Figure 17.). At six months of age they were still smaller and only two-thirds of the weight of a wild-type animal (Figure 16. C).

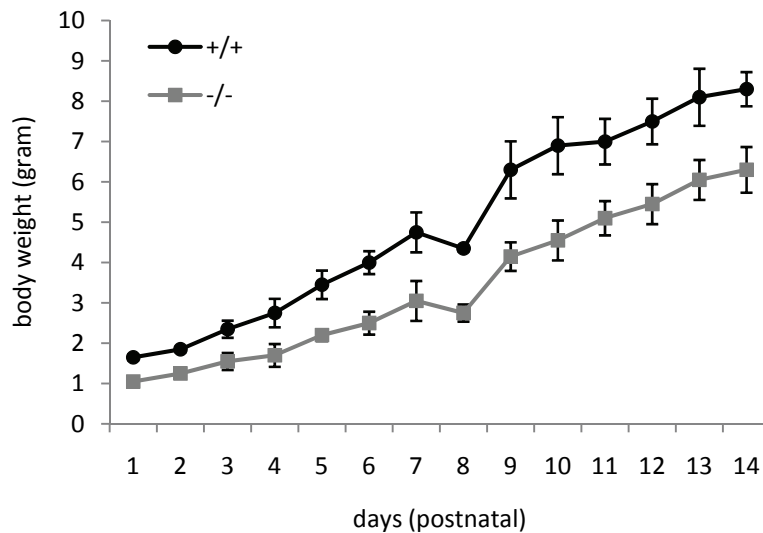


Figure 17. Growth curve of *Mad212*^{-/-} newborns and wild-type littermates.

The graph displays animals from a representative litter. Error bars indicate standard errors of the means.

***Mad212* targeted MEF's show decelerated proliferation**

Primary embryonic fibroblasts were isolated from 13.5 and 14.5 dpc embryos to study the consequences of *Mad212* deficiency under well-defined culture conditions. As the life span of primary cultured mouse embryonic fibroblasts is limited, and the mortality of *Mad212*^{-/-} embryos was above-average, the attempt to establish a MEF cell line with permanent growth features was undertaken. There are two major pathways to establish an immortalized MEF cell line, including transformation by overexpression of one or more oncogenes and serial passage of primary MEF's until they pass their growth-crisis (Aaronson and Todaro, 1968; Todaro and Green, 1963). In order to establish an immortalized *Mad212* deficient cell line a serial of passages was done but *Mad212*^{-/-} cells failed to grow after several passages and thinned out with each passage. In contrast, the wild-type cells could be passaged and presumably would have given rise to an immortalized cell line.

Due to these observations the plating efficiency as well as the growth rate of *Mad212*^{-/-} MEF's and their wild-type equivalents was monitored. The plating efficiency of *Mad212*^{-/-} MEF's did not significantly differ from their wild-type counterparts but the growth rate was substantially reduced (Figure 18. A & B).

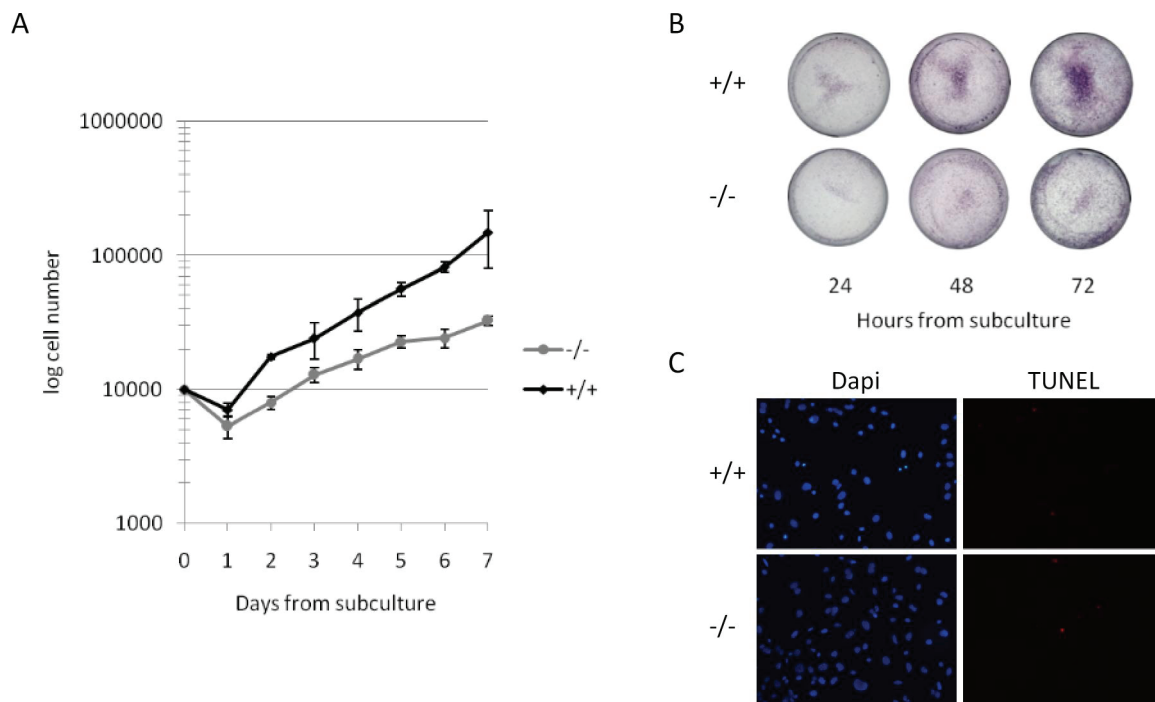


Figure 18. Influence of *Mad212* deficiency on plating efficiency and proliferation rate of MEF's.

(A) The cell number of wild-type and *Mad212*^{-/-} MEF's was monitored for seven days after subculture. The plating efficiency was only slightly different but the proliferation rate of wild-type cells was higher. Error bars indicate standard errors of the means. (B) Giemsa staining of wild-type and *Mad212* deficient MEF's. The population of *Mad212*^{-/-} cells seems to be almost constant between 48 and 72 hours of subculture. (C) TUNEL assay displayed no significant differences in the occurrence of apoptosis.

To address the question whether the *Mad212*^{-/-} MEF's had either a reduced growth rate or a higher ratio of mortality the occurrence of apoptosis was assessed. Observations of the cell cultures revealed no obvious apoptosis visible to the eye therefore a TUNEL assay was performed. The *Mad212* deficient cells showed no sign of elevated apoptosis, as there was no increase in TUNEL-positive nuclei compared to the wild-type control cells (Figure 18. C). This observation was further strengthened by FACS analysis. Apoptosis will ultimately lead to nuclear condensation followed by segmentation into apoptotic bodies. These apoptotic bodies appear in a FACS analysis in front of the G1 peak that represents all cells with a diploid DNA content (Darzynkiewicz et al., 1997). The FACS analysis showed no significant nuclear debris in front of the G1 peak in both wild-type and *Mad212* deficient cells (Figure 19. A).

***Mad212* deficient MEF's show an altered cell cycle phase distribution**

Due to the involvement of *Mad212* in cell cycle control by the regulation of the Cdh1-APC complex (Chen and Fang, 2001; Pflieger et al., 2001) as well as in DNA damage repair

(Lawrence, 2002; Okada et al., 2005) an effect of MEF's lacking Mad212 on cell cycle distribution could not be excluded. In addition, the previously described proliferation phenotype (Figure 18) suggested the possibility of alterations in the cell cycle. To address this question *Mad212*^{-/-} and wild-type MEF's were cultured until they reached 80-90% confluency before they were analyzed by flow cytometry.

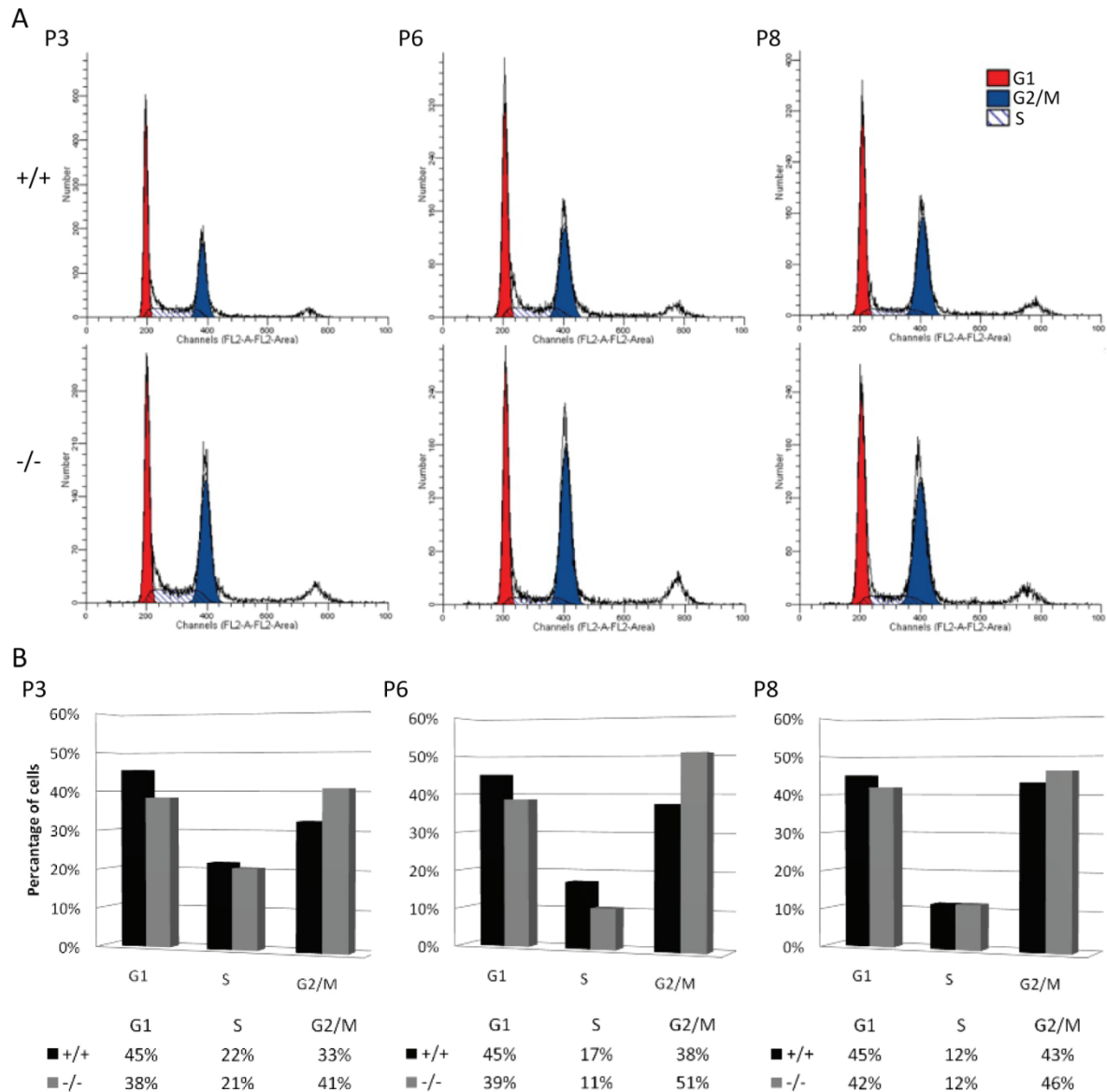


Figure 19. FACS analysis of *Mad212* deficient MEF's.

(A) Cell cycle distribution of wild-type and *Mad212* deficient MEF's at different passages. (B) The percentage of *Mad212*^{-/-} MEF's in the G1 phase is reduced whereas there are more *Mad212*^{-/-} cells in the G2/M phase throughout all the different passages. P = passage.

The early passages of primary MEF's (passage 3 and 6) displayed a significant alteration in the cell cycle phase distribution. The percentage of cells in the G1 phase was reduced in

the *Mad2l2* knockout situation compared to the wild-type cells whereas the number of *Mad2l2*^{-/-} cells in the G2/M phase was significantly increased (Figure 19. B). In one of the later passages (passage 8) the difference was not as obvious but still present. In addition there was a small population of wild-type and knockout cells that seemed to be octaploid (Figure 19. A).

Accumulation of γ -H2AX in *Mad2l2* deficient MEF's

The phosphorylation of histone H2AX (γ -H2AX) at Ser¹³⁹ is an early response to DNA double-strand breaks that occurs within minutes. These phosphorylated molecules are cytologically visible as foci (Paull et al., 2000; Rogakou et al., 1998). To investigate whether *Mad2l2* deficiency leads to an increase of double-strand breaks due to unrepaired lesions, immunofluorescent staining of γ -H2AX was performed. Under normal culture conditions the *Mad2l2* deficient MEF's displayed an elevated level of γ -H2AX foci in comparison to their wild-type counterparts (Figure 20. A & B). This elevated expression was confirmed by western blot analysis of whole cell extract lysates (Figure 20. C).

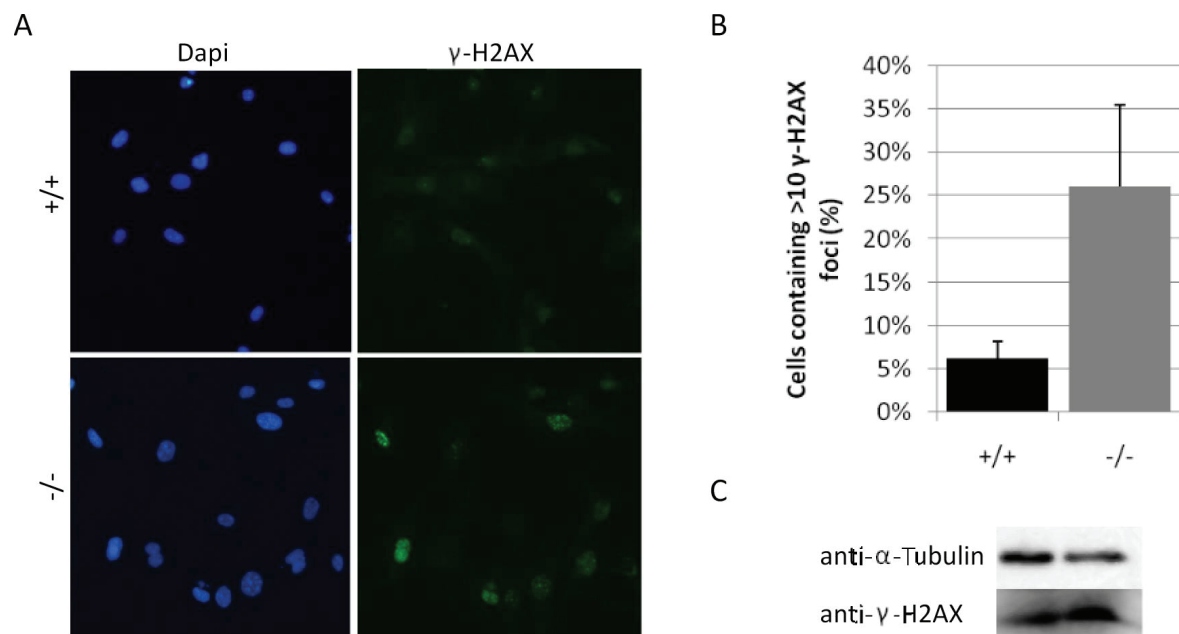


Figure 20. Elevation of γ -H2AX expression levels in *Mad2l2* deficient MEF's.

(A) Immunofluorescent staining of γ -H2AX revealed an elevated level in *Mad2l2*^{-/-} MEF's compared to wild-type cells. (B) Quantitation of cells containing >10 γ -H2AX foci. Error bars indicate standard errors of the means. (C) Western blot analysis displayed an increase of γ -H2AX in *Mad2l2*^{-/-} MEF's.

Pituitary gland displays impaired cell differentiation

Mad2l2 deficient mice displayed no obvious developmental and morphological defects in the anterior central nervous system as it was previously observed in mice lacking *Hesx1* (Dattani et al., 1998). Since intra-uterine lethality was observed among *Mad2l2*^{-/-} mice, the animals which were born probably display only a mild phenotype. To further investigate the molecular mechanism of the binding of Mad2l2 to Hesx1 and the developmental as well as cellular consequences of *Mad2l2* deficiency, the pituitary gland was used as a model system. Generally, the different anterior pituitary gland cell types appear from a common premordium in a precise spatial and temporal order (Japon et al., 1994; Simmons et al., 1990). *Hesx1* deficiency and misexpression results in phenotypes especially in the four ventral cell types (somatotropes, lactotropes, thyrotropes and gonadotropes; (Table 1.; Dasen et al., 2001).

An initial hematoxylin and eosin staining of a newborn *Mad2l2*^{-/-} animal revealed a morphologically intact pituitary gland. The pituitary consisted of an anterior lobe, an intermediate lobe and a posterior lobe sitting on top of the cartilage element of the sphenoid bone (Figure 21).

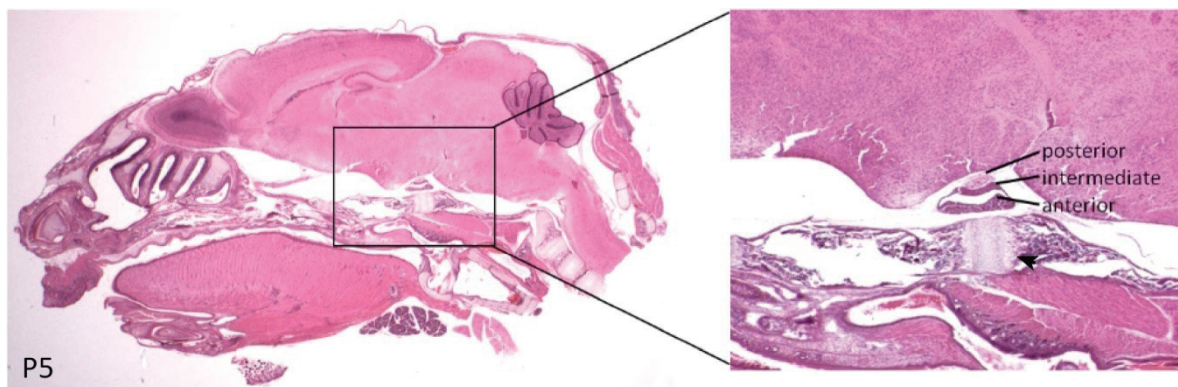


Figure 21. *Mad2l2* deficient mice display a morphologically normal pituitary.

H&E staining of P5 *Mad2l2*^{-/-} mouse head mid-sagittal section. Mice display a morphological normal pituitary gland consisting of a posterior, intermediate and anterior lobe sitting on the cartilage element of the sphenoid bone (arrow head).

To assess the specification of the different cell types of the anterior pituitary in the *Mad2l2* deficient mice, an immunohistochemical analysis was performed. Cell types were identified by their expression of the specific hormones. α GSU is a shared common subunit of the heterodimeric peptide hormones FSH, LH and TSH which can be detected in cells

becoming gonadotropes or thyrotropes respectively. Its expression can be detected as early as 11.5 dpc; ACTH is secreted by the corticotropes from 12.5 dpc on; TSH is secreted by the thyrotropes at around 14.5 dpc; GH is secreted from somatotropes and can be detected around 15.5 dpc; at the same stage PRL secretion starts from the lactotropes and FSH and LH are secreted by gonadotropes around 16.5 dpc and 17.5 dpc respectively.

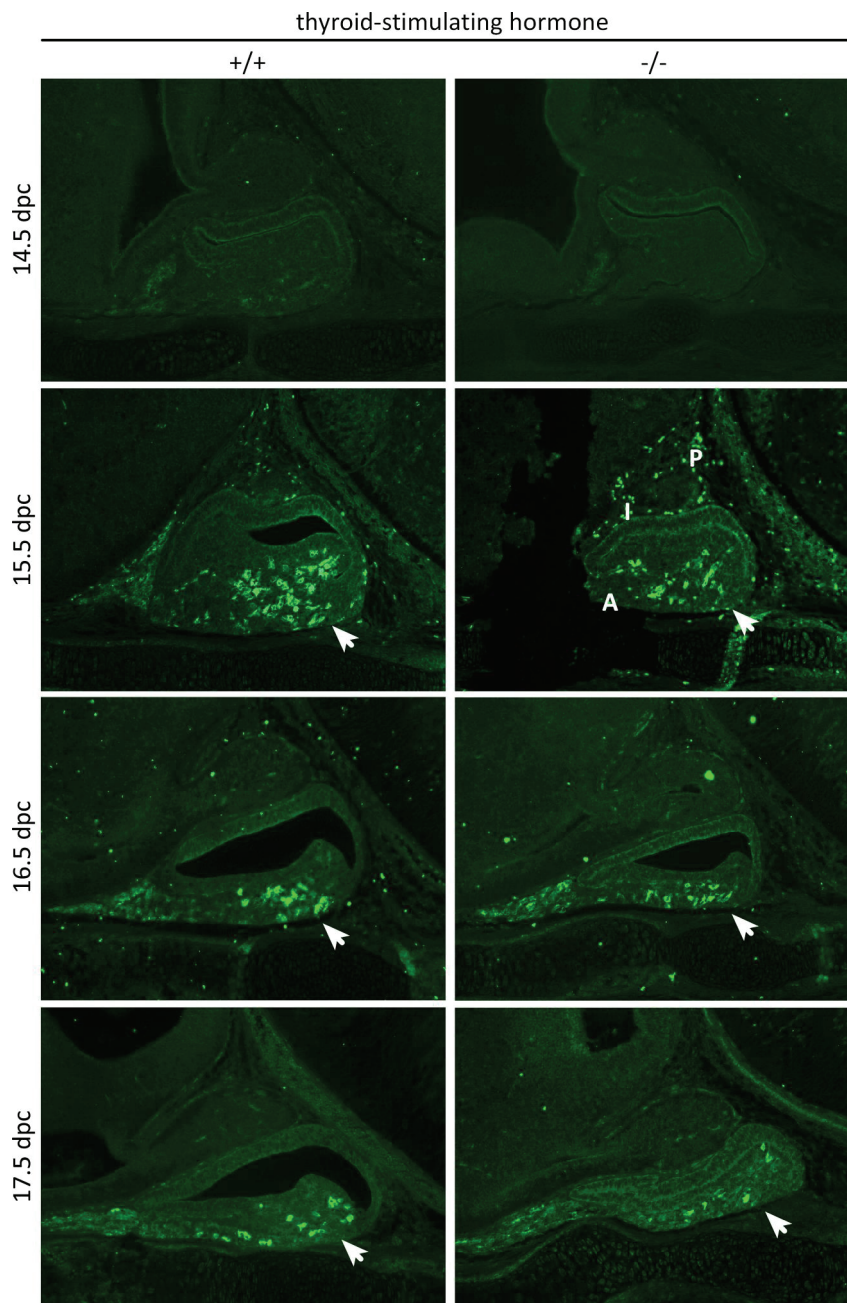


Figure 22. Expression of TSH in the developing pituitary gland.

Thyroid-stimulating hormone (TSH β) expression in the developing anterior pituitary gland displays no differences between wild-type and *Mad212* deficient embryos. The expression starts around 15.5 dpc. Arrow heads pointing at the TSH expressing cell population within the anterior lobe of the pituitary gland. P = posterior lobe, I = intermediate lobe and A = anterior lobe. Immunostaining outside the developing pituitary gland (Figure 22. & Figure 23. 15.5 dpc) is considered to be unspecific binding of the antibody.

The analysis was done with embryos from 12.5 dpc to 17.5 dpc because most of the cell types appear around these stages. Staining with α GSU, ACTH, TSH β , PRL and LH β specific antisera did not reveal any significant changes in the *Mad212*^{-/-} embryos compared to the

wild-type (data not shown and Figure 22.). There might be a minor delay in the expression of the respective hormones in the mutant embryos but so far this could not be specified.

The appearance of the somatotrophic cell lineage secreting GH was significantly delayed. In the wild-type embryos a lot of somatotropes populated the anterior pituitary gland already around 16.5 dpc whereas the *Mad2l2* deficient embryos displayed no GH secreting cells at this stage. At 17.5 dpc some somatotropes could be detected in the mutant embryos but the number was severely reduced (Figure 23.). In addition, one 17.5 dpc *Mad2l2* deficient embryo displayed an aberration of the cartilage element usually underlying the developing anterior pituitary gland (asterisk, Figure 23.).

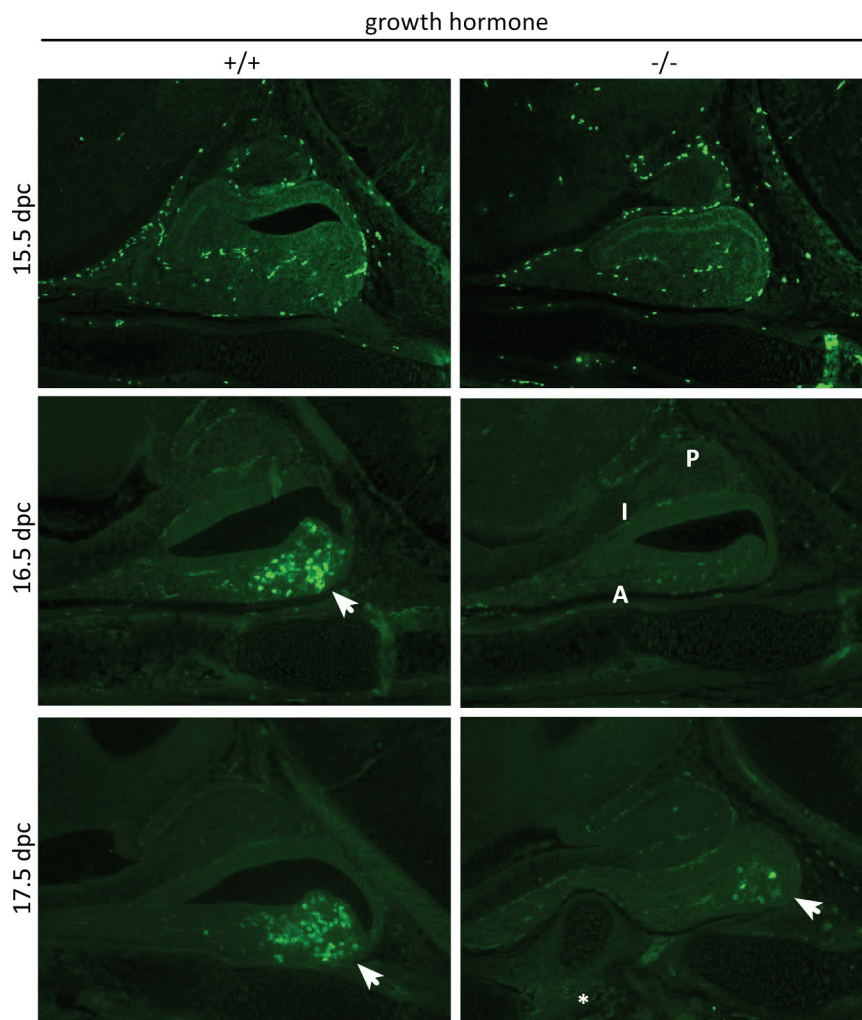


Figure 23. GH expression in the developing anterior pituitary gland.

Growth hormone (GH) expression in the developing anterior pituitary gland shows a significant delay in *Mad2l2*^{-/-} embryos. The expression starts in wild-type mice around 16.5 dpc whereas in the *Mad2l2*^{-/-} mice only a few cells appear at 17.5 dpc. Note the disturbed cartilage element in the mutant embryo at 17.5 dpc (asterisk). Arrow heads pointing at the GH expressing cells.

Altogether, these results present a cell type specific anterior pituitary gland phenotype in *Mad2l2* deficient embryos. The somatotrophic cell lineage was significantly delayed or reduced, whereas all other pituitary gland cell lineages appeared to develop normal.

DISCUSSION

Understanding the functional significance of the coordinate expression and interaction of homeobox transcription factors remains a critical question in developmental biology. *Hesx1* is an important transcriptional repressor during forebrain and pituitary gland development (Dattani et al., 1998; Martinez-Barbera et al., 2000). Mutations in the human *Hesx1* gene are linked to the congenital disorder septo optical dysplasia, isolated growth hormone deficiency and combined pituitary hormone deficiency. However, the overall frequency of *Hesx1* mutations in patients displaying SOD, IGHD or CPHD is less than 5% (reviewed in Reynaud et al., 2004). This observation suggests that mutations in other known or unknown genes may participate in this complex disorder. Some of these genes are possibly involved in regulation and fine-tuning of the activity of transcription factors involved in normal development of the forebrain and pituitary.

The present study has extended the regulative network in which *Hesx1* is embedded and identified so far unknown mechanisms of *Hesx1* regulation, involving binding to Mad2I2 and ubiquitination through the E3 ligase Cdh1-APC.

Hesx1 regulation through Mad2I2 and Cdh1-APC

Mad2I2 prevents Hesx1 from DNA binding

Hesx1 and Mad2I2 are co-expressed and interact

In a previous study, Mad2I2 was isolated in a yeast two-hybrid screen as a potential binding partner of *Hesx1* (Pilarski, 2004). The present work has verified this interaction using a yeast two-hybrid assay, by GST pull-down experiments and co-immunoprecipitation (Figure 5. A-C). Interestingly, there was potent interaction detected in the yeast two-hybrid system and the co-immunoprecipitation experiments, but only very weak binding in the GST pull-down. This discrepancy might result from differences of the assay approaches. The yeast two-hybrid system and the co-immunoprecipitations have in common that they detect interactions in an *in vivo* environment, whereas the GST pull-down, even though the transcription/translation process takes place in a reticulocyte lysate, is an *in vitro* assay. However, direct binding was detected in the peptide array. These results eventually suggest that the binding of Mad2I2 to *Hesx1* is assisted by co-factors which strengthen the interaction.

RNA expression profiling revealed that *Mad2l2* is, not abundantly but ubiquitously, expressed in the mouse embryo as well as in adult tissues (Figure 7. A & C). These results may account for the non-conclusive *in situ*-hybridization results but are similar to the results found in *Homo sapiens* and *Xenopus laevis* (Chan et al., 2001; van den Hurk et al., 2004; Ying and Wold, 2003). This expression pattern is in contrast with the restricted and dynamic expression of *Hesx1* (Figure 6.; Hermes et al., 1996; Thomas and Beddington, 1996).

In context of the finding that both *Hesx1* and *Mad2l2* are co-localized in the nucleus (Figure 7. B), these results make a biological significant interaction possible.

Mad2l2 binds the N-terminal arm of the homeodomain

Mapping of the *Mad2l2* binding domain within *Hesx1* revealed a binding to a highly conserved domain at the N-terminal arm of *Hesx1* homeodomain (Figure 8.). This conservation beyond the homeodomain indicates a critical role within the protein. Interestingly, the N-terminal arm of the homeodomain contributes substantially to both the DNA binding ability and to sequence recognition by contacting the minor groove of the DNA helix (Figure 24.; Kissinger et al., 1990; Kornberg, 1993; Wilson et al., 1995).

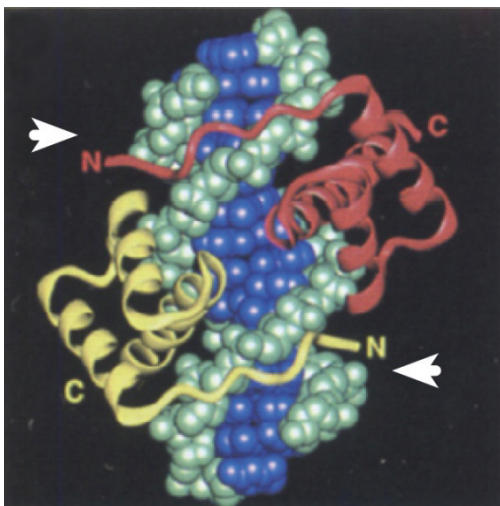


Figure 24. The N-terminal arm of paired homeodomains is involved in DNA binding.

Structure of paired homeodomains that are binding as homodimers to a palindromic PIII site. The N-terminal arm of the paired homeodomain binds to the minor groove of the DNA helix (arrow heads). The DNA is displayed in a space-filling model with phosphoribose backbone in green and bases in blue. The homeodomains are indicated as ribbons (red and yellow) representing the polypeptide backbone (Wilson et al., 1995).

Furthermore, binding of *Mad2l2* prevents *Hesx1* from binding a palindromic PIII site (Figure 9.). This finding suggests that *Mad2l2* is involved in the regulation of *Hesx1* activity. Binding of *Mad2l2* might prevent *Hesx1* from binding its target promoters.

In summary, these results indicate a role of *Mad2l2* in the regulation of *Hesx1* on the protein level by interfering with its ability to bind to target DNA. This inhibitory

mechanism might be critical during pituitary gland cell differentiation when Hesx1 levels need to be precisely downregulated in order to allow a normal anterior lobe development (Dasen et al., 2001; Sornson et al., 1996). Downregulation of Hesx1 might therefore occur at three levels: (1) the transcriptional level and the protein level, which can be subdivided into (2) the functional control and (3) the control of protein half-life (discussed below). Mad2l2 binding to Hesx1 might be involved in regulating Hesx1 at the functional level.

The Cdh1-APC complex controls Hesx1 stability

Cdh1 and Hesx1 are co-expressed and interact

Since Mad2l2 is an inhibitor of the Cdh1-APC complex (Chen and Fang, 2001; Pflieger et al., 2001), the observed Mad2l2-Hesx1 interaction led to the idea that Hesx1 might be a substrate of Cdh1. Co-immunoprecipitation experiments confirmed the hypothesis that Cdh1 binds to Hesx1 (Figure 5. D). Furthermore, *Cdh1* displays an almost ubiquitous expression pattern in *Mus musculus*, *Gallus gallus* and *Xenopus laevis* (Gieffers et al., 1999; Wan and Kirschner, 2001; Zhou et al., 2002). Together with the data from the RT-PCR analysis, a spatially and temporally overlapping expression of *Cdh1* and *Hesx1* is very likely. In addition, Hesx1 presents two motifs in its amino acid sequence that are similar to Cdh1 recognition motifs, the D-box and the KEN-box. These motifs are located within the homeodomain, and Cdh1 has been shown to bind within this region (Figure 10. B).

This observation also reduces the possibility of unspecific binding. Both the Hesx1 co-repressor TLE1 and Cdh1 contain WD40 domains that have been shown to be responsible for the interaction with the Hesx1 eh1 domain and target substrates, respectively (Dasen et al., 2001; Kraft et al., 2005). The co-immunoprecipitation of Cdh1 with a Hesx1 deletion mutant lacking the eh1 domain diminishes the eventuality that Cdh1 binds unspecific to the eh1 domain (Figure 10. B). Nevertheless, co-immunoprecipitation experiments with Hesx1 bearing mutations in the recognition motifs should strengthen this result.

Hesx1 is ubiquitinated in vivo

The finding that Hesx1 is a target for ubiquitination *in vivo* together with the observed interaction with Cdh1 suggests that Hesx1 is a target of the E3 ligase Cdh1-APC complex (Figure 10.). The observation that Mad2l2 co-expression diminishes this polyubiquitination supports this idea. Mad2l2 might inhibit the Cdh1-APC complex, and

the subsequent ubiquitination or binding of Mad212 to Hesx1 might block its accessibility. The finding that co-expression of Cdh1 did not increase the polyubiquitination pattern might be due to the fact that the overall level of ubiquitination in the presence of the proteasome inhibitor MG132 is already relatively high. Cdh1 knockdown or *in vitro* experiments with purified APC complexes should be performed in the future to confirm Cdh1-APC as the E3 ubiquitin ligase involved in Hesx1 ubiquitination.

Taken together, these experiments show that Hesx1 is targeted for degradation via the ubiquitin pathway. Since downregulation on the transcriptional level can only ensure an indirect control of Hesx1 activity, these findings suggests a precise tuning of Hesx1 at the protein level. This regulation on the protein level might be crucial during anterior pituitary gland development. At the border between proliferation and differentiation a removal of present Hesx1 protein might promote the switch from one state into the other (Figure 25.). Evidence for such a function for Hesx1 comes from ES cells where Hesx1-RNA levels are downregulated upon differentiation (Thomas et al., 1995). Furthermore, a similar role of Cdh1-APC was found to be involved in terminal lens differentiation where the complex is responsible for the coordination of proliferation, cell cycle arrest and differentiation (Wu et al., 2007).

Therefore, Cdh1-APC may have a similar function in pituitary gland development by regulating the exit of the cell cycle and at the same time coordinating the onset of differentiation by targeting most probably among other proteins, Hesx1.

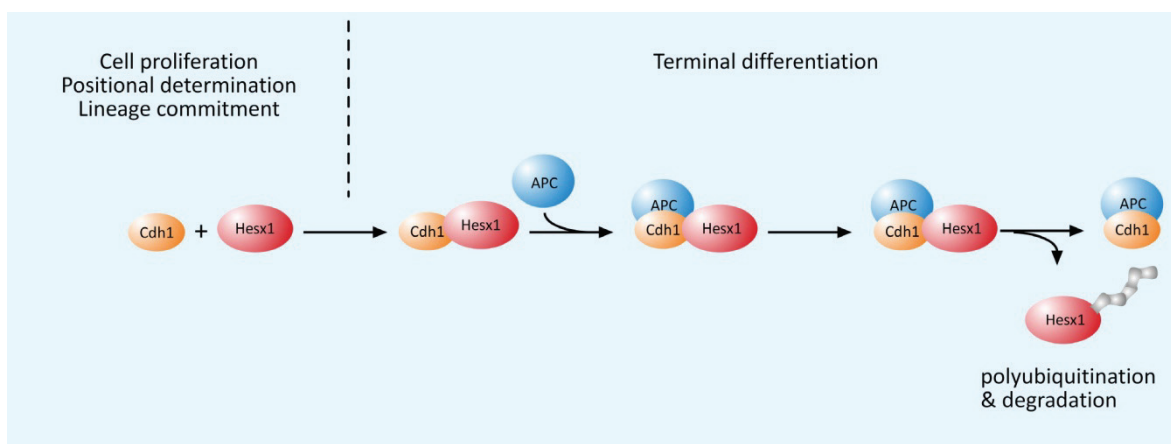


Figure 25. Possible model of Hesx1 ubiquitination during anterior pituitary gland development.

Targeting of Hesx1 for ubiquitination and subsequent degradation might allow terminal differentiation of the specific cell lineages within the anterior pituitary lobe.

At present there is no evidence indicating that Mad2l2 is involved in substrate recognition or binding, suggesting that Hesx1 ubiquitination and interaction with Mad2l2 might be two independent processes. However, Mad2l2 was found to function as an adapter between JNK MAP kinases and the transcription factor Elk-1 (Zhang et al., 2007). Therefore, a similar role could be conceivable during the ubiquitination process of Hesx1, especially if one considers the low *in vitro* binding affinity of Hesx1 and Mad2l2. To address this question, ubiquitination experiments of Hesx1 in *Mad2l2* deficient MEF's might be elucidative.

Phenotypical analysis of *Mad2l2* deficiency

In order to gain further insight into the function of Mad2l2 during mouse development as a subunit of polymerase ζ and as an inhibitor of the Cdh1-APC complex, *Mad2l2* deficient mice were generated. *Mad2l2* heterozygous mice were viable, morphologically normal and fertile. In contrast, homozygous *Mad2l2* deficient mice displayed a non-mendelian distribution with the occurrence of intra-uterine lethality. *Mad2l2*^{-/-} embryos and adult mice were smaller in size and infertile. MEF's generated from *Mad2l2* deficient embryos showed a reduced proliferation rate, an accumulation of cells in the G2/M phase and an elevated level of γ -H2AX. Moreover, the developing anterior pituitary gland in *Mad2l2* deficient mice displayed a significant delay in the differentiation of somatotropes.

Infertility, reduced viability and size in *Mad2l2* deficient embryos

Offspring of *Mad2l2*^{+/-} mice intercrosses did not correspond to the expected Mendelian frequency. Only 13% of the offspring were homozygous *Mad2l2* mutants, indicating intra-uterine lethality (Figure 15.). The exact point in time of lethality could not be determined so far. Most of the examined stages did not agree with the expected number of *Mad2l2* deficient animals according to Mendelian rules.

Mad2l2 deficient embryos and mice could be distinguished readily by their size compared to wild-type and heterozygous littermates (Figure 16.). Besides proportional growth retardation, the embryos seemed not to be significantly retarded in development, which was confirmed by later molecular analysis of the anterior lobe of the pituitary. Furthermore, neither embryos nor adult mice displayed any morphological anterior forebrain or eye abnormalities as it was found in Hesx1 deficient mice (Dattani et al.,

1998; Martinez-Barbera et al., 2000), suggesting that an interaction of Mad212 and Hesx1 is not essential at these early stages of development.

Both processes, TLS by polymerase ζ and ubiquitination mediated by the Cdh1-APC complex, involve the regulatory function of Mad212 and are of comprehensive relevance during mouse embryonic development (Bemark et al., 2000; Esposito et al., 2000; Wirth et al., 2004; Wittschieben et al., 2000).

On the one hand, the observed phenotype could be linked to Mad212 and its role in DNA damage repair. The rapidly dividing cells of the developing embryo might progressively accumulate DNA damage caused by e.g. endogenous metabolic byproducts. These lesions would be normally efficiently bypassed by polymerase ζ . Since Mad212 increases the catalytic activity of Rev3 by up to 20 to 30 folds (Nelson et al., 1996), cells lacking Mad212 might not be able to sufficiently repair lesions. As a consequence, cells of the embryo that accumulated too many unrepaired lesions and subsequent double-strand breaks might undergo apoptosis (reviewed in Borges et al., 2008).

On the other hand, this phenotype could be caused by a failure in cell cycle progression due to a diminished Cdh1-APC regulation, even though the mechanisms which induce Mad212 mediated inhibition are not yet understood. The timing of the exit from mitosis or entry into the S phase might be disturbed, leading to cell cycle arrest or apoptosis.

Nevertheless, some embryos survived and gave rise to viable *Mad212*^{-/-} animals. The observed variability in survival rates could be explained with the fact that Mad212 acts in both processes as a regulatory subunit. Rev3 is the catalytical subunit of polymerase ζ and able to bypass lesions even in the absence of Mad212 (Nelson et al., 1996), and the Cdh1-APC complex is regulated by a variety of mechanisms which might compensate the lack of Mad212 (reviewed in Peters, 2006). Therefore, some embryos survive development without accumulating too much DNA damage and deregulation of the cell cycle. However, these embryos and mice might lose cells due to apoptosis resulting in the observed proportional small size of embryos and adult mice.

Interestingly, *Mad212* deficient mice exhibited infertility. This infertility was shown to be independent of gender. Since *Mad212* is highly expressed in *Mus musculus* (Figure 7. C), human (Nelson et al., 1999) and *Xenopus laevis* (van den Hurk et al., 2004) testes, and to

a lesser extent in ovaries, this phenotype is consistent with the expression pattern of *Mad2l2*. The high expression could implicate two possible functions of Mad2l2 during gametogenesis: (1) Mad2l2 might be involved in regulating meiosis by inhibiting Cdh1-APC (Marangos et al., 2007; Reis et al., 2007) or (2) the elevated level of *Mad2l2* in testes accounts for the increased requirement of polymerase ζ to maintain the genomic stability in the constantly proliferating gametes. The loss of Mad2l2 suggests either an increased rate of apoptosis in the gonads due to genomic instability or a meiotic phenotype which needs to be further investigated.

In summary, these observations indicate that Mad2l2 is an important factor for normal embryonic development. The fact that Mad2l2 is involved in the regulation of two fundamental processes during development, namely cell cycle control and TLS to maintain genomic stability, may account for the observed more general phenotypes. The high *Mad2l2* expression levels in testes and ovaries are consistent with the infertility phenotype in *Mad2l2*^{-/-} mice, and suggest a critical role of Mad2l2 in gametogenesis. Furthermore, an interaction of Hesx1 and Mad2l2 during anterior forebrain development seems not to be essential, since surviving embryos display no obvious malformations of the anterior forebrain structures or behavioral phenotypes.

Proliferation and DNA damage in *Mad2l2* deficient MEF's

MEF's isolated from *Mad2l2* deficient embryos had a reduced proliferation rate and failed to give rise to an immortalized proliferating cell line. Early passages showed neither a significant increase in apoptosis nor a significant difference in the plating efficiency. But MEF's lacking *Mad2l2* had an elevated number of cells in the G2/M phase and displayed an accumulation of γ -H2AX foci.

These observations suggest that Mad2l2 is a critical component in the TLS pathway. MEF's lacking Mad2l2 accumulate DNA lesions which are not repaired due to the diminished activity of Rev3. These lesions subsequently give rise to DNA double-strand breaks, as indicated by the elevated levels of γ -H2AX foci (Rogakou et al., 1998). The accumulation of DNA double-strand breaks could explain the observed increased number of cells present in the G2/M phase. The approximate threshold for activating the G2/M DNA damage checkpoint has been shown to be around 10-20 double-strand breaks per nucleus (Deckbar et al., 2007; reviewed in Lobrich and Jeggo, 2007). *Mad2l2* deficient

MEF's may have an activated G2/M checkpoint due to an increased level of DNA double-strand breaks which would account for the low proliferation rate. Furthermore, this could explain why these cells did not give rise to a proliferating cell line. The DNA damage that is accumulated in these cells over time might induce cellular senescence with an arrest in G2/M. The MEF's cease proliferation and may potentially become resistant to apoptosis, both characteristics are probably mediated among others by the tumor suppressor protein p53 (reviewed in Campisi and d'Adda di Fagagna, 2007). The mechanism by which senescent cells escape apoptosis is not completely clear, but this characteristic could explain why the *Mad212*^{-/-} MEF's did not display an increase in apoptotic cells in comparison to their wild-type counterparts. Interestingly, these results are consistent with observation from *Rev3L* deficient MEF's. Cells lacking *Rev3L* divided poorly and entered a quiescent state with apoptosis occurring over weeks to months (Wittschieben et al., 2006). Moreover, *Rev3L* deficient MEF's in a *p53* null background proliferate, even though slower than wild-type cells, and display an increased frequency of cells in the G2/M phase together with an elevated sensitivity to genotoxic agents (Wittschieben et al., 2006; Zander and Bemark, 2004).

Results from other cell lines and experiments targeting *Mad212* differ from the observation in *Mad212* null MEF's. In chicken DT40 cells, the disruption of *Mad212* leads to proliferating cells. These cells showed retarded growth kinetics, an higher apoptosis rate and an increased sensitivity towards genotoxic treatments (Okada et al., 2005). Interestingly, the chicken DT40 cells do not express p53 (Takao et al., 1999) a certainty which might explain the ability to proliferate and the increased apoptotic rate. Knockdown experiments in several cell lines revealed similar results (Cheung et al., 2006; Iwai et al., 2007; McNally et al., 2008) but these cells may have residual levels of *Mad212* left. Low levels of *Mad212* may be enough to repair most lesions and therefore preventing the cells from going into senescence which subsequently leads to a less pronounced phenotype.

In summary, these results provide evidence for a vital role of *Mad212* in mouse embryonic fibroblasts. Cells lacking *Mad212* may induce the G2/M DNA damage checkpoint due to an accumulation of unrepaired DNA lesions and subsequent double-strand breaks. Finally, cells could be driven into senescence which would explain the observed phenotype

(Figure 26.). Further analysis using senescence markers, such as p16 or senescence-associated β -galactosidase (reviewed in Campisi and d'Adda di Fagagna, 2007) should provide evidence for this hypothesis. In addition, transfection of Mad212 to rescue the MEF phenotype could provide additional information to dissect the function of Mad212 in vivo.

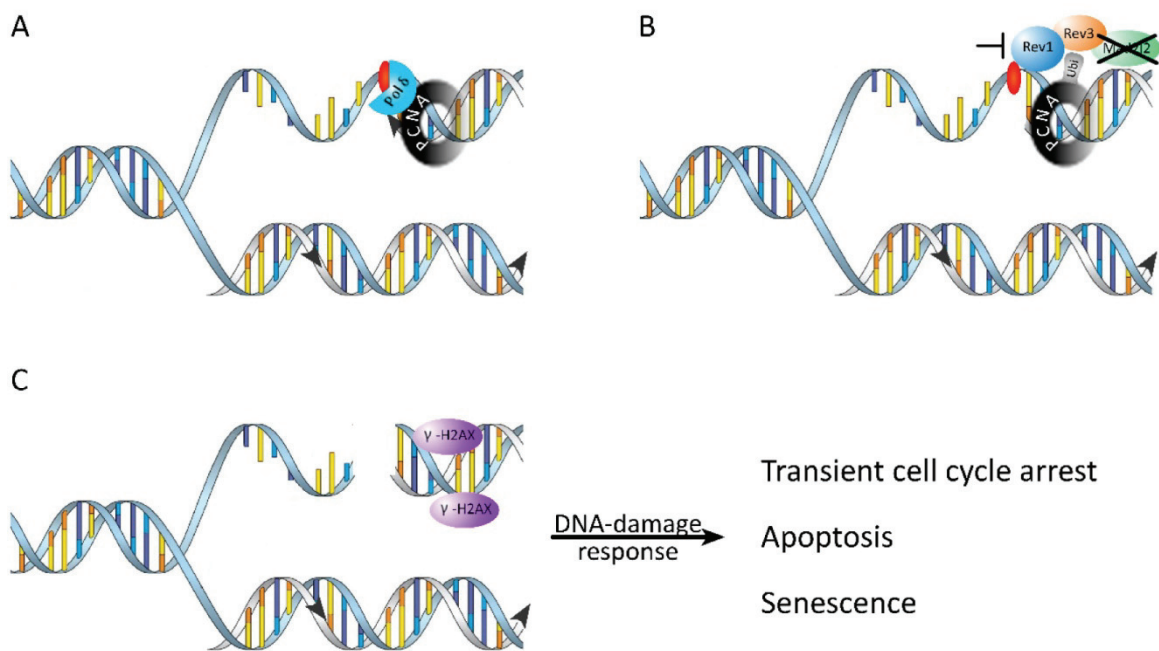


Figure 26. DNA lesion bypass by polymerase ζ might be disturbed in *Mad212*^{-/-} mice.

(A) DNA replication polymerase δ is unable to bypass the non-coding lesion (red) and is stalled. (B) The stalled replication fork induces the mono-ubiquitination (Ubi; grey) of PCNA. Mono-ubiquitination of PCNA causes the “polymerase switch” from polymerase δ to TLS polymerases. Lack of Mad212 might reduce the bypass efficiency of Rev3 and result in unrepaired lesions (C) Unrepaired lesions subsequently give rise to double-strand breaks which induce H2AX phosphorylation (γ -H2AX), followed by transient cell cycle arrest, apoptosis or senescence.

Furthermore, a cell cycle effect of *Mad212* deficiency in MEF’s cannot be excluded. The observed accumulation of cells in the G2/M phase might indicate a perturbation of the Cdh1-APC regulation at the exit of mitosis. Cells might not be able to finish mitosis and are blocked within the M phase.

***Mad212* deficiency impairs pituitary cell lineage differentiation**

Since Mad212 binding of Hesx1 showed not to be substantial for morphologically normal anterior forebrain development, the developing anterior pituitary gland provided an

excellent model system to monitor any *Hesx1* dependent alteration. *Mad2l2* deficient embryos displayed no alteration in the differentiation of corticotropes, thyrotropes, lactotropes and gonadotropes as indicated by the expression of α GSU, ACTH, TSH β , PRL and LH β . Strikingly, the somatotrophic cell lineage identified by the expression of GH was almost absent in all investigated stages so far (Figure 23.).

Interestingly, *Prop-1* deficiency leads to a prolonged expression of *Hesx1* and a hypoplasia of all *Pit-1* dependent cell types, including thyrotropes, somatotropes and gonadotropes (Nasonkin et al., 2004; Sornson et al., 1996). A prolonged expression of *Hesx1* together and without *TLE1* confirmed that these lineages are dependent among other transcription factors on the downregulation of *Hesx1* (Dasen et al., 2001). Moreover, there is a human mutation in *Hesx1* that impairs the interaction with the co-repressor TLE1 which was shown to reduce partially the repressor function of *Hesx1*. This patient displayed GH deficiency and subsequently developed gonadotropin, ACTH and TSH deficiencies (Carvalho et al., 2003). Furthermore, loss-of-function or gain-of-function mutations in the homozygotic or heterozygotic state in humans involve, among other phenotypes, a variable degree of GH deficiency (reviewed in Dattani, 2004, 2005). These findings suggest, that the somatotrophic cell lineage is most sensitive to perturbances of *Hesx1* activity and this could explain why only the somatotrophic cell lineage is affected in *Mad2l2* deficient mice.

These observations, together with the finding that *Mad2l2* deficient mice display a delay in the differentiation of somatotropes, suggest that *Mad2l2* binding of *Hesx1* is of biological significance and might be necessary to negatively regulate its activity at the onset of *Pit-1* dependent cell lineage differentiation. Whether this effect is due to the interference of *Mad2l2* on *Hesx1* DNA binding capacity or due to a disturbed degradation via the Cdh1-APC complex needs to be determined. Therefore, prolonged *Hesx1* activity may be the reason for a delay in the somatotrophic cell lineage differentiation due to a retarded *Pit-1* activation through *Prop-1* (Figure 27.; Dasen et al., 2001).

A complete absence of the somatotropes in *Mad2l2* deficient mice is unlikely because the postnatal growth rate (despite of their smaller stature) is only mildly affected. Analysis of later stages, expression of transcription factors like *Pit-1* and down-stream targets like IGF-1 levels in the blood, should clarify this. In addition, future analyses need to be done

in order to monitor the presence of all cell lineages of the pituitary gland and to determine whether there is a loss during postnatal development as described in human patients (reviewed in Dattani, 2004, 2005). The loss of e.g. gonadotropes could be an additional reason for the observed infertility phenotype.

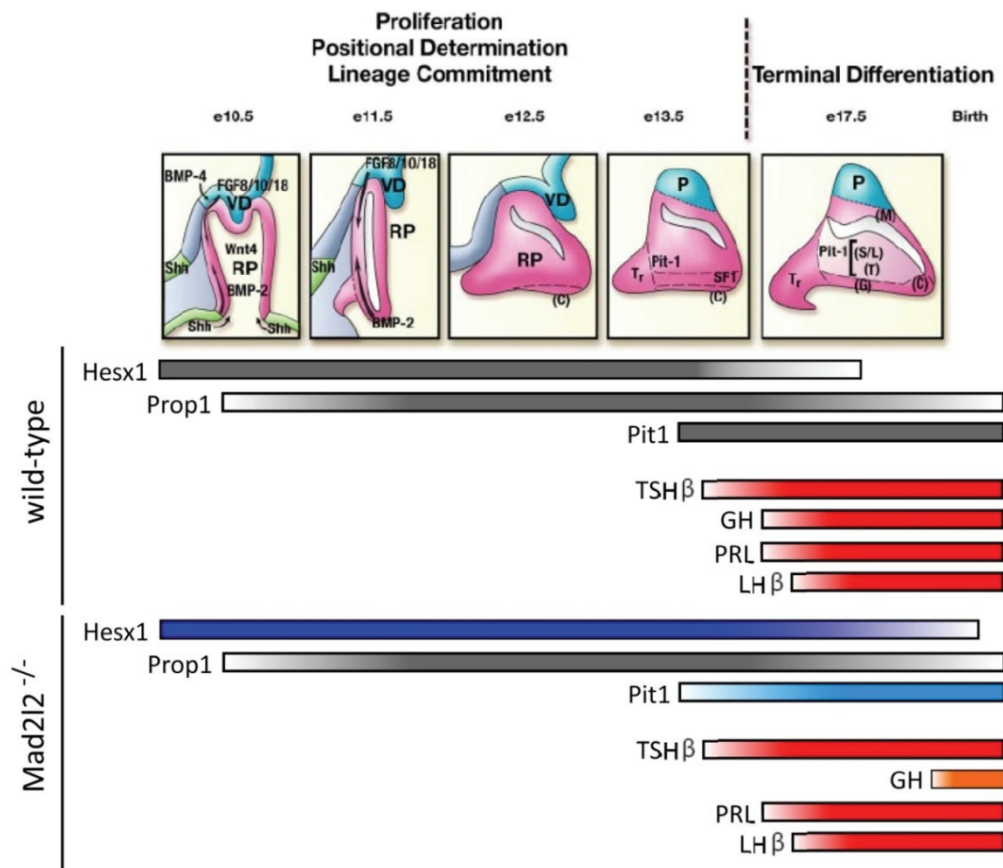


Figure 27. Delayed somatotrope differentiation in *Mad2l2* deficient mice.

A possible prolonged Hesx1 presence and activity (blue bar) in *Mad2l2* deficient mice may be the reason for a delay in somatotrophic lineage (GH; orange bar) differentiation due to a retarded *Pit-1* (light blue bar) activation through Prop-1 (adapted from Zhu et al., 2007).

SUMMARY AND CONCLUSIONS

Hesx1 is a *paired*-like homeodomain transcription factor, which is required for normal forebrain and pituitary gland formation. Its dynamic expression pattern especially during anterior pituitary gland development has been shown to be crucial for normal development. *Hesx1* deficient mice display variable degrees of forebrain and pituitary gland defects. A comparable phenotype in humans is septo optical dysplasia (SOD) and humans harboring mutations in *HESX1* were observed to display some form of SOD.

In a previous study, Mad2l2 was identified as a so far unknown binding partner of Hesx1 (Pilarski, 2004). Mad2l2 has been shown to be involved in the regulation of the cell cycle progression and DNA damage repair, probably coordinating both events. The observed interaction raised the question whether broader functionality of Mad2l2 towards transcriptional regulation could be found. Furthermore, the function of Mad2l2 in inhibiting the E3 ligase Cdh1-APC-complex led to the question if Hesx1 might be targeted for ubiquitination by this complex. Both processes might be involved in the regulation of Hesx1 at the protein level.

In this study the interaction of Mad2l2 with Hesx1 was confirmed in several independent experiments. The binding of Mad2l2 to Hesx1 was shown to take place at the N-terminal region of the homeodomain and resulted in a diminished ability of Hesx1 to bind target DNA. Furthermore, a binding of Cdh1 to Hesx1 was found and Hesx1 could be identified as a target of the Cdh1-APC complex. Hesx1 was found to be polyubiquitinated and subsequently degraded via the 26S proteasome.

To study the consequence of Mad2l2 inactivation in mice, knockout animals were produced. These animals displayed a variable intra-uterine lethality, growth retardations and infertility. Mouse embryonic fibroblasts generated from these mice display a DNA damage phenotype confirming a crucial role of Mad2l2 as a subunit of polymerase ζ and translesion synthesis. Taken together, Mad2l2 showed to be a crucial factor during embryonic development.

Furthermore, Mad2l2 deficient mice displayed a delay in the differentiation of somatotropes within the developing anterior pituitary gland. Hesx1 activity during anterior pituitary development has been shown to be involved in the initial organ

commitment and to keep cells in a proliferative state. Differentiation has been shown to require Hesx1 to be downregulated. This study provides evidence that besides transcriptional control which is a more indirect process, Hesx1 may also be regulated on the protein level. Hesx1 protein activity and levels within the differentiating cells may be negatively regulated by Mad2l2 by interfering with the ability of Hesx1 to bind to target DNA and by degradation mediated through ubiquitination by the E3 ubiquitin ligase Cdh1-APC complex.

Eventually, the present study has extended the regulative network in which Hesx1 is embedded and identified so far unknown mechanisms of Hesx1 regulation at the protein level.

MATERIAL AND METHODS

Isolation, analysis and manipulation of nucleic acids

Total RNA isolation from eukaryotic cells or mouse embryos

Total RNA from cultured eukaryotic cells or mouse embryonic tissues was isolated using the RNeasy® Mini Kit (QIAGEN), as described by the manufacturer.

Genomic DNA extraction from mammalian cells or mouse tissues

In 10 cm dishes cultured mammalian cells were washed with PBS twice and trypsinized in 2 ml Trypsin (0.05% Trypsin/EDTA; Gibco BRL®). The Trypsin digestion was stopped by adding 8 ml of culture medium and the cells were transferred into a 15 ml Falcon™ tube. Cells were collected by centrifugation at 210 g (Heraeus Megafuge 1.0 - 1000rpm) for five minutes. The cell pellet was washed with PBS twice and resuspended in 500 µl DNA lysis buffer (100 mM Tris-Cl, pH 8.0, 5 mM EDTA, 0.2% SDS, 200 mM NaCl) containing freshly added 25 µl of 100 µg/ml Proteinase K. The cells were incubated at 55°C shaking for 6 hours. Afterwards, the lysis product was centrifuged at 13000 rpm for five minutes. 450 µl of the supernatant was transferred into a new 1.5 ml tube. The DNA was now precipitated by the addition of 350 µl of isopropanol and subsequent vigorous shaking. The DNA was pelleted by centrifugation at 13000 rpm for five minutes, washed with 70% ethanol and air dried. DNA was dissolved in 200-300 µl TE buffer (10 mM Tris-Cl, pH 7.5, 1 mM EDTA) shaking at 37°C for 30 minutes.

Mouse tissues were washed with PBS once and incubated in 500 µl DNA lysis buffer at 55°C o/n. The following treatments were the same as described above for mammalian cells.

Plasmid DNA isolation from *E. coli*

To isolate plasmid DNA from *E. coli*, the QIAprep® Spin Miniprep Kit (QIAGEN) was used to isolate up to 20 µg from a 3 to 5 ml o/n culture and the QIAfilter™ Plasmid Maxi Kit (QIAGEN) was used to isolate up to 500 µg, from a 100 to 250 ml o/n culture. Both systems are based on alkaline lysis of bacterial cells (Birnboim and Doly, 1979) followed by an absorption of DNA onto silica or an anion-exchange resin, respectively. The procedure was done according to the instructions of the manufacturer. The plasmid DNA was eluted or re-dissolved using dH₂O.

P1-derived artificial chromosome (PAC) isolation from *E. coli*

The following protocol was used in order to isolate large PAC's from *E.coli*. Buffers P1, P2, N3 and TE were used from the QIAprep® Miniprep Kit (QIAGEN).

A 5 ml overnight culture was inoculated and harvested by centrifugation for five minutes at 5000 rpm. The supernatant was removed; the cell pellet dissolved in 250 µl P1 Buffer and everything was transferred into a 1.5 ml eppendorf tube. 250 µl P2 Buffer was added, mixed thoroughly and incubated for five minutes at room temperature to lyse the cells. Afterwards 350 µl of N3 Buffer was added, mixed and placed on ice for five minutes. The mixture was centrifuged two times for five minutes at 13200 rpm and each time the supernatant was transferred into a new tube. To precipitate the DNA, 750 µl isopropanol was added, mixed and placed on ice for 10 minutes. Now, it was centrifuged for 10 minutes at 13200 rpm, the supernatant was removed and the pellet was washed with 1 ml of 70% ethanol. Finally, the DNA was dissolved in 50 µl TE Buffer at 37°C for three hours. Only freshly prepared DNA was used for transformations.

Standard and Genomic polymerase chain reaction (PCR)

The PCR (Saiki et al., 1988) was used to selectively amplify DNA fragments. Annealing temperatures were adjusted to fit the respective primer melting temperature (approximately 5°C below). Extension times were matched to fit the length of the DNA fragment and the speed of the respective polymerase. To minimize the probability of mutations (exchange, deletion, etc.) a Pwo DNA polymerase (Roche) or the *PfuUltra*® Hotstart DNA polymerase (Stratagene) was used. These polymerases possess a 3'-5' exonuclease activity (proofreading activity) which results in an over 10-fold increased fidelity of DNA synthesis compared to Taq DNA polymerase. The GoTaq® DNA polymerase (Promega) was used for genotyping. All polymerases were used according to the instructions of the manufacturer. The thermocycling program (Table 2) was carried out using the Mastercycler® Gradient (Eppendorf).

Segment	Number of cycles	Temperature	Duration
1) Initial denaturation	1	94°C	2 minutes
2) Denaturation	30-40	94°C	30 seconds
Annealing		55-65°C	30 seconds
Elongation		72°C	1-2 minutes
3) Final elongation	1	72°C	10 minutes

Table 2. Standard thermocycling program for PCR.

Reverse transcriptase – polymerase chain reaction (RT-PCR)

The QIAGEN® OneStep RT-PCR Kit (QIAGEN) was used to amplify selectively DNA fragments from RNA templates. This kit is designed to carry out reverse transcription and PCR sequentially in the same tube. The enzyme mix contains the Omiscript and Sensiscript reverse transcriptases for efficient and specific reverse transcription and the HotStarTaq DNA polymerase for subsequent amplification. Annealing temperatures were adjusted approximately 5°C below the respective primer melting temperature. Extension times were matched to fit the length of the DNA fragment. The RT-PCR was performed according to the instructions of the manufacturer. The thermocycling program (Table 3) was carried out using the Mastercycler® Gradient (Eppendorf).

Segment	Number of cycles	Temperature	Duration
1) Reverse Transcription	1	50°C	30 minutes
2) Initial PCR activation step	1	95°	15 minutes
3) Initial denaturation	1	94°C	2 minutes
4) Denaturation	30-40	94°C	30 seconds
Annealing		55-65°C	30 seconds
Elongation		72°C	1-2 minutes
5) Final elongation	1	72°C	10 minutes

Table 3. Standard thermocycling program for RT-PCR.

Purification of PCR products

PCR products were purified using the QIAquick® PCR Purification Kit (QIAGEN), following the instructions of the manufacturer.

PCR-Primers

Primers were designed using the Sequencher™ 3.1.1 software (Gene Codes Corporation), the CLC Free Workbench 4.0.3 program (CLC bio A/S; <http://www.clcbio.com>) and the online tool Oligo Calc (<http://www.basic.northwestern.edu/biotools/oligocalc.html>). This program calculates the physical constants of the oligonucleotide, checks self-

complementarity and allows a direct access to the NCBI BLAST interface. Oligonucleotides were obtained either from IBA (Goettingen, Germany) or Operon (Cologne, Germany).

Name/Purpose	Direction	Tag	Sequence (5'→3')
Cloning			
Mad2l2_5'Sall	Forward	Sall	ACGCGTCGACGCCAAGGATGACCACC
Mad2l2_3'NotI	Reverse	NotI	ATAAGAATGCGGCCGCGCCCTCAGCTGTTCTTATGC
Map-1_5'Sall	Forward	Sall	ACGCGTCGACGAGCACCATGACACTGAG
Map-1_3'NotI	Reverse	NotI	ATAGTTTAGCGGCCGCGGGTCAAGTGCAATAGCCT
Importin13_5'EcoRI	Forward	EcoRI	GGAATTCCAAAGATGGAGCGGGCGGG
Importin13_3'NotI	Reverse	NotI	ATAGTTTAGCGGCCGCGCCCTCAGTAGTCAGCTGTG
Traf4_5'Sall	Forward	Sall	ACGCGTCGACGCCCCGCCATGCCCGGC
Traf4_3'NotI	Reverse	NotI	ATAAGAATGCGGCCGCTCTACTCAGCTGAGGATC
pGEX_Hesx1_BamHI	Forward	BamHI	CGGGATCCCAGAAGAGAATGTCTCCAGCC
pGEX_Hesx1_HindIII	Reverse	HindIII	CCCAAGCTTCTACCTATTTCAGAAGATCTGGG
5'GST-Mad2l2 SmaI	Forward	SmaI	TCCCCCGGGGATGACCACCCTCACGC
3'GST-Mad2l2 XbaI	Reverse	XbaI	GCTCTAGACCTCAGCTGTTCTTATGCG
pSP64_Mad2l2_3'XbaI	Reverse	XbaI	GCTCTAGAGCCCTCAGCTGTTCTTATG
Cdh1 5' EcoRI	Forward	EcoRI	GGAATTCCCATGGACCAGGACTATGAGC
Cdh1 3' Sall	Reverse	Sall	ACGCGTCGACCCTGCGGGGTCTATCGGATC
Hesx1 5' EcoRI	Forward	EcoRI	GGAATTCAATGTCTCCAGCCTTCG
Hesx1 3' BamHI	Reverse	BamHI	CGGGATCCTACCTATTTCAGAAGATCTGG
Hesx1*3'ΔHD BamHI	Reverse	BamHI	CGGGATCCTCAAGTCTCACTGGGAAGATC
Hesx1*5'Δeh1 EcoRI	Forward	EcoRI	GGAATTCTCCTTGCCAGTGGATCACC
Northern blot analysis			
Mad2l2northernS5	Forward	-	GACCTCAACTTTGGCCAAG
Mad2l2northernS3	Reverse	-	GGTTGTGATCCAGGACAG
Mad2l2 cko vector - recombineering			
A	Forward	NotI	ATAAGAATGCGGCCGCACTCCAGTTCAGGTTATCCG
B	reverse	SpeI	GGACTAGTTTACATAATAAGAGTCCTCTCC
Y	Forward	SpeI	GGACTAGTAGCTTCTGAGTGGAAATCTAGG
Z	Reverse	BamHI	GGATCCCCATGAGAGAGTCTGTCTG
C	Forward	Sall	ACGCGTCGACCTGAAGATTTATTGAGTCAACTCC
D	Reverse	EcoRI, BglI	GGAATTTCGCTGCAGGGCCGAGCTAAACCGCCTTTGG
E	Forward	BamHI	CGCGGATCCTTCTTGAGATTCCTGTAGC
F	Reverse	NotI	ATAAGAATGCGGCCGCTCCCTCTCGGCGGAAATCC
G	Forward	Sall	ACGCGTCGACACTTCAGGCTCGAATCTGC
H	Reverse	EcoRI, DraI	GGAATTCTTTAAATACACATGTTTCATCCTGTTTGG
I	Forward	BamHI	CGCGGATCCTCGAAGCTGCCCTGAGAAG
J	Reverse	NotI	AGAATGCGGCCGCTTCTCTGATTACCCTCCAGG
Southern blot analysis			
S1 DraI (3' Probe)	Forward	-	GGAGAAGCTGTCATCAGATGTC
S2 DraI (3' Probe)	Reverse	-	GCT CCT TAG TGC TTG GAA CAC
S3*BglI (5' Probe)	Forward	-	GTC AGC TTC TTG CCA CTC TCC
S4*BglI (5' Probe)	Reverse	-	CAT CTA CTG GCC ATG CAC ACC
EMSA			
PrdQ-EMSA-sense	Forward	-	AGCTTGAGTCTAATTGAATTAAGTGTAC
PrdQ-EMSA-antisense	Reverse	-	GTACAGTTAATTCAATTAGACTCAAGCT
Genotyping			
neoF	Forward	-	CAGCTGTGCTCGACGTTGTCAGT

neoR	Reverse	-	CCATGATATTCGGCAAGCAGGCATCG
3' out of neo	Forward	-	CAGCGCATCGCCTTCTATC
M2I25genotyp (#1)	Forward	-	GCTCTTATTGCCTTGACATGTGGCTGC
M2I23genotyp (#2)	Reverse	-	GGACACTCAGTTCTGGAAAGGCTGG
M2I25loxPgenotyp (#3)	Forward	-	CTGAGCCCAATTCGATCATATTCAATAAC
GAPDH 5'	Forward	-	ACCTTCGATGCCGGGGCTG
GAPDH 3'	Reverse	-	ATGAGGTCCACCACCCTGTTG

Table 4. List of PCR-primers

DNA electrophoresis and purification from agarose gel

To analyze and separate fragments of restriction digests or products of PCR reactions agarose gels were made. Depending on the fragment size 0.3–2% agarose gels (Table 5) were prepared in 1x TBE buffer (89 mM Tris-base, 89 mM Boric acid, 2 mM EDTA 0.5 M, pH 8) containing 10 µg/ml of ethidium bromide. The DNA was mixed with an appropriate amount of 6x gel loading buffer (0,25% (w/v) Bromophenol blue, 0,25% (w/v) Xylene cyanol FF, 30% (v/v) Glycerol in dH₂O) before being loaded into the gel. The gel was run at a voltage of 80 to 110 in 1x TBE. UV-light (Biometra TI2) with a wave length of 258 nm was used to visualize DNA for analytical purposes. AlphaEase™FC software was used for documentation. Preparative Gels were examined at a wave length of 366nm with less intensity to prevent DNA damage.

Agarose concentration (% w/v)	DNA fragment range (kb)
0.3	5–60
0.5	1–30
0.7	0.8–12
1.0	0.5–10
1.2	0.4–7
1.5	0.2–3
2.0	0.05–2

Table 5. Concentration of agarose used for separating DNA of different sizes.

Modified from Qiagen Bench Guide, 2001.

Quantification of nucleic acids

The concentration of DNA or RNA was determined using the BioPhotometer (Eppendorf) or the NanoDrop® Spectrometer ND-1000 (Thermo Fisher Scientific). Readings were taken at wavelength of 260 nm and 280 nm. The reading of 260 nm allows calculation of the concentration of nucleic acid, whereas the ratio of OD₂₆₀/OD₂₈₀ provides an estimate of the purity. Pure preparations have values in the range of 1.8 and 2.0.

Restriction digest of DNA

Restriction digests of DNA using restriction endonucleases were performed as recommended by the manufacturer (New England Biolabs, Roche). Double digestions

could be performed if both enzymes needed the same conditions. Otherwise a sequential digestion was performed and the DNA was purified, using the QIAquick® PCR Purification Kit (QIAGEN), between the different digestions. For analytical digests 5U restriction enzyme was used per µg DNA. The digest was accelerated by using a microwave oven two times for 12 seconds at half power and afterwards incubating the reaction for an half an hour at 37°C. Preparative digests were performed using up to 10U of restriction endonuclease per µg of DNA and the reaction mix was incubated for two to four hours at 37°C. If cleavages close to the end of a DNA fragment were desired the incubation was o/n at room temperature. If required, BSA was added to a final concentration of 100 µg/ml.

Dephosphorylation of DNA fragments

Dephosphorylations of cloning vectors were performed to prevent religation of the vector itself. The alkaline phosphatase hydrolyzes the 5'-phosphate group at the DNA. The reaction assay was adjusted with one tenth volumes of the 10x dephosphorylation buffer and 1U alkaline phosphatase (1U/µl, Roche) was subsequently added. The reaction was incubated at 37°C for one hour. Afterwards the vector DNA was purified using the QIAquick® PCR Purification Kit (QIAGEN).

DNA ligation

DNA ligations were performed using T4 DNA Ligase (MBI Fermentas). 25-100 ng vector DNA was used and the insert DNA mass was determined according to the following equation: $mass_{insert}[ng] = \frac{5 \times mass_{vector}[ng] \times length_{insert}[bp]}{length_{vector}[bp]}$ (Mülhardt, 2004). The ligation reaction was performed in 10 µl and contained 1 µl of ligase (3U/µl), 1 µl 10x ligation buffer, the appropriate amount of DNA and dH₂O. Incubation took place for one hour at room temperature or overnight at 16°C. At the end of the incubation time the reaction was heat inactivated for 10 min at 65°C.

Name	Backbone (supplier)	Insert	Purpose	Reference
IRAVp968E0724D6	pCMV-SPORT6 (RZPD)	Mad2l2	General cloning	RZPD clone
IRAKp961H2324Q	pCMV-SPORT6 (RZPD)	Importin13	General cloning	RZPD clone
IRAKp961C2016Q	pCMV-SPORT6 (RZPD)	Traf 4	General cloning	RZPD clone
2610209C10	Modified	Map-1	General cloning	RIKEN

	bluscript 1			(Fantom 1 library) RZPD clone
IRAVp968A1021D6	pCMV-SPORT6 (RZPD)	Cdh1	General cloning	
pDBLeu	(Gibco BRL®)	-	Yeast Two-Hybrid Screen	(Chevray and Nathans, 1992)
pDBLeu-Hesx1	pDBLeu (Gibco BRL®)	Hesx1	Yeast Two-Hybrid Screen	(Pilarski, 2004)
pPC86	(Gibco BRL®)	-	Yeast Two-Hybrid Screen	(Chevray and Nathans, 1992)
pPC86-Mad2l2	pPC86 (Gibco BRL®)	Mad2l2	Yeast Two-Hybrid Screen	This study
pPC86-Map-1	pPC86 (Gibco BRL®)	Map-1	Yeast Two-Hybrid Screen	This study
pPC86-Traf 4	pPC86 (Gibco BRL®)	Traf 4	Yeast Two-Hybrid Screen	This study
pPC86-Imp13	pPC86 (Gibco BRL®)	Importin13	Yeast Two-Hybrid Screen	This study
pGEX-KT/mHesx1	pGEX-KT (Amersham Biosciences)	Hesx1	GST-Hesx1 protein expression and purification	This study
pGEX-KT/Mad2l2	pGEX-KT (Amersham Biosciences)	Mad2l2	GST-Mad2l2 protein expression and purification	This study
pSP64/Mad2l2	pSP64 Poly (A) (Promega)	Mad2l2	<i>In vitro</i> transcription/translation	This study
pSP64/Hesx1	pSP64 Poly (A) (Promega)	Hesx1	<i>In vitro</i> transcription/translation	This study
pCMV-HA/Mad2l2	pCMV-HA (Clontech)	Mad2l2	Co-immunoprecipitation, Ubiquitination assay	This study
pCMV-HA/Cdh1	pCMV-HA (Clontech)	Cdh1	Co-immunoprecipitation, Ubiquitination assay	This study
pFLAG-CMV/Hesx1	pFLAG-CMV™-2 (Sigma)	Hesx1	Co-immunoprecipitation, Ubiquitination assay	This study
pFLAG-CMV/Hesx1 Δ HD	pFLAG-CMV™-2 (Sigma)	Hesx1 Δ HD	Co-immunoprecipitation	This study
pFLAG-CMV/Hesx1 Δ eh1	pFLAG-CMV™-2 (Sigma)	Hesx1 Δ eh1	Co-immunoprecipitation	This study
pFLAG-CMV/Hesx1 Δ 2/3 HD	pFLAG-CMV™-2 (Sigma)	Hesx1 Δ 2/3 HD	Co-immunoprecipitation	This study
pGEM-T/Hesx1	pGEM®-T (Promega)	Hesx1	<i>Whole mount in situ</i> -hybridization	(Pilarski, 2004)
pEGFP-N2	(Clontech)	GFP	Transfection control	-
pcDNA3.1(-)-His ₆ Ubiquitin	pcDNA3.1(-) (Invitrogen)	His ₆ Ubiquitin	Ubiquitination assay	F. Melchior lab.
RPCIP711B01141Q6	pPAC4 (RZPD)	Mad2l2 genomic region	Recombineering	(Osoegawa et al., 2000)
PL451	(NCI-Frederick)	<i>Frt-Pgk-em7-Neo-Frt-loxP</i>	Recombineering - targeting	(Liu et al., 2003)
PL452	(NCI-Frederick)	<i>loxP-Pgk-em7-Neo-loxP</i>	Recombineering - targeting	(Liu et al., 2003)
PL253	pBluescript (NCI-Frederick)	<i>Mc1</i> -driven Thymidine Kinase (<i>TK</i>)	Recombineering - retrieving	(Liu et al., 2003)

Table 6. List of plasmids.

Sequencing

Sequencing was performed in the Molecular Cell Biology department by Sigurd Hille using Taq Dye Deoxy Terminator Kits (Perkin Elmer) and an ABI Prism 377 DNA Sequencer (Applied Biosystems) or by GATC Biotech (Konstanz).

Sequence analysis was performed with the Sequencher™ 3.1.1 software (Gene Codes Corporation) or the CLC Free Workbench 4.0.3 program (CLC bio A/S; <http://www.clcbio.com>). Database analysis was performed using the different databases of the National Center for Biotechnology Information (NCBI, <http://www.ncbi.nih.org>), the exPASy Molecular Biology Server (<http://us.expasy.org>), Ensemble (<http://www.ensembl.org/index.html>) and Mouse Genome Informatics (MGI) (<http://www.informatics.jax.org>).

Dig-labeled antisense RNA probe preparation

Dig-labeled antisense RNA *in vitro* transcription was performed from a linearized plasmid which contains the cDNA of the gene which transcripts should be monitored in the tissue. The linearization of the plasmid DNA was done with restriction enzymes which leave a 5'-overhang to prevent the RNA polymerase from "turning" around and synthesizing a sense strand. The transcription reaction was done in a total volume of 20 µl containing 1 µl linearized plasmid (1 µg/µl), 2 µl 10x transcription buffer (Roche), 2 µl DIG RNA labeling mix (Roche), 2 µl RNasin (40 U/µl), 1 µl RNA polymerase and 12 µl dH₂O. This reaction was mixed and incubated for 2 hours at 37°C. Digoxigenin-11-UTP is incorporated in the antisense RNA during the *in vitro* transcription, which was later on detected by anti-DIG-AP conjugated antibodies. To purify the RNA probes ProbeQuant G-50 columns (GE Healthcare) were used. After the elution 30 µl dH₂O was added to give a final volume of 100 µl. 5 µl of the reaction were controled on a non-denaturing 1% agarose gel and should result in one strong and a possibly second weaker band. The sizes of the single stranded RNA just fits very roughly to the DNA marker.

Preparation of random radioactively labeled DNA probes

The DNA probes for northern and southern blot analysis were prepared using the Amersham Rediprime II Random Prime Labelling System (GE Healthcare) and [α -³²P]-dCTP (Amersham Biosciences). The labeling reaction was performed as recommended by the manufacturer.

Purification of labeled nucleic acids

ProbeQuant G-50 Sephadex Micro Columns (GE Healthcare) were used to purify DIG or radioactively labeled nucleic acids. The Micro Columns were used according to the instruction of the manufacturer. The specific activity of radioactive labeled DNA was measured using the LS 1701 scintillation counter (BeckMan).

Phenol extraction and ethanol precipitation of DNA

The DNA solution was first extracted with a phenol/chloroform/isoamyl alcohol mixture to remove protein contaminants, and then precipitated with 100% ethanol. The DNA was pelleted after the precipitation step, washed with 70% ethanol to remove salts and small organic molecules, and resuspended in dH₂O at a concentration suitable for further experimentation.

An equal volume of phenol/chloroform/isoamyl alcohol (25:24:1 (v/v/v)) was added to the DNA solution to be purified in a 1.5 ml microcentrifuge tube. This was vigorously vortexed for 10 seconds and microcentrifuged 15 seconds at maximum speed, room temperature. The top (aqueous) phase containing the DNA was removed using a 200 µl pipettor and transferred to a new tube. The same step was performed using 24:1 chloroform/isoamyl alcohol (24:1 (v/v)). Now, 1/10 volume of sodium acetate (3 M, pH 5.2) was added to the solution of DNA and mixed by vortexing briefly. Subsequently, 2 to 2.5 vol (calculated after salt addition) of ice-cold 100% ethanol was added, again mixed by vortexing and placed in a -20°C freezer for at least 30 min. Afterwards the tube was microcentrifuged for five minutes at maximum speed and the supernatant removed. 1 ml room temperature 70% ethanol was added, the tube several times inverted and microcentrifuged as previously described. The supernatant was removed and the pellet dried at room temperature. The dry DNA pellet was dissolved in an appropriate volume of dH₂O.

Northern blot analysis

Northern blot analysis was performed using the FirstChoice™ Northern Blot Mouse Blot I (Ambion), which is a ready-to-hybridize Northern blot of different mouse tissues. The assay was done using a radioactive labeled PCR amplified DNA probe (1×10^6 cpm/ml) and a hybridization temperature of 42°C. Otherwise the analysis was done using the

ULTRAhyb™ ULTRASensitive Hybridization Solution and the NorthernMax High and Low Stringency Wash Solutions (Ambion) following the instructions of the manufacturer.

Southern blot analysis

Restriction digestions of genomic DNA were set up in a total volume of 50 μ l. 5-10 μ g genomic DNA was digested with the appropriate restriction enzyme (10 U/ μ g of DNA) and 2 μ l RNase A (1 mg/ml stock) was added. The reaction was incubated at 37°C overnight. Agarose gel electrophoresis of this reaction was performed using a 0.7 % gel in 0.5 \times TBE containing 10 μ g/ml of ethidium bromide. 6 \times gel loading buffer was mixed to the samples to load them on the gel. If the digested DNA was stored at 4°C, it was heated to 56°C for two to three minutes before it was applied on the gel. The gel was run at < 1 V/cm at approximately 30 V overnight. Afterwards the upper part of the gel above the wells and all unnecessary parts were removed. On edge of the gel was marked by cutting off a piece, and a photo with a ruler adjacent to the gel was taken under UV-light. In order to prepare the gel for blotting it was shaken for 15 minutes in 0.25 M HCl and afterwards washed with dH₂O. Again it was shaken for 40 minutes in Blot Buffer I (1.5 M NaCl, 0.5 M NaOH), washed with dH₂O and shaken for 40 minutes in Blot Buffer II (1 M Tris, pH 7.2, 1.5 M NaCl). The gel was now transferred into 20 \times SSC (3 M NaCl, 300 mM Na-Citrate) and shaken for 20 minutes. Meanwhile the nylon membrane (GeneScreen™ Hybridization Transfer Membrane, PerkinElmer) was first incubated in dH₂O and afterwards shaken for >10 minutes in 20 \times SSC until the color had totally changed to light grey and no white areas were left. The blotting was performed for 24-48 hrs in 20 \times SSC. The wells of the gel were marked on the membrane with a pencil before the gel was removed. Cross linking of the DNA to the membrane was done by UV irradiation (0.5 J/cm², Fluo Link). The radiolabeled probes were prepared and purified as described earlier. Probes were used if they had more than 800.000 cpm/ μ l. After the blotting, membranes were transferred in roller bottles and washed with prewarmed (65°C) 2 \times SSC containing 0.5% SDS for 30 minutes at 65°C. Blots were prehybridized in approximately 0.1 ml prewarmed prehybridization solution/cm² membrane (5 \times Denhardt's solution, 5 \times SSPE, 0.5% SDS and 5 mg/ml Salmon sperm DNA; 50 \times Denhardt's (10 g Ficoll 400, 10 g Polyvinylpyrrolidone, 10 g BSA in 1 liter dH₂O); 20 \times SSPE (174 g NaCl, 27.4 g NaH₂PO₄xH₂O, 7.4 g EDTA, pH 7.4 in 1 liter dH₂O)) for at least two hours at 65°C. For hybridization the prehybridization solution was poured off and replaced with fresh hybridization solution (prehybridization solution

containing the probe (1×10^6 cpm/ml)). Hybridization took place overnight while gently rotating at 65°C. The next day the hybridization solution was removed and the membranes were washed twice with prewarmed (65°C) 2× SSC containing 0.5% SDS for 30 minutes. Afterwards they were washed once with prewarmed (65°C) 0.1× SSC containing 0.5% SDS for an half an hour. Now blots were air dried for 30 min on a Whatman 3MM paper. The corners of the blots were stuck to a Whatman 3MM paper and everything was wrapped in Saran wrap. The wrapped membranes were transferred into a film cassette. In the dark room, an X-ray film (Biomax MR film, Kodak) was placed on it. Exposure took place at -70°C. Optimal exposure times were empirically determined and were probe dependent.

Transformation of *E. coli*

Bacterial strains

Name	Purpose	Supplier/Reference
DH5-α	Propagation of plasmid DNA	Invitrogen
DH10B	Propagation of plasmid DNA	Invitrogen
BL21-CodonPlus® (DE3)-RIL	Protein expression	Stratagene
Rosetta	Protein expression	Novagen
SW102	Recombineering (temperature-sensitive <i>exo</i> , <i>bet</i> , and <i>gam</i> genes)	(Warming et al., 2005)
SW105	Recombineering (<i>ara</i> -inducible <i>Flpe</i> gene)	(Warming et al., 2005)
SW106	Recombineering (<i>ara</i> -inducible <i>Cre</i> gene)	(Warming et al., 2005)

Table 7. Bacterial strains used in this study.

Preparation of electrocompetent *E. coli*

A single colony was inoculated in 2x 10 ml LB medium (10 g tryptone, 5 g yeast extract, 10 g NaCl and dH₂O up to 1 liter, autoclaved) and incubated at 37°C shaking at 220 rpm for o/n. These starter cultures were used to inoculate 2x 1 liter LB medium, which were incubated at 37°C until they reached an OD₆₀₀ of ~0.6-0.8 (mid-log phase). Now the cells were chilled on ice for 20 minutes and harvested at 5000 x *g* for 20 minutes at 4°C. The cells were washed 1:1 (referring to the 2x 1 liter culture) with prechilled dH₂O while not disturbing the pellet and harvested again. Afterwards the cells were washed 1:10, 1:50 and 1:500 with prechilled 10% glycerol/dH₂O and harvested at 5500 x *g* for 10 minutes (5

minutes last step) at 4°C. They were resuspended with prechilled 10% glycerol/dH₂O and divided in 50 µl aliquots. The aliquots were frozen in liquid nitrogen and then stored at -80°C.

Preparation of *E. coli* competent for heat shock transformation

One colony was inoculated in 5 ml LB medium and grown overnight at 37°C. This pre-culture was inoculated in 50 ml LB medium. Cells were grown to reach an OD₆₀₀ of ~0.7 (mid-log phase). They were harvested for 10 minutes at 2000 rpm and resuspended in 25 ml of ice-cold CaCl₂ (50 mM). After an additional centrifugation for 10 minutes at 2000 rpm, cells were resuspended with 3 ml of ice-cold CaCl₂/glycerol (50 mM, 10% glycerol) and aliquoted (50 µl). These aliquots were frozen in liquid nitrogen and then stored at -80°C.

Transformation of *E. coli* by electroporation

Electro competent *E. coli* were thawed on ice and mixed with 5 µl of a ligation reaction or ~1-10 ng plasmid DNA. This mixture was pipetted in an *E. coli* Pulser[®] Cuvette (BioRad). The electroporation was performed using the Gene Pulser (BioRad, capacity: 25 µF, voltage: 2.5 kV, resistance: 200 Ω). An efficient transformation required a pulse length of 3.8-4.6 msec. After the electroporation the bacteria were directly mixed with 950 µl of prewarmed LB medium and incubated for an half an hour shaking at 200 rpm at 37°C. 50 µl of this culture were put on prewarmed LB-agar plates containing either ampicillin, kanamycin (50 µg/ml) or chloramphenicol (25 µg/ml), depending on the resistance gene included in the plasmid DNA. The plates were cultured at 37°C o/n. (Dower et al., 1988)

Transformation of *E. coli* by heat shock

The heat shock competent cells were thawed on ice and transferred into a Falcon™ 2059 polypropylene tube (BD Falcon). 10 ng plasmid DNA or 5 µl ligation reaction was directly added to the competent cells and mixed well by gently flicking. The mixture was incubated on ice for 30 minutes, heat shocked at 42 °C for 1 minute, and incubated on ice for 1.5-2 minutes. Afterwards, 950 µl prewarmed LB medium was added to the heat shocked cells, and they were incubated at 37 °C rotating for 1 hour. The recovered cells were subsequently spun down at 3000 rpm for 2 minutes, resuspended in 200 µl LB medium and plated on appropriate LB-agar plates.

Cryopreservation of *E. coli*

For long term storage of bacterial clones, 800 μ l of a colony, grown until stationary phase, were mixed with 300 μ l autoclaved 80% glycerol/dH₂O, frozen in liquid nitrogen and then stored at -80°C. If aliquots were taken from this glycerol stock and used for inoculation of a culture, the glycerol stock was kept frozen.

Yeast Two-Hybrid Assay

The yeast two-hybrid assay was performed using the ProQuest™ Two-Hybrid System (Gibco BRL®), essentially according to the instructions of the manufacturer.

Transformation of yeast

LiAc was used to make competent yeast cells which are able to take up plasmid DNA (Ito et al., 1983). To increase the efficiency of genetic transformation heat denatured sonicated salmon sperm DNA (Stratagene) was used as carrier DNA (Schiestl and Gietz, 1989)

Several isolated colonies of the yeast strain MaV203 (*MAT α* , *leu2-3,112*, *trp1-901*, *his3 Δ 200*, *ade2-101*, *gal4 Δ* , *gal80 Δ* , *SPAL10::URA3*, *GAL1::lacZ*, *HIS3_{UAS} GAL1::HIS3@ LYS2*, *can1^R*, *cyh2^R*) (Vidal, 1997) were suspended in 50 μ l dH₂O and spread onto the center of an YPDG plate (10 g Bacto-yeast extract, 20 g Bacto-peptone, 20 g Dextrose, 100 mg Adenine sulfate, 20 g bacteriological-grade agar, dH₂O ad 1 liter). They were incubated at 30°C o/n. The next day they were scraped from the plate and resuspended in 5 ml dH₂O. This cell suspension was used to inoculate a 100 ml YPDG broth (10 g Bacto-yeast extract, 20 g Bacto-peptone, 20 g Dextrose, 100 mg Adenine sulfate, dH₂O ad 1 liter) to a final OD₆₀₀ of 0.1. They were incubated shaking (180 rpm) at 30°C until the OD₆₀₀ reached ~0.4. Now the 100 ml culture was split into two 50 ml aliquots and centrifuged at 3000 x *g* for five minutes at room temperature. The supernatant was discarded and each pellet suspended in 20 ml dH₂O. The cells were harvested by centrifugation at 3000 x *g* for five minutes at room temperature, the supernatant was discarded and each pellet was suspended in 10 ml freshly prepared 1x TE/LiAc solution (10 mM Tris-HCl (pH 7.5), 1 mM EDTA, 100 mM lithium acetate). The cells were harvested again by centrifugation at 3000 x *g* for five minutes at room temperature, the supernatant was poured of and each pellet was suspended in 175 μ l fresh 1x TE/LiAc solution. Booth suspensions were pooled.

For each transformation 50 μl cells were combined with 5 μl freshly boiled carrier DNA (10 $\mu\text{g}/\mu\text{l}$, five minutes boiled and stored on ice to prevent annealing) and 100 ng of each plasmid DNA. This was gently mixed by pipetting up and down; 300 μl PEG/LiAc (10 mM Tris-HCl (pH 7.5), 1 mM EDTA, 100 mM lithium acetate, 40% PEG-3350) was added and the solution was mixed again. All transformations were incubated for 30 minutes at 30°C and afterwards heat shocked for 15 minutes at 42°C. The cells were harvested at 7000 x *g* for 20 seconds and the supernatant was removed. 500 μl dH₂O was used to suspend the pellet and 100 μl undiluted and 100 μl of a 1:10 dilution were plated on appropriated selection plates. These plates were incubated at 30°C for 48-72 hours.

Characterization of transformants

The two monitored reporter genes in this system (*HIS3* and *lacZ*) were induced in MaV203 cells that contain pDBLeu-Hesx1 and pPC86-Y encoding interacting proteins. To analyze the colonies grown on SC-Leu-Trp-His+50 mM 3AT selection plates, two freshly single purified colonies of control strains A-F and MaV203 (pDBLeu-Hesx1, pPC86) and three colonies of each potential positive clone were plated onto a single SC-Leu-Trp plate. After an incubation of 18 hours at 30°C every plate was replica plated onto an YPDG plate containing a Nytran® N membrane (Schleicher & Schuell) and a SC-Leu-Trp-His+50 mM 3AT plate, which was replica cleaned afterwards. All plates were incubated for ~24 hours at 30°C and the X-Gal assay was performed with the colonies grown on the Nytran® N membranes. The other plates were replica cleaned again, incubated for 2 additional days and analyzed.

X-Gal assay

To detect the induction of the *lacZ* reporter gene, 10 mg X-Gal was dissolved in 100 μl DMF and combined with 60 μl β -mercaptoethanol and 10 ml Z-buffer (16.1 g Na₂HPO₄*7H₂O, 5.5 g NaH₂PO₄*H₂O, 0.75 g KCl, 0.25 g MgSO₄*7H₂O in a total volume of 1 liter). Two round Whatman® 541 filter were stacked and saturated with the X-Gal containing solution removing any air bubble. The Nytran® N membrane was immersed in liquid nitrogen for 20-30 seconds to lyse the cells, and then placed colony side up onto the soaked Whatman® filters. The plates were slightly tipped to prevent accumulation of X-Gal solution on the membrane and incubated at 37°C for 24 hours. The appearance of blue color was monitored over this 24 hour period.

Long term storage of yeast

Yeast strains can be stored for periods of 6-12 months on tightly sealed agar plates. For longer periods yeast strains were stored in 50% (v/v) glycerol at -70°C.

Purification and analysis of proteins

Expression and purification of GST-fused recombinant proteins

GST-fused Hesx1 and Mad2l2 protein were expressed in and purified from *E. coli*. Full-length *Hesx1* and *Mad2l2* cDNAs were cloned in frame with the N-terminal GST-tag into the pGEX-KT vector. This vector contains a thrombin cleavage site between the GST-tag and the multiple cloning site, which allows a subsequent removal of the tag. pGEX-KT/Hesx1 was transformed via thermal shock into chimiocompetent BL21-CodonPlus® (DE3)-RIL cells and pGEX-KT/Mad2l2 was transformed by electroporation into Rosetta cells.

Single colonies were used to inoculate 100 ml LB medium containing the appropriate antibiotics for selection. 50 µg/ml ampicillin (Sigma) was used for BL21-CodonPlus® (DE3)-RIL cells or ampicillin and 25 µg/ml chloramphenicol (Boehringer) was used for the Rosetta strain. This culture was grown overnight at 37°C, shaking at 150 rpm. 50 ml of the overnight culture was added to 1 l fresh prewarmed LB medium supplemented with the required antibiotics. The culture was grown at 37°C and 150 rpm until it reached an OD₆₀₀ of 0.6-0.7 (mid-log phase). Protein expression was induced by the addition of 1 mM isopropyl-β-D-thiogalactopyranoside (Sigma). The culture was grown at 37°C for two hours (pGEX-KT/Hesx1) or at 22°C for six hours (pGEX-KT/Mad2l2) shaking at 140 rpm. Afterwards, cells were harvested in at 5000 rpm at 4°C for 25 minutes. The supernatant was discarded slowly, and the pellets with the remaining medium was resuspended and transferred into 50 ml Falcon™ tubes. The resuspension was centrifuged at 4000 rpm at 4°C for 30 minutes and the supernatant discarded again. The cell pellet was frozen at -70°C overnight. The pellet was resuspended in 40 ml protein lysis buffer (50 mM Tris, pH 7.5, 500 mM NaCl, 2 mM EDTA, 5 mM DTT, 10% glycerol, freshly added 1 mM PMSF and Complete™-EDTA protease inhibitor tablet (Roche)) on ice. Lysosyme at a concentration of 10 mg/10 ml resuspension solution was added and incubated on ice for 30 minutes. The resuspension was then sonicated on ice six times with 20 pulses and a one minute break in between each round. Sonication was done with the 1 cm tip using the Cell

Disruptor B15 (Branson Sonifier) under the condition of Output Option 5 and 50 % Duty Cycle. The lysate was centrifuged at 4°C for 1 hour at 15300 rpm. The supernatant was incubated with 500 µl prewashed Glutathione Sepharose 4B (Amersham Biosciences) at 4 °C on a rotating wheel for at 2-5 hours or at room temperature for 30 minutes. The mixture was centrifuged at 800 rpm at 4°C for one minute and the supernatant was discarded. The beads were applied to a 10 ml column (Pierce) and washed three times with 1x PBS containing freshly added Complete™-EDTA protease inhibitor tablet (Roche). The elution was done twice, each time with 2 ml elution buffer (GST-Hesx1 - 50 mM Tris, pH 8.0, 20 mM Glutathione or GST-Mad2I2 - 500 mM Tris, pH 8.0, 100 mM Glutathione both supplemented with protease inhibitor) rotating 30 minutes at room temperature. The proteins were dialyzed in dialysis buffer (20mM Tris-Cl pH 7.5, 1mM EDTA, 1mM DTT) using a dialysis cassettes (Pierce) at 4°C overnight. The protein concentrations were measured and determined according to the standard curve. If necessary, the protein was concentrated using Vivaspin concentrators (VIVASCIENCE). The purified protein was aliquoted, shock-frozen in liquid nitrogen and stored at -80°C.

Thrombin cleavage of GST-fused recombinant proteins

GST-Mad2I2 protein was cleaved with Thrombin protease (Amersham Bioscience) in order to obtain Mad2I2 protein without tag. Cleavage was done on the glutathione sepharose matrix with 50 U thrombin in 950 µl 1x PBS. The cutting was performed at 22°C overnight. The cleavage was stopped by adding 1 mM PMSF and two elutions were performed, by washing the beads with 1x PBS. The elutions were passed through HiTrap Benzamidine FF (high sub) (Amersham Biosciences) columns to remove the thrombin.

Quantification of protein concentrations

For protein quantification, the Bio-Rad Protein Assay (BioRad) was used following the manufacturer's instructions. BSA of known concentrations was used to generate standard curves (Figure 28). These curves were used to deduce the concentration of the protein solutions.

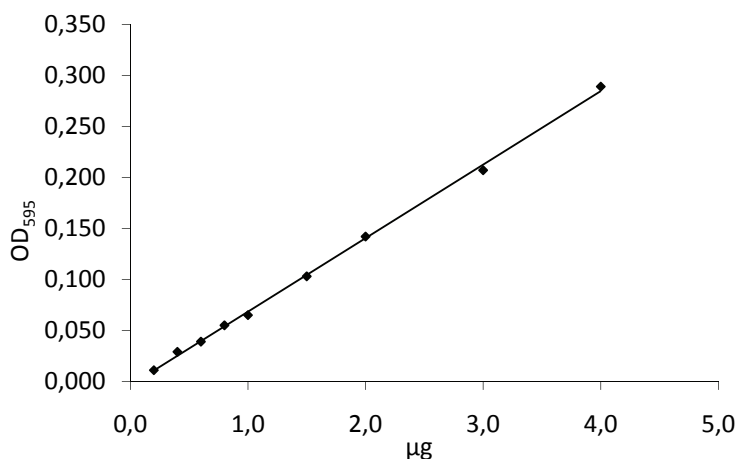


Figure 28. Standard curve for the determination of protein concentrations.

BSA in different concentrations was used to generate standard curves.

***In vitro* transcription/translation**

The TNT[®] Reticulocyte Lysate System (Promega) was used for the expression of radiolabeled proteins. The cDNA fragment of interest was cloned into the pSP64 Poly (A) vector (Promega), maxipreparation were performed and the plasmid purified by phenol extraction and ethanol precipitation. The assay was performed according to the instructions of the manufacturer using Redivue™ L-[³⁵S] methionine (Amersham Biosciences).

SDS-polyacrylamide gel electrophoresis of proteins (SDS-PAGE)

The SDS-PAGE was carried out using the Mini-Protean II cell system (BioRad). Different SDS-gel concentrations were used to obtain an optimal protein size resolution (Table 8). The preparation of the different gel parts was done using 4x separating gel buffer (1.5 M Tris, pH 8.8, 0.4% SDS) and 4x stacking gel buffer (0.5 M Tris, pH 6.8, 0.4% SDS). The separation gel was cast and immediately overlaid with isopropanol to give a smooth surface of the boundary stacking – separation gel. After polymerization the isopropanol was discarded and the stacking gel was poured. The protein samples were mixed with either 2x SDS loading buffer (125 mM Tris, pH 6.8, 20% glycerol, 0.02% bromphenol blue, 2% β-mercaptoethanol, 4% SDS) or with 6x SDS loading buffer (350 mM Tris, pH 6.8, 30% glycerol, 0.012% bromphenol blue, 0.6 M DTT, 10% SDS) and heated at 95°C for five minutes or in boiling water for three minutes. After loading of the protein samples and markers (BenchMark™ Pre-stained, MagicMark™XP (Invitrogen)), electrophoresis was done in 1x SDS electrophoresis buffer (25 mM Tris-base, 0.1% SDS, 192 mM glycine, pH 8.75) running the gel at 20 mA for approximately one hour. Subsequently, the gel was used directly for western blotting, or fixed (45% methanol, 7.5% acetate) for five minutes

and stained with Coomassie blue (0.25% Coomassie brilliant blue R 250, 45% methanol, 10% acetate) for one hour. Destaining of the gel was achieved by washing with 10% acetate for several hours or overnight.

Separating gel	12% (14-100 kDa)	15% (8-80 kDa)	Stacking gel	5%
4x Separation gel buffer	2.5 ml	2.5 ml	4x Stacking gel buffer	1 ml
30% Acrylamide-bisacrylamide solution	4 ml	5 ml	30% Acrylamide-bisacrylamide solution	670 μ l
dH ₂ O	3.4 ml	2.4 ml	dH ₂ O	2.3 ml
APS (10%)	100 μ l	100 μ l	APS (10%)	40 μ l
TEMED	4 μ l	4 μ l	TEMED	4 μ l

Table 8. SDS-polyacrylamide gel preparation.

Western blot analysis

After SDS-PAGE, western blotting and subsequent immunostaining was performed using primary and secondary antibodies specified in Table 9. For western blotting a Protran BA 85 nitrocellulose membrane (Schleicher & Schuell) and 4 pieces of Whatman 3MM paper were prepared at similar sizes to the gel, with the Whatman paper slightly larger. The membrane and the papers were presoaked in blot buffer (48 mM Trisbase, 3.9 mM glycine, 0.037% SDS, 20% methanol). The SDS-gel was placed on top of a double-layered Whatman paper, the nitrocellulose membrane was placed onto the gel followed by a double layer of Whatman paper, carefully avoiding any air bubble in between this sandwich. Electrophoretic transfer was performed in blot buffer using the Mini Trans-Blot electrophoretic Transfer cell (Bio-Rad) with the membrane close to the anode and the gel close to the cathode. Blotting was done at 15 V overnight or 100 V for one hour with a cooling chamber. The following steps were performed in small plastic boxes on a rocker (Biotetra). After the transfer was completed the membrane was briefly washed in wash buffer A (10 mM Tris, pH 7.4, 0.9% NaCl, 0.05% Tween 20), and then incubated in Ponceau S for 5 min to control if the protein transfer had worked. The membrane was then almost completely destained in wash buffer A and afterwards blocked in blocking buffer A (5% low fat milk powder in wash buffer A) for one hour at room temperature. The primary antibody was applied in the right concentration, diluted in 1% blocking buffer A, and the membrane was incubated at 4 °C with shaking overnight (preferred) or at room temperature for 1-2 hours. Afterwards the membrane was washed rocking at room temperature using the following sequence: wash buffer A, twice wash buffer B (0.9% NaCl, 0.5% Triton X-100, 0.1% SDS), buffer A (each step for 10 minutes). The secondary

HRP-conjugated antibody was diluted in 1% blocking solution and incubated at room temperature rocking for 40 minutes. The membrane was washed again in the same way as described before. Finally, the bound antibodies were detected by using the SuperSignal® West Pico or Femto Chemiluminescent Substrate (Pierce) and a phosphorimager (Lumimager™, Boehringer Mannheim) by exposing the membrane for 1 second to 20 minutes to a Lumi-Imager (Boehringer Mannheim) or to CL-Xposure™ films (Pierce) followed by developing with the Curix 60 developing machine (Agfa).

Antibodies

Name	Host and type	Dilution WB	Dilution IHC	Company/Source
Primary antibody				
Anti-FLAG	Rabbit polyclonal	1:1000	1:1000	Sigma
Anti-alpha-Tubulin	Mouse monoclonal	1:4000	-	Sigma
Anti-MAD2B (Mad2I2)	Mouse monoclonal	1:1000	-	BD Biosciences
Anti-γ-H2A.X (phospho S139)	Rabbit polyclonal	1:1000	1:100	Abcam
Anti-HA	Rat monoclonal	1:500	1:100	Roche
Anti-Hesx1	Goat polyclonal	1:500	-	Santa Cruz
Anti-rACTH	Rabbit antiserum	-	1:1000	NHPP
Anti-rTSHβ	Rabbit antiserum	-	1:1000	NHPP
Anti-mGH	Rabbit antiserum	-	1:1000	NHPP
Anti-rLHβ	Rabbit antiserum	-	1:1000	NHPP
Anti-rPRL	Rabbit antiserum	-	1:1000	NHPP
Anti-αGSU	Rabbit antiserum	-	1:200	NHPP
Secondary antibody				
Anti-rabbit-HRP	Goat antiserum	1:5000	-	Covance
Anti-mouse-HRP	Goat polyclona	1:10000	-	Dianova
Anti-goat-HRP	Rabbit polyclonal	1:7500	-	Abcam
Anti-rat-HRP	Goat polyclonal	1:5000	-	Dianova
Anti-rat-Alexa 594	chicken	-	1:1000	MoBiTec
Anti-rabbit-Alexa 488	goat	-	1:1000	MoBiTec

Table 9. List of antibodies.

Analysis of protein-protein interactions

GST Pull-down assay

The GST pull-down analysis was used to study the protein-protein interactions *in vitro*. The whole procedure was performed at 4°C. 50 µl (40 µl bed volume) Glutathione Sepharose 4B beads (Amersham Bioscience) were prewashed with 500 µl pull-down binding buffer (20 mM Tris, pH 7.5, 100 mM NaCl, 1 mM EDTA, 0.1% NP-40, freshly added 1 mM PMSF and Complete™-EDTA protease inhibitor (Roche)). The beads were sedimented by centrifugation at 500 g for five minutes and the supernatant discarded. 40-50 µg GST-Hesx1/Mad2l2 and GST were coupled to the beads in 500 µl pull-down binding buffer rotating overnight. Beads were sedimented by brief centrifugation and washed once with 500 µl pull-down binding buffer rotating for three minutes, to remove unbound protein. In a next step the beads were spun down again, the supernatant was discarded and the beads were incubated with 45 µl *in vitro* transcription/translation product in 500 µl pull-down binding buffer rotating for two hours. The remaining 5 µl of the *in vitro* transcription/translation product was mixed as a control with 2x SDS loading buffer and boiled at 95°C for five minutes. After the binding reaction, the beads were again sedimented and washed with pull-down binding buffer twice rotating for five minutes each. Two more washing steps were performed using pull-down washing buffer (20 mM Tris, pH 7.5, 150 mM NaCl, 1 mM EDTA, 0.1% NP-40, freshly added 1 mM PMSF and Complete™-EDTA protease inhibitor (Roche)) rotating for five minutes each step. Finally, the beads were spun down again and the supernatant was carefully aspirated. The protein was eluted by the addition of 40 µl 2x SDS loading buffer and subsequent heating at 95°C for five minutes. The beads were sedimented again and 20 µl supernatant and 10 µl control were subjected to SDS-PAGE. After electrophoresis the gel was placed on a wet Whatman paper and dried with a vacuum gel drier (Biometra) at 60°C for three hours. The dried gel together with the Whatman paper was wrapped in cling film and fixed in a film cassette. After exposure to an X-ray film (Biomax MR film, Kodak) at -70°C overnight, the film was subsequent developed with the Curix 60 developing machine (Agfa).

Peptide array analysis

The peptide array was done to further characterize the protein-protein interaction site. A Hesx1 PepSpots™ peptide membrane (JPT Peptide Technologies GmbH) was used to

determine the interaction site with Mad2l2. The entire Hesx1 sequence was spotted as overlapping peptides on a Whatman 50 cellulose support. The peptides were covalently bound to the membrane with their C-terminus and were N-terminal acetylated to repress degradation. The sequence was synthesized as 20meric peptides which were overlapping by 17 amino acids.

The peptide membrane was rinsed with a small volume of ethanol for one minute. Afterwards the membrane was washed three times with TBS (50 mM Tris, pH 8.0, 137mM NaCl, 2.7 mM KCl) rocking for 10 minutes each time. Blocking of the membrane was achieved by incubating the membrane in blocking solution (1.5% BSA in western wash buffer A) rocking for three hours at room temperature. The membrane was washed once with T-TBS (50 mM Tris, pH 8.0, 137mM NaCl, 2.7 mM KCl, 0.05% Tween 20) for 10 minutes and then incubated in blocking solution containing 1 µg/ml recombinant Mad2l2 protein overnight at room temperature. The next day, the membrane was washed three times for one minute with T-TBS. For the semi-dry blotting the peptide membrane was placed on Whatman paper presoaked with cathode buffer (25mM Tris, pH 9.2, 40 mM 6-aminohexanoic acid, 20% methanol). The PVDF membrane was briefly rinsed with methanol and equilibrated in anode buffer I (30 mM Tris, 20% methanol) for at least 10 minutes. This PVDF membrane was placed on top of the peptide membrane and then covered with two sheets of Whatman paper presoaked with anode buffer I and two sheets presoaked with anode buffer II (300 mM Tris, 20% methanol). Blotting took place at 1.0 mA/cm² for 30 minutes. The blotting process was repeated twice, the third time blotting was done for one hour. Afterwards the PVDF membranes were washed with western wash buffer A, twice with wash buffer B and again with wash buffer A for 10 minutes each time. The following steps were the same as described for western blotting, starting from the incubation of the primary antibody. Regeneration of the peptide membranes was done as described by the manufacturer.

Co-immunoprecipitation

To study protein-protein interactions *in vivo*, co-immunoprecipitation experiments were performed. COS-7 cells were cultured in 10 cm dishes and transiently co-transfected with different combination of the following plasmids: pCMV-HA/Mad2l2, pCMV-HA/Cdh1, pFLAG-CMV/Hesx1, pFLAG-CMV/Hesx1 Δ HD, pFLAG-CMV/Hesx1 Δ eh1, pFLAG-

CMV/Hesx1 Δ 2/3 HD and pFLAG-CMVTM-2. Cells were harvested 24-36 hours after the transfection. Immunoprecipitation was performed using the FLAG[®] Tagged Protein immunoprecipitation Kit (SIGMA). The assay was carried out according to the manufacturer's instructions, including the optional washing step to remove any traces of unbound ANTI-FLAG antibody. The binding step was carried out for at least three hours and protein elution was mostly done under native conditions by a competition with 3x FLAG peptide.

***In vivo* ubiquitination assay**

The *in vivo* ubiquitination was performed in NIH-3T3 cells. Cells were cultured in 10 cm dishes and transiently co-transfected with different combinations of the pCMV-HA/Mad2l2, pCMV-HA/Cdh1, pFLAG-CMV/Hesx1, pEGFP-N2 and pcDNA3.1(-)-His₆Ubiquitin plasmids. The cells were incubated for 24 hours after the transfection. 10 hours before harvesting, the proteasome inhibitor MG 132 (10-25 μ M, SIGMA) was added to the culture medium. Cells were washed twice with ice-cold PBS and then lysed with 6 ml Guanidium-HCl buffer (6 M Guanidium Hydrochloride, 100 mM Na₂HPO₄/NaH₂PO₄, pH 8.0, 10 mM Tris-HCl, pH 8.0 and 10 mM β -mercaptoethanol added directly before use). Cells were collected by scrapping, and transferred into 15 ml FalconTM tubes. The cell lysate was sonicated with the Cell Disruptor B15 (Branson Sonifier) under the condition of Output Option 5 and 50 % Duty Cycle for one minute on ice. Meanwhile 160 μ l (50% slurry, per 10 cm dish) Ni-NTA Agarose (QIAGEN) was washed twice with Guanidium-HCl buffer and spun down at 800 x g for 10 seconds. 150 μ l of the cell lysate was taken as input control and subject to MeOH/CHCl₃ precipitation (see below). The remaining lysate was incubated with 160 μ l Ni-NTA resin (50% slurry) and 30 μ l of 2 M imidazole rotating for three hours at room temperature or overnight at 4°C. Resin was sedimented by centrifugation at 800 x g for 10 seconds and transferred into a 1.5 ml tube. The following washing steps were performed at room temperature rotating for 10 minutes each step, sedimenting the resin was carried out by centrifugation as described above. Resin was washed with 1.2 ml each time: 1) Guanidium-HCl buffer containing 10 mM imidazole, 2) urea buffer (8 M urea, 100 mM Na₂HPO₄/NaH₂PO₄, 10 mM Tris-HCl, pH 8.0) containing 10 mM imidazole, 3) urea buffer (8 M urea, 100 mM Na₂HPO₄/NaH₂PO₄, 10 mM Tris-HCl, pH 6.3) containing 10 mM imidazole, 4) urea buffer (8 M urea, 100 mM Na₂HPO₄/NaH₂PO₄, 10 mM Tris-HCl, pH 6.3) containing 10 mM imidazole and 0.2% Triton-X-100, 5) urea

buffer (8 M urea, 100 mM Na₂HPO₄/NaH₂PO₄, 10 mM Tris-HCl, pH 6.3) containing 10 mM imidazole and 0.1% Triton-X-100 and finally with urea buffer (8 M urea, 100 mM Na₂HPO₄/NaH₂PO₄, 10 mM Tris-HCl, pH 6.3) containing 10 mM imidazole. The buffer was completely removed after the last washing step using a Hamilton™ syringe. Proteins were eluted by incubating the resin with 60 µl 2x SDS loading buffer containing 250 mM imidazole in boiling water for six minutes. The eluate was transferred into a new 1.5 ml tube and together with the input control subject to SDS-PAGE and western blotting as described earlier.

MeOH/CHCl₃ precipitation

Protein precipitation from the *in vivo* ubiquitination cell lysate input control (2 ml tube) was performed by adding four volumes of methanol and two volumes of CHCl₃. This was mixed and briefly centrifuged at 9000 x g for 10 seconds. Afterwards, three volumes of dH₂O were added and everything vortexed for one minute. To separate the different phases, a centrifugation step at 9000 x g for five minutes was carried out and the upper phase was subsequently removed. Three volumes (in relation to initial volume) methanol were added, and the tube was mixed. After a centrifugation at 9000 x g for two minutes, the supernatant was carefully removed, and the protein pellet air dried for two to six minutes. Finally, the pellet was dissolved in 50 µl SDS loading buffer and boiled for 10 minutes.

Analysis of protein-DNA associations

Electrophoretic mobility shift assay (EMSA)

Gel retardation assays were performed to study *in vitro* the influence of Mad2l2 on the ability of Hesx1 to bind to DNA. It is known that Hesx1 protein binds to an oligonucleotide containing a palendromic PIII site (PrdQ) (Dattani et al., 1998; Sornson et al., 1996; Wilson et al., 1993). The oligo used for EMSAs is described in Table 4. The radioactive labeled PrdQ oligonucleotide was created by incubating 1 µl sense strand (0.1 nmol), 2 µl polynucleotide kinase buffer (Roche), 3 µl γ-[³²P]-dATP (30mCi, Amersham Biosciences), 0.2 µl polynucleotide kinase (Roche) and 13.8 µl dH₂O at 37°C for 45 minutes. The labeling reaction was filled up with dH₂O to 50 µl and then purified with a ProbeQuant G-50 Sephadex Micro Column (GE Healthcare). The approximately 60 µl of flow through were mixed with 6 µl 1 M KCl and 1 µl of the antisense strand (0.1 nmol) and then completely

denatured at 95°C in a thermoblock. Annealing of the sense and antisense strand was achieved by switching off the thermoblock to allow a slow cool down over several hours. The radioactivity of the double-stranded oligo was determined by using the LS1701 counter (Beckman) and the oligo was diluted with dH₂O to get 20000 cpm/μl. Binding reaction was setup, preincubating 4 μl in vitro transcribed/translated Hesx1 with 7.5 μl 4x binding buffer (40 mM Tris-HCl (pH 8), 200 mM KCl, 4 mM EDTA, 4 mM DTT, 40% glycerol and 4mg/ml BSA) and dH₂O for 15 minutes on ice. 0-6 μg of recombinant Mad2l2 protein was added followed by an additional incubation of 30 minutes. Then, 100 ng poly[di-dC] was added and the reaction incubated for five minutes at 30 °C. Finally, 1 μl of the diluted radioactive oligo was given to the reaction and it was incubated for additional 30 minutes at 30°C. The shift was performed on a 9% acrylamid gel (6 ml 30% acrylamide-bisacrylamide 29:1, 200 μl glycerol, 13.69 ml 0.5x TBE, 106.5 μl 10% APS and 10.65 μl TEMED – total volume of 20 ml). The gel polymerized within an hour and was pre-run for 45 minutes at 200 V and 4°C using 0.5% TBE buffer. Afterwards, the samples were applied and electrophoresis was performed at 200 V and 4°C for two and an half hours. The gel was fixed with cling film on one of the glass plates in a film cassette and exposed to a Biomax MR film (Kodak) at -70°C for 12-36 hours. The film was subsequent developed with the Curix 60 developing machine (Agfa).

Generation of the *Mad2l2* conditional knockout vector via recombineering

In order to generate *Mad2l2* deficient mice, a conditional knockout (cko) targeting vector was designed. This vector was created using a method described as recombineering (recombination-mediated genetic engineering) or recombinogenic engineering (Liu et al., 2003; Muyrers et al., 2001; Warming et al., 2005). Recombineering is based on homologous recombination via the gap repair mechanism. The method makes use of *E. coli* strains containing a defective λ prophage in the bacterial genome. This defective prophage expresses the recombination genes *exo*, *bet* and *gam* from the λ P_L promoter, which is under the control of the temperature-sensitive repressor λ *cl857*. *exo* encodes a 5'-3' exonuclease (Exo) that creates single-stranded overhangs on introduced linear DNA, *bet* encodes a pairing protein (Beta) which protects these overhangs and promotes the subsequent recombination process and *gam* encodes for the Gam protein that prevents degradation of linear DNA by inhibiting *E. coli* RecBCD protein. When the bacteria are

cultured at 32°C no recombinant proteins are expressed, at 42°C the repressor is inactive and *exo*, *bet* and *gam* are produced. Linear DNA with 300-500 bp of homology in the 5' and 3' ends to the target DNA (already present in the bacteria) can now be electroporated into the cells and undergoes homologous recombination with the target molecule (Liu et al., 2003; Warming et al., 2005). After each retrieval and targeting 1 ng of the plasmid was retransformed into wild-type DH10B cells and subsequently isolated. This process was done since the repression of *E. coli* RecBCD protein might lead to rolling circle replication and will eventually convert the plasmid into multimers (Feiss et al., 1982). Retransformation favors plasmid monomers and therefore eliminates the plasmid multimers.

To create *Mad2l2* deficient mice the entire coding sequence was flanked by *loxP* sites to generate a null allele upon expression of Cre. To minimize the probability of deleting an intronic sequence conserved among species which might have a regulatory function, introns were analyzed using the databases of the National Center for Biotechnology Information (NCBI, <http://www.ncbi.nih.org>). The overall size of the targeting region was 12193 bp and the *loxP* sites were introduced 113 bp upstream of the first coding exon and 20 bp downstream of the last exon, deleting finally a region of 5330 bp. The 5' homology arm was 3853 bp and the 3' homology arm 3012 bp. For gene targeting in ES cells a NotI site was introduced at the 5' end of the construct to be able to linearize it prior to the electroporation into ES cells. The different steps in the recombineering process are described in Figure 29 and below.

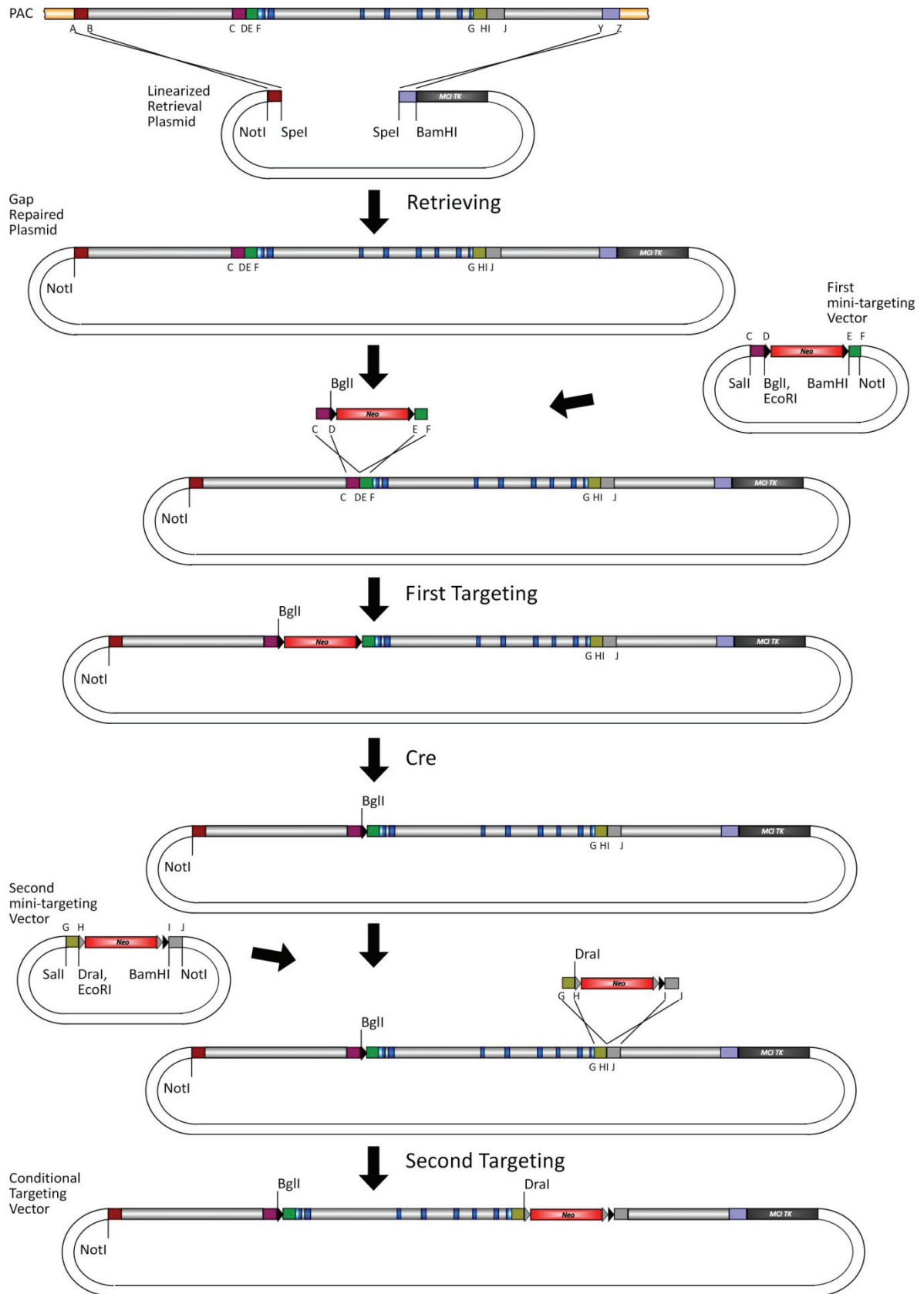


Figure 29. Generation of the *Mad212* conditional knockout vector via recombineering.

Targeting region is depicted in grey. Blue are *Mad212* coding exons and light blue display untranslated regions. Black arrow heads are *loxP* sites and grey arrow heads are *frt* sites. The *Neo* cassette is depicted in red whereas the *tk* cassette is grey.

Construction of retrieval and targeting vectors

To obtain the genomic DNA for the targeting construct, the Mouse PAC (RPCI-21) library 711 (Strain: 129/SvevTACfBR) (RZPD; now imaGenes; (Osoegawa et al., 2000)) was screened using a radioactive labeled probe of the *Mad2l2* orf. The assay and analysis was performed according to the instructions of the manufacturer. Positive clones were ordered and analyzed by PCR if they contained the genomic region needed to construct the targeting vector.

Primer sequences used for the generation of the *Mad2l2* conditional knockout vector are listed in Table 4. These primers were used to amplify the following homology fragments using the genomic PAC clone as a template: 378 bp with A, B; 403 bp with Y, Z; 420 bp with C, D; 304 bp with E, F; 459 bp with G, H and 483 bp with I, J. All PCRs were done using Pwo DNA polymerase (Roche) to prevent the occurrence of mutations.

The retrieval vector was created by ligating the PCR fragment A, B (NotI/SpeI) and Y, Z (SpeI/BamHI) into plasmid PL253 (NotI/BamHI). This plasmid contains a *Mc1*-driven Thymidine Kinase (*tk*) cassette for negative selection in ES cells.

The first mini targeting vector was generated by cloning the PCR fragments C, D (Sall/EcoRI) and E, F (BamHI/NotI) into PL452, a vector containing a neomycin (*neo*) cassette flanked by two *loxP* sites. Expression of the *neo* gene is achieved by a prokaryotic promoter (*em7*) a eukaryotic promoter (*PgK*). A new BglII restriction site was created in front of the 5' *loxP* site that was later used to identify correctly targeted ES cells by southern blot.

The second mini targeting vector was created by cloning the fragments G, H (Sall/EcoRI) and I, J (BamHI/NotI) into the PL451 vector, generating a DraI site upstream of the 5' *frt* site which was used for southern blot analysis. The PL451 plasmid contains a *neo* cassette flanked by two *frt* and one *loxP* site. The expression of the *neo* gene is as well regulated by the *em7* and *PgK* promoter.

Transformation of PAC or plasmid DNA into recombinogenic strains

For each transformation the electrocompetent recombinogenic bacterial strains were prepared fresh. A 5 ml overnight culture of the recombinogenic strain was inoculated from the glycerol stock (or a single colony from a plate containing already the target

plasmid) and incubated shaking at 32°C. The next day, the overnight culture was diluted 1:50 in 25 ml LB medium and incubated three to five hours at 32°C until bacteria had reached an OD₆₀₀ of 0.6. Now the culture was cooled down in an ice/waterbath for a few minutes and spun down in 50 ml Falcon™ tubes for five minutes at 5000 rpm and 4°C. The supernatant was poured off and the pellet in 1 ml ice-cold 10% glycerol resuspended by gently shaking the tube in the ice/waterbath. The cells were transferred in an eppendorf tube and spun down for 20 seconds at 13200 rpm at 4°C. This step was repeated twice, and the cells were resuspended in the residual amount of 10% glycerol (volume should be around 50 µl). For the electroporation the cells were mixed with the DNA (1-10 ng plasmid DNA; 1-5 µg freshly prepared PAC DNA or 100 ng purified targeting cassette) to be transformed and incubated on ice for 5 min. Transformation was done by electroporation as described earlier. After the transformation the bacteria were transferred into 950 µl of LB medium and incubated at 32°C in a shaking heat block for one hour. Finally the bacteria were plated on selective medium and incubated at 32°C for 18-24 hours. Several colonies were analyzed by restriction digestion.

Retrieving and targeting

SW102 (temperature-sensitive *exo*, *bet*, and *gam* genes) bacteria containing the target plasmid or PAC were cultured as described above. When the culture reached an OD₆₀₀ of 0.6, 10 ml were transferred into a 50 ml Falcon™ tube and incubated shaking at 42°C for 15 minutes. This heat-shock enables the bacteria to produce a sufficient amount of recombination proteins for the subsequent homologous recombination. The rest of the bacteria served as a control and were put back at 32°C. The heat shock-induced and the uninduced cultures were now cooled down by gently shaking them in an ice/waterbath for a few minutes and transformed as describe above.

Excision of the Neo cassette

To excise the first *neo* cassette leaving only the 5' *loxP* site and to control if all *loxP* and *frt* sites were functional, the target plasmid was transformed into arabinose induced SW106 (*ara*-inducible *Cre* gene) or SW105 (*ara*-inducible *Fpe* gene) bacteria. The bacteria were cultured as described earlier until they reached an OD₆₀₀ of 0.6. 10 ml of the culture were transferred into a 50 ml Falcon™ tube and 100 µl of 10% L(+) arabinose (Sigma-Aldrich) was added. The induction took place at 32°C shaking for one hour, and the remainder of

the culture was used for the control experiment. Transformation was performed as described above.

Gene targeting in mouse ES cells and production of chimeras

The *Mad2l2* cko-targeting vector was subsequently linearized with NotI, a phenol extraction and ethanol precipitation was performed. 40 µg of the vector was electroporated into the MPI-II ES cells. ES cells underwent positive/negative selection with G418 and ganciclovir (Ganc) respectively. Cells containing the *neo* cassette survive the exposure to G418. If a targeted homologous recombination occurred, the ES cells lost the *tk* cassette and survive as well the exposure to ganciclovir. Electroporation, selection and culture of the ES cells was carried out by Sharif Mashur. The G418^r Ganc^r ES cells colonies were picked for southern analysis to confirm targeted insertion of the cko-construct. Positive ES cells were used for the production of aggregation chimeras. The ES cells were aggregated with diploid CD-1[®]/ICR morula-stage embryos and cultured to the blastocyst-stage. The aggregated blastocyst was transferred into the oviduct of pseudopregnant female recipient mice. Aggregation and oviduct transfer was performed by Ulrich Franke. Chimeric mice which gave germ-line transmission were crossed with CMV-Cre mice (CMV promoter driven Cre recombinase; (Schwenk et al., 1995)) to generate *Mad2l2*^{+/-} (heterozygous) offspring.

Isolation and analysis of embryos and mice

Dissection and fixation of mouse embryos

Dissection of mouse embryos was performed in the whole as described in “Manipulating the Mouse Embryo: A Laboratory Manual” (Nagy et al., 2003). Briefly, pregnant mice at the desired stage of embryonic development were sacrificed by cervical dislocation. The abdominal cavity was opened and the uterus was dissected by cutting the uterus below the oviduct and separating it from the mesometrium and cutting across the cervix. After the uterus was dissected it was washed in ice-cold PBS and opened by cutting the antimesometrial wall with the tip of a pair of fine scissors. The decidua were now shelled out of the uterus with forceps. Embryos were dissected from the decidua and a tissue sample from the yolk sack, the amnion or the tail was taken from each embryo. These samples were used to extract genomic DNA for genotyping. The embryos were staged

according to “The anatomical basis of mouse development” (Kaufman and Bard, 1999) and fixed in 4% PFA/PBS overnight and subsequently washed in PBS.

Bouin’s fixation of postnatal mouse heads

Postnatal mice were sacrificed, the head was cut off and the skin was removed. The head was briefly washed in ice-cold PBS and then incubated for two to four days in Bouin’s Fix (Sigma). Bouin’s fix has the advantage that it decalcifies the skull which simplifies sectioning later on. After fixation, the heads were dehydrated using an ascending ethanol concentration (70%, 80%, 90%, 95% 97,5% 100%) and a final incubation in isopropanol. Each step was done overnight at 4°C. Then, they were incubated for two days in toluol at room temperature and for three days in liquid paraplast 60°C (replacing it every day). The embedding and sectioning procedure was performed as describe below.

Paraffin embedding and sectioning

The PFA fixed embryos were washed three times with PBS to remove the fixative and three times with 0.86% NaCl to wash out salt crystals. Each washing step was performed for one hour at 4°C. Following this washing steps the embryos were dehydrated with an ascending ethanol concentration. They were incubated twice in 50% ethanol for 15 minutes, two times in 70% ethanol for 15 minutes (or overnight), three times in 80% ethanol for 20 minutes, three times in 90% ethanol for 30 minutes, four times in 96% ethanol for 30 minutes and five times in pure ethanol for 20 minutes at 4°C. Finally the embryos were transferred into isopropanol and incubated for overnight at 4°C. The infiltration procedure was done at room temperature. The embryos were incubated in 25% toluol/isopropanol, 50% toluol/isopropanol and 75% toluol/isopropanol each step for 30 minutes. Afterwards they were incubated three times in 100% toluol for one hour before they were transferred into liquid paraplast (60°C). Paraplast was changed every day for three days. The embryos were embedded in appropriate paraplast filled blocks. The resulting blocks were stored at 4°C. 10 µm thick sections were produced using a microtome (Leica). Right after cutting, the sections were transferred into a heated water-bath (43°C) to allow them to spread. Afterwards the sections were collected on microscope glass slides, dried overnight at 37°C and stored at 4°C.

Hematoxylin and Eosin staining (H&E staining)

The H&E staining was used to get a histological overview of the examined tissue. Hematoxylin is a basic dye, which colors basophilic structures of the cell, mostly nucleic acids with blue-purple hue. The alcohol-based eosin Y colors intra- and extracellular protein. It stains predominantly the cytoplasm in pink.

Paraffin sections were deparaffinized by washing them three times for three minutes with Xylene and rehydrated in decreasing concentrations of ethanol (100%, 90%, 70% and 50%, each for two minutes). Sections were placed in deionized H₂O for five minutes and afterwards stained with Hematoxylin (Sigma HHS16) for ten minutes. Then, the sections were washed three times for three minutes with tap water and destained with acid ethanol (5 ml concentrated HCl + 400 ml 70% ethanol) for 20 seconds. Afterwards the sections were washed again two times with deionized H₂O and stained with Eosin for 15 seconds. Sections were dehydrated, and placed in Xylene three times for three minutes. Finally, stained sections were mounted on coverslips using Eukitt (Kindler) mounting medium, and dried overnight in the hood.

Whole mount in situ-hybridization

The whole mount in situ-hybridization analysis was performed as described (Pilarski, 2004). In brief, after fixation the embryos were transferred into nets, which fit into six well plates. They were dehydrated and the plasma membranes were removed by an ascending methanol series. Afterwards the embryos were rehydrated and bleached by H₂O₂ to increase the transparency of the tissue. The proteinase K (10µg/ml) digest was done to reach a higher permeability of the tissue and to remove proteins which are bound to RNA and therefore making the RNA easier accessible for the antisense RNA probe. To increase the tissue permeability again, the embryos were incubated in RIPA buffer (150 mM NaCl, 50 mM Tris pH 8.0, 1 mM EDTA pH 8.0, 1% NP40 (Nonidet[®] P40), 0.5% DOC, 0.1% SDS). The embryos were then refixed in PFA because the proteinase K digest and the RIPA buffer treatment reduced their mechanical stability extensively. The prehybridization (50% Formamide, 5x SSC pH 4.5, 1% SDS, 50 µg/ml yeast tRNA, 50 µg/ml heparin) as well as the hybridization (antisense RNA probe in a volume ratio 1:100 to the prehybridization buffer) was performed shaking at 70°C. Hybridization was performed overnight. To remove the unspecific bound antisense RNA probes the embryos were

brought through several, solution 2 (10 ml 20x SSC, pH 7, 50 ml Formamide, 100 µl Tween-20 and dH₂O ad 100 ml.) and MABT (100 mM Maleic acid, 150 mM NaCl, pH 7.5, adjusted using NaOH, 0.1% Tween-20), washing steps. In addition they were incubated in freshly prepared RNase A (100 µg/ml) in RNase buffer (10 ml 5 M NaCl, 1 ml 1 M Tris-HCl, pH 7.5, 0.1 ml Tween-20 and dH₂O ad 100 ml.) to reduce the unspecific background and in blocking solution (12 ml MABT, 4 ml heat inactivated FCS and 4 ml 10% BBR/MAB) to block unspecific binding site for the antibody. Finally the embryos were brought into blocking solution containing anti-digoxigenin-AP, Fab fragments (Roche, 1:2000) and incubated overnight at 4°C. Unspecific bound antibodies were removed by several washing steps in MABT and subsequently NTMT (100 mM NaCl, 100 mM Tris-HCl pH 9.5, 50 mM MgCl₂ and 1 % Tween-20). After passing through the washing steps the embryos were transferred into small glass bottles and on a rotor to optimize the washing procedure. The color reaction varies dramatically corresponding to the number of transcripts therefore it was necessary to monitor it all the time. The embryos were brought back into nets and 6 well plates. The staining solution NBT/BCIP (Roche) was diluted 1:50 in NTMT containing 2 mM levamisol. The reaction was performed under light exclusion and stopped by washing with PBT. Afterwards embryos were refixed with PFA and brought into 80% glycerin where they can be stored at 4°C. They were documented on agarose dishes using the Olympus SZX 12 binocular.

Immunohistochemistry

Deparaffinization of paraffin-sections was done using Histoclear (Vogel GmbH). Slides were dewaxed twice for three minutes, transferred into 50% Histoclear/ethanol for additional three minutes and washed twice in 100% ethanol for three minutes. Individual sections were then encircled with the ImmEdge™ Pen (Vector Laboratories) and rehydrated in a descending concentration of ethanol (95%, 70%, 50%) and finally tap water for three minutes each step. The slides were boiled in Antigen Unmasking Solution (1:100 in dH₂O, Vector Laboratories) for five minutes and immediately washed with running tap water. Afterwards the sections were washed twice for five minutes in PBS and then twice in 0.025% Triton X-100/PBS for five minutes. The long incubations were all done in a wet-chamber to prevent the sections from drying out. To block unspecific binding sites, the slides were incubated in blocking solution (10% FCS, 1% BSA, in PBS) for 45 minutes to two hours. The primary antibody was applied diluted in blocking solution

for overnight at 4°C. The next day slides were rinsed in 0.025% Triton X-100/PBS twice for five minutes and the fluorophore-conjugated secondary antibody diluted in blocking solution was applied. This incubation as well as the following steps were done in the dark to avoid photobleaching. Incubation took place at room temperature for two hours. The sections were washed in PBS three times for five minutes and mounted with VECTASHIELD® Mounting Medium with DAPI (Vector Laboratories). The coverslip was sealed using nail polish.

Cell culture

Cell lines

Cell line	Cell type	DSMZ no.	Morphology	Reference	Culture medium
COS-7	African green monkey kidney	ACC 60	Fibroblast-like	(Gluzman, 1981)	DMEM + 4mM L-glutamine + 4,5 mg/ml glucose +10% FCS
NIH-3T3	Swiss mouse embryo	ACC 59	Fibroblast	(Aaronson and Todaro, 1968)	DMEM + 4mM L-glutamine + 4,5 mg/ml glucose +10% FCS
MPI-II	Mouse embryonic stem cells	-	Embryonic stem cells	Gruss, P. 1993	DMEM +20% FCS +1% non-essential amino acids +1% sodium pyruvate (100mM) +1% L-glutamine (200mM)+ Lif 1000U/ml +0.1mM β-mercaptoethanol
Primary cells					
MEF-Mad2l2 (+/+; -/-)	Mouse embryo		Fibroblast	(This study)	DMEM + 4mM L-glutamine + 4,5 mg/ml glucose +10% FCS

Table 10. Cell lines used in this study.

Revival, subculture and cryopreservation of cells

Cell vials from the liquid nitrogen storage were thawed as rapidly as possible in a 37°C water bath, to minimize intracellular ice crystal growth during the warming process. The cell suspension was then transferred into a 15 ml Falcon™ tube and slowly diluted in 10 ml of the appropriate culture medium. Rapid dilution reduces cell viability because sudden dilution may cause severe osmotic damage. The cells were centrifuged at 210 x g for five minutes and the medium was carefully aspirated. Subsequently, cells were resuspended in the appropriate volume of culture medium by pipetting up and down. The cell suspension was plated on an appropriate culture dish and gently shaken (five times

left-right and back and forth) to distribute the cells equally. The cells were cultured in a humidified BBD 6220 incubator (Heraeus) at 37°C and a 5% CO₂ atmosphere.

Generally cells were passaged when they had reached 70-95% of confluence. The culture medium was removed and the cells were washed twice with the same amount of prewarmed PBS (37°C). Cells were dissociated applying an appropriate amount of Trypsin (0.05% Trypsin/EDTA; Gibco BRL®) on the dish (2 ml/10 cm dish), followed by an incubation of five minutes in a humidified incubator. Right after the incubation the dish was shaken until all the cells were floating and then five times the amount of culture medium was added to the dish. The cell suspension was pipetted up and down a few times to disperse the cells and subsequently transferred into 15 ml Falcon™ tubes. To sediment the cells they were centrifuged at 210 x g for five minutes and afterwards resuspended in the desired volume of culture medium. For subculture, the cells were usually diluted 1:6. If necessary the concentration of the cell suspension was determined using a Hemocytometer slide (improved Neubauer). 10 µl of the cell suspension were applied to the Hemocytometer and four of the 1 mm² squares were counted to improve accuracy of the result. The following equation was used to determine the concentration:

$$\text{concentration}_{(\text{cells/ml})} = \frac{\text{number of cells}}{4} \times 10^4 .$$

If the cells were subjected to cryopreservation, the cells of a 10 cm dish were resuspended in 2 ml of culture medium. 500 µl of this cell suspension was transferred into a CryoTube™ (NUNC™) containing 500 µl of 2x freezing medium (culture medium, 16.6% DMSO, 20% FCS) and mixed by inverting. The tubes were frozen at -20°C for three hours to overnight, then transferred to -80°C for overnight up to a month and finally stored in liquid nitrogen.

Cell transfection

Cells were transfected by lipofection with one or several plasmids using FuGENE® 6 Transfection Reagent (Roche). Plasmid DNAs used for transfections were always subject to phenol extraction and ethanol precipitation to prevent contamination of the cell cultures. The entire procedure was performed according to the instructions of the manufacturer.

Preparation of primary mouse embryonic fibroblasts (MEF's)

The uterus of a pregnant mouse (13.5 dpc) was dissected into warm (37°C) PBS and transferred in a cell culture hood. Embryos were dissected from the uterus into fresh PBS (10 cm dishes). In a next step, individual embryos were transferred into fresh PBS and extremities, head, tail and inner organs were removed. The tail was used for isolation of genomic DNA and subsequent genotyping. The remaining corpus of the embryos was placed in a 35 mm Petri dish containing 2 ml of Trypsin (0.05% Trypsin/EDTA; Gibco BRL®). Embryos were first disrupted, using two forceps until only small cell clusters remained. Afterwards they were transferred into 15 ml Falcon™ tubes. Cell clusters were disrupted by pipetting up and down. To remove the Trypsin, cells were centrifuged for five minutes at 210 x g (Heraeus Megafuge 1.0 - 1000rpm). Carefully, the trypsin was (might be problematic due to the viscosity) removed with a pipette and the cell pellet redissolved in culture medium. One embryo resulted in enough cells for a 15 cm dish. After cells were attached the medium was replaced.

Measurement of cell proliferation rates

The quantification of culture growth was done to determine the characteristic of growth pattern of Mad212^{-/-} MEF's and wild type MEF's. For an initial quantification a series of 12 well plates with cultures at three different cell concentrations (1 x 10⁴/ml, 3 x 10⁴/ml, 1 x 10⁴/ml) was set up and counted with a Hemocytometer at a daily basis for three days. In addition a duplicate at each density was stained with Giemsa and documented. To monitor the growth rate over a longer period, cells were seeded in 24-, 12- and 6-well plates at a concentration of 1 x 10⁴. The cell suspension was added slowly from the center of the well and not shaken to prevent an accumulation of cells in the middle of the well. Cell concentration was determined at daily intervals by trypsinizing (volume was adjusted according to the well size) the culture and counting the cells with the Hemocytometer.

Giemsa staining

Giemsa stain is a polychromatic stain which stains the nucleus pink-magenta, the nucleoli dark blue, and the cytoplasm pale gray-blue. It provides a convenient method for staining complete culture dishes. The Giemsa solution was prepared by mixing 500 ml glycerol with 500 ml methanol and subsequent addition of 8.5 g of Giemsa-stain (Sigma). The staining solution was incubated mixing at room temperature overnight. To stain the cells

directly in the multiwell plate, the medium was removed and was washed once with PBS. Afterwards 50% methanol/PBS was added and the culture was incubated for two minutes. The 50% methanol/PBS solution was removed and displaced by methanol. After an incubation of 10 minutes the methanol was removed and the culture was briefly rinsed with fresh methanol. Giemsa stain was added in a way that the entire cell monolayer was covered. The culture was incubated for two minutes, before the staining solution was diluted (1:5) with water and it was incubated agitated gently for a further two minutes. The stain was displaced with water so that the scum that forms due to oxidation was carefully removed without coating the cells. Now the cells were gently washed in running tap water for ten to twenty seconds and then washed once with dH₂O. The cells were examined and documented while still wet using the SZX12 stereo microscope and cell[^]D software (both Olympus). The cultures can be stored dry, and are rewetted to re-examine.

Immunohistochemistry

The cells were passaged and cultured on coverslips in 24-well plates. When the cells reached the desired confluency the medium was removed and the cells were washed twice with PBS. The cells were fixed with 4% PFA for 20 minutes at room temperature and three times rinsed with PBS incubating them for five minutes each step. To permeabilize the cells they were incubated with 0.5% Triton X-100/PBS for five minutes and then washed twice with PBT (0.1% Tween 20/PBS) for five minutes each time. Blocking of unspecific binding sites was done in blocking solution (10% FCS, 1% BSA, in PBT) at room temperature for one to two hours. The incubation with the appropriately diluted primary antibody was performed in blocking solution in a wet-chamber at 4°C overnight. The next day coverslips were washed with PBT twice and once with blocking solution for five minutes each time. Afterwards the cells were incubated with the diluted fluorophore-conjugated secondary antibody at room temperature and in the dark for one hour. Finally, cells were washed three times with PBT for five minutes, rinsed briefly with water and subsequently mounted with VECTASHIELD[®] Mounting Medium with DAPI (Vector Laboratories). The coverslips were sealed using nail polish. The samples were monitored and documented with the BX-60 fluorescence microscope (Olympus) using the cell[^]P software (Olympus).

TUNEL assay

The TUNEL (Terminal deoxynucleotidyltransferase-mediated dUTP-biotin nick end labeling) assay was used to examine the occurrence of apoptosis in transgenic MEF's. This method detects DNA strand breaks enzymatically by labeling the free 3'-OH termini with modified nucleotides (Gavrieli et al., 1992). This labeling is the basis of the ApopTag® Red *In Situ* Apoptosis Detection Kit (CHEMICON® International) which was used in this study. The MEF's were cultured on coverslips in 24 well plates for two days. The assay was carried out according to the instructions of the manufacturer and the coverslips were mounted with VECTASHIELD® Mounting Medium with DAPI (Vector Laboratories). The coverslips were sealed using nail polish. The samples were examined and documented with the BX-60 fluorescence microscope (Olympus) using the cell^P software (Olympus).

FACS analysis of mouse embryonic fibroblasts

Flow cytometric analysis was performed to determine the cell-cycle phase distribution of the wild type and transgenic MEF's. The CycleTEST™ PLUS DNA Reagent Kit (Becton Dickinson) was used to stain cell nuclei with propidium iodide. The procedure involves dissolving of the cell membrane lipids with a nonionic detergent, removing the cytoskeleton and nuclear proteins with trypsin and digesting the RNA. The nuclear chromatin is stabilized with spermine and in the clean, isolated nuclei DNA is bound stoichiometrically by propidium iodide.

The medium of the MEF's was collected and used to resuspend the cells after the trypsinization. After removal of the medium, cells were washed with PBS and incubated with trypsin (0.05% Trypsin/EDTA; Gibco BRL®) in a humidified incubator at 37°C for five minutes. The trypsin was inactivated by transferring the previously removed medium into the culture dish and pipetting up and down for a few times. Cell concentration was determined using a Hemocytometer as described earlier. 1×10^6 cells were transferred into a 15 ml Falcon™ tube and sedimented by centrifugation at $210 \times g$ for five minutes. Afterwards the medium was carefully removed without disturbing the cell pellet. Cells were twice resuspended in 2 ml PBS and sedimented. Finally the cell pellet was resuspended in 1 ml of PBS, transferred into a freezer-safe tube with screw cap and rapidly frozen in a mixture of dry ice and 99% ethanol. Samples were stored at -80°C. Right before analysis the cells were thawed as fast as possible in a water-bath at 37°C

without allowing them to reach this temperature. The cell suspension was transferred into 12 x 75 mm capped polypropylene tubes (Becton Dickinson Falcon) and centrifuged at 400 x g for five minutes at room temperature. The supernatant was carefully removed and residual drops were removed with a tissue. 250 µl Solution A (trypsin buffer) was added, the tube was mixed by gently tapping and it was incubated for 10 minutes at room temperature. This procedure was repeated by adding an additional 200 µl of Solution B (RNase buffer). After an incubation time of 10 minutes, 200 µl of ice cold Solution C (propidium iodide stain solution) was added, the suspension was gently mixed and incubated for 10 minutes in the dark on ice. The samples were now ready for analysis and needed to run on the flow cytometer within three hours. The tubes were vortexed immediately before the measurement with the FACS Calibur Flow Cytometer (Beckton Dickinson) and the obtained data were analyzed with the Modifit LT software (Verify Software House Inc.). The staining procedure as well as the flow cytometry analysis was performed in the group of Prof. Dr. Detlef Doenecke (Biochemie und Molekulare Zellbiologie, Georg-August University of Göttingen) with the help of Krisitina Haenecke and Dr. Nicole Happel.

BIBLIOGRAPHY

Aaronson, S.A., and Todaro, G.J. (1968). Development of 3T3-like lines from Balb-c mouse embryo cultures: transformation susceptibility to SV40. *J Cell Physiol* **72**, 141-148.

Andersen, B., and Rosenfeld, M.G. (2001). POU domain factors in the neuroendocrine system: lessons from developmental biology provide insights into human disease. *Endocr Rev* **22**, 2-35.

Andersen, P.L., Xu, F., and Xiao, W. (2008). Eukaryotic DNA damage tolerance and translesion synthesis through covalent modifications of PCNA. *Cell Res* **18**, 162-173.

Andoniadou, C.L., Signore, M., Sajedi, E., Gaston-Massuet, C., Kelberman, D., Burns, A.J., Itasaki, N., Dattani, M., and Martinez-Barbera, J.P. (2007). Lack of the murine homeobox gene *Hesx1* leads to a posterior transformation of the anterior forebrain. *Development* **134**, 1499-1508.

Araki, M., Yu, H., and Asano, M. (2005). A novel motif governs APC-dependent degradation of *Drosophila* ORC1 in vivo. *Genes Dev* **19**, 2458-2465.

Aravind, L., and Koonin, E.V. (1998). The HORMA domain: a common structural denominator in mitotic checkpoints, chromosome synapsis and DNA repair. *Trends Biochem Sci* **23**, 284-286.

Bashir, T., Dorrello, N.V., Amador, V., Guardavaccaro, D., and Pagano, M. (2004). Control of the SCF(Skp2-Cks1) ubiquitin ligase by the APC/C(Cdh1) ubiquitin ligase. *Nature* **428**, 190-193.

Bayramov, A.V., Martynova, N.Y., Eroshkin, F.M., Ermakova, G.V., and Zaraisky, A.G. (2004). The homeodomain-containing transcription factor X-nkx-5.1 inhibits expression of the homeobox gene *Xanf-1* during the *Xenopus laevis* forebrain development. *Mech Dev* **121**, 1425-1441.

Bemark, M., Khamlichi, A.A., Davies, S.L., and Neuberger, M.S. (2000). Disruption of mouse polymerase zeta (*Rev3*) leads to embryonic lethality and impairs blastocyst development in vitro. *Curr Biol* **10**, 1213-1216.

Birnboim, H.C., and Doly, J. (1979). A rapid alkaline extraction procedure for screening recombinant plasmid DNA. *Nucleic Acids Res* **7**, 1513-1523.

Borges, H.L., Linden, R., and Wang, J.Y. (2008). DNA damage-induced cell death: lessons from the central nervous system. *Cell Res* **18**, 17-26.

Brickman, J.M., Clements, M., Tyrell, R., McNay, D., Woods, K., Warner, J., Stewart, A., Beddington, R.S., and Dattani, M. (2001). Molecular effects of novel mutations in *Hesx1/HESX1* associated with human pituitary disorders. *Development* **128**, 5189-5199.

Cahill, D.P., da Costa, L.T., Carson-Walter, E.B., Kinzler, K.W., Vogelstein, B., and Lengauer, C. (1999). Characterization of *MAD2B* and other mitotic spindle checkpoint genes. *Genomics* **58**, 181-187.

Camper, S.A., Saunders, T.L., Katz, R.W., and Reeves, R.H. (1990). The *Pit-1* transcription factor gene is a candidate for the murine Snell dwarf mutation. *Genomics* **8**, 586-590.

Campisi, J., and d'Adda di Fagagna, F. (2007). Cellular senescence: when bad things happen to good cells. *Nat Rev Mol Cell Biol* **8**, 729-740.

- Carvalho, L.R., Woods, K.S., Mendonca, B.B., Marcal, N., Zamparini, A.L., Stifani, S., Brickman, J.M., Arnhold, I.J., and Dattani, M.T. (2003). A homozygous mutation in HESX1 is associated with evolving hypopituitarism due to impaired repressor-corepressor interaction. *J Clin Invest* *112*, 1192-1201.
- Chan, S.H., Hung, F.S., Chan, D.S., and Shaw, P.C. (2001). Trichosanthin interacts with acidic ribosomal proteins P0 and P1 and mitotic checkpoint protein MAD2B. *Eur J Biochem* *268*, 2107-2112.
- Charles, M.A., Suh, H., Hjalt, T.A., Drouin, J., Camper, S.A., and Gage, P.J. (2005). PITX genes are required for cell survival and Lhx3 activation. *Mol Endocrinol* *19*, 1893-1903.
- Chen, J., and Fang, G. (2001). MAD2B is an inhibitor of the anaphase-promoting complex. *Genes Dev* *15*, 1765-1770.
- Cheung, H.W., Chun, A.C., Wang, Q., Deng, W., Hu, L., Guan, X.Y., Nicholls, J.M., Ling, M.T., Chuan Wong, Y., Tsao, S.W., *et al.* (2006). Inactivation of human MAD2B in nasopharyngeal carcinoma cells leads to chemosensitization to DNA-damaging agents. *Cancer Res* *66*, 4357-4367.
- Chevray, P.M., and Nathans, D. (1992). Protein interaction cloning in yeast: identification of mammalian proteins that react with the leucine zipper of Jun. *Proc Natl Acad Sci U S A* *89*, 5789-5793.
- Chou, S.J., Hermes, E., Hatta, T., Feltner, D., El-Hodiri, H.M., Jamrich, M., and Mahon, K. (2006). Conserved regulatory elements establish the dynamic expression of Rpx/Hesx1 in early vertebrate development. *Dev Biol* *292*, 533-545.
- Christensen, K.L., Brennan, J.D., Aldridge, C.S., and Ford, H.L. (2006). Cell cycle regulation of the human Six1 homeoprotein is mediated by APC(Cdh1). *Oncogene*.
- Cohen, R.N., Cohen, L.E., Botero, D., Yu, C., Sagar, A., Jurkiewicz, M., and Radovick, S. (2003). Enhanced repression by HESX1 as a cause of hypopituitarism and septooptic dysplasia. *J Clin Endocrinol Metab* *88*, 4832-4839.
- Couly, G., and Le Douarin, N.M. (1988). The fate map of the cephalic neural primordium at the presomitic to the 3-somite stage in the avian embryo. *Development* *103 Suppl*, 101-113.
- Curtis, M.J., and Hays, J.B. (2007). Tolerance of dividing cells to replication stress in UVB-irradiated Arabidopsis roots: requirements for DNA translesion polymerases eta and zeta. *DNA Repair (Amst)* *6*, 1341-1358.
- Cushman, L.J., Watkins-Chow, D.E., Brinkmeier, M.L., Raetzman, L.T., Radak, A.L., Lloyd, R.V., and Camper, S.A. (2001). Persistent Prop1 expression delays gonadotrope differentiation and enhances pituitary tumor susceptibility. *Hum Mol Genet* *10*, 1141-1153.
- Darzynkiewicz, Z., Juan, G., Li, X., Gorczyca, W., Murakami, T., and Traganos, F. (1997). Cytometry in cell necrobiology: analysis of apoptosis and accidental cell death (necrosis). *Cytometry* *27*, 1-20.
- Dasen, J.S., Barbera, J.P., Herman, T.S., Connell, S.O., Olson, L., Ju, B., Tollkuhn, J., Baek, S.H., Rose, D.W., and Rosenfeld, M.G. (2001). Temporal regulation of a paired-like homeodomain repressor/TLE corepressor complex and a related activator is required for pituitary organogenesis. *Genes Dev* *15*, 3193-3207.

- Dattani, M.T. (2004). Novel insights into the aetiology and pathogenesis of hypopituitarism. *Horm Res 62 Suppl 3*, 1-13.
- Dattani, M.T. (2005). Growth hormone deficiency and combined pituitary hormone deficiency: does the genotype matter? *Clin Endocrinol (Oxf)* *63*, 121-130.
- Dattani, M.T., Martinez-Barbera, J.P., Thomas, P.Q., Brickman, J.M., Gupta, R., Martensson, I.L., Toresson, H., Fox, M., Wales, J.K., Hindmarsh, P.C., *et al.* (1998). Mutations in the homeobox gene HESX1/Hesx1 associated with septo-optic dysplasia in human and mouse. *Nat Genet* *19*, 125-133.
- Deckbar, D., Birraux, J., Krempler, A., Tchouandong, L., Beucher, A., Walker, S., Stiff, T., Jeggo, P., and Lobrich, M. (2007). Chromosome breakage after G2 checkpoint release. *J Cell Biol* *176*, 749-755.
- Diaz, M., Verkoczy, L.K., Flajnik, M.F., and Klinman, N.R. (2001). Decreased frequency of somatic hypermutation and impaired affinity maturation but intact germinal center formation in mice expressing antisense RNA to DNA polymerase zeta. *J Immunol* *167*, 327-335.
- Diffley, J.F. (2004). Regulation of early events in chromosome replication. *Curr Biol* *14*, R778-786.
- Dower, W.J., Miller, J.F., and Ragsdale, C.W. (1988). High efficiency transformation of *E. coli* by high voltage electroporation. *Nucleic Acids Res* *16*, 6127-6145.
- Eagleson, G.W., and Harris, W.A. (1990). Mapping of the presumptive brain regions in the neural plate of *Xenopus laevis*. *J Neurobiol* *21*, 427-440.
- Eeken, J.C., Romeijn, R.J., de Jong, A.W., Pastink, A., and Lohman, P.H. (2001). Isolation and genetic characterisation of the *Drosophila* homologue of (SCE)REV3, encoding the catalytic subunit of DNA polymerase zeta. *Mutat Res* *485*, 237-253.
- Ermakova, G.V., Alexandrova, E.M., Kazanskaya, O.V., Vasiliev, O.L., Smith, M.W., and Zarsisky, A.G. (1999). The homeobox gene, *Xanf-1*, can control both neural differentiation and patterning in the presumptive anterior neurectoderm of the *Xenopus laevis* embryo. *Development* *126*, 4513-4523.
- Ermakova, G.V., Solovieva, E.A., Martynova, N.Y., and Zarsisky, A.G. (2007). The homeodomain factor *Xanf* represses expression of genes in the presumptive rostral forebrain that specify more caudal brain regions. *Dev Biol* *307*, 483-497.
- Eroshkin, F., Kazanskaya, O., Martynova, N., and Zarsisky, A. (2002). Characterization of cis-regulatory elements of the homeobox gene *Xanf-1*. *Gene* *285*, 279-286.
- Esposito, G., Godindagger, I., Klein, U., Yaspo, M.L., Cumano, A., and Rajewsky, K. (2000). Disruption of the Rev3l-encoded catalytic subunit of polymerase zeta in mice results in early embryonic lethality. *Curr Biol* *10*, 1221-1224.
- Fang, G., Yu, H., and Kirschner, M.W. (1998). Direct binding of CDC20 protein family members activates the anaphase-promoting complex in mitosis and G1. *Mol Cell* *2*, 163-171.
- Fang, S., and Weissman, A.M. (2004). A field guide to ubiquitylation. *Cell Mol Life Sci* *61*, 1546-1561.

- Feiss, M., Siegele, D.A., Rudolph, C.F., and Frackman, S. (1982). Cosmid DNA packaging in vivo. *Gene* 17, 123-130.
- Furuta, T., Tuck, S., Kirchner, J., Koch, B., Auty, R., Kitagawa, R., Rose, A.M., and Greenstein, D. (2000). EMB-30: an APC4 homologue required for metaphase-to-anaphase transitions during meiosis and mitosis in *Caenorhabditis elegans*. *Mol Biol Cell* 11, 1401-1419.
- Gabellini, D., Colaluca, I.N., Vodermaier, H.C., Biamonti, G., Giacca, M., Falaschi, A., Riva, S., and Peverali, F.A. (2003). Early mitotic degradation of the homeoprotein HOXC10 is potentially linked to cell cycle progression. *EMBO J* 22, 3715-3724.
- Gage, P.J., Brinkmeier, M.L., Scarlett, L.M., Knapp, L.T., Camper, S.A., and Mahon, K.A. (1996). The Ames dwarf gene, *df*, is required early in pituitary ontogeny for the extinction of *Rpx* transcription and initiation of lineage-specific cell proliferation. *Mol Endocrinol* 10, 1570-1581.
- Gan, G.N., Wittschieben, J.P., Wittschieben, B.O., and Wood, R.D. (2008). DNA polymerase zeta (*pol zeta*) in higher eukaryotes. *Cell Res* 18, 174-183.
- Gavrieli, Y., Sherman, Y., and Ben-Sasson, S.A. (1992). Identification of programmed cell death in situ via specific labeling of nuclear DNA fragmentation. *J Cell Biol* 119, 493-501.
- Gieffers, C., Peters, B.H., Kramer, E.R., Dotti, C.G., and Peters, J.M. (1999). Expression of the CDH1-associated form of the anaphase-promoting complex in postmitotic neurons. *Proc Natl Acad Sci U S A* 96, 11317-11322.
- Gleiberman, A.S., Fedtsova, N.G., and Rosenfeld, M.G. (1999). Tissue interactions in the induction of anterior pituitary: role of the ventral diencephalon, mesenchyme, and notochord. *Dev Biol* 213, 340-353.
- Glotzer, M., Murray, A.W., and Kirschner, M.W. (1991). Cyclin is degraded by the ubiquitin pathway. *Nature* 349, 132-138.
- Gluzman, Y. (1981). SV40-transformed simian cells support the replication of early SV40 mutants. *Cell* 23, 175-182.
- Golden, A., Sadler, P.L., Wallenfang, M.R., Schumacher, J.M., Hamill, D.R., Bates, G., Bowerman, B., Seydoux, G., and Shakes, D.C. (2000). Metaphase to anaphase (*mat*) transition-defective mutants in *Caenorhabditis elegans*. *J Cell Biol* 151, 1469-1482.
- Hermesz, E., Mackem, S., and Mahon, K.A. (1996). *Rpx*: a novel anterior-restricted homeobox gene progressively activated in the prechordal plate, anterior neural plate and Rathke's pouch of the mouse embryo. *Development* 122, 41-52.
- Hermesz, E., Williams-Simons, L., and Mahon, K.A. (2003). A novel inducible element, activated by contact with Rathke's pouch, is present in the regulatory region of the *Rpx/Hesx1* homeobox gene. *Dev Biol* 260, 68-78.
- Hershko, A., and Ciechanover, A. (1998). The ubiquitin system. *Annu Rev Biochem* 67, 425-479.
- Hoegge, C., Pfander, B., Moldovan, G.L., Pyrowolakis, G., and Jentsch, S. (2002). RAD6-dependent DNA repair is linked to modification of PCNA by ubiquitin and SUMO. *Nature* 419, 135-141.

- Holbeck, S.L., and Strathern, J.N. (1997). A role for REV3 in mutagenesis during double-strand break repair in *Saccharomyces cerevisiae*. *Genetics* *147*, 1017-1024.
- Hsu, J.Y., Reimann, J.D., Sorensen, C.S., Lukas, J., and Jackson, P.K. (2002). E2F-dependent accumulation of hEmi1 regulates S phase entry by inhibiting APC(Cdh1). *Nat Cell Biol* *4*, 358-366.
- Irniger, S., Piatti, S., Michaelis, C., and Nasmyth, K. (1995). Genes involved in sister chromatid separation are needed for B-type cyclin proteolysis in budding yeast. *Cell* *81*, 269-278.
- Ito, H., Fukuda, Y., Murata, K., and Kimura, A. (1983). Transformation of intact yeast cells treated with alkali cations. *J Bacteriol* *153*, 163-168.
- Iwai, H., Kim, M., Yoshikawa, Y., Ashida, H., Ogawa, M., Fujita, Y., Muller, D., Kirikae, T., Jackson, P.K., Kotani, S., *et al.* (2007). A bacterial effector targets Mad2L2, an APC inhibitor, to modulate host cell cycling. *Cell* *130*, 611-623.
- Japon, M.A., Rubinstein, M., and Low, M.J. (1994). In situ hybridization analysis of anterior pituitary hormone gene expression during fetal mouse development. *J Histochem Cytochem* *42*, 1117-1125.
- Jimenez, G., Paroush, Z., and Ish-Horowicz, D. (1997). Groucho acts as a corepressor for a subset of negative regulators, including Hairy and Engrailed. *Genes Dev* *11*, 3072-3082.
- Juo, P., and Kaplan, J.M. (2004). The anaphase-promoting complex regulates the abundance of GLR-1 glutamate receptors in the ventral nerve cord of *C. elegans*. *Curr Biol* *14*, 2057-2062.
- Kannouche, P.L., Wing, J., and Lehmann, A.R. (2004). Interaction of human DNA polymerase eta with monoubiquitinated PCNA: a possible mechanism for the polymerase switch in response to DNA damage. *Mol Cell* *14*, 491-500.
- Kaufman, M.H., and Bard, M.H. (1999). *The anatomical basis of mouse development*. Academic Press.
- Kawamura, K., J, O.W., Bahar, R., Koshikawa, N., Shishikura, T., Nakagawara, A., Sakiyama, S., Kajiwarra, K., Kimura, M., and Tagawa, M. (2001). The error-prone DNA polymerase zeta catalytic subunit (Rev3) gene is ubiquitously expressed in normal and malignant human tissues. *Int J Oncol* *18*, 97-103.
- Kazanskaya, O.V., Severtzova, E.A., Barth, K.A., Ermakova, G.V., Lukyanov, S.A., Benyumov, A.O., Pannese, M., Boncinelli, E., Wilson, S.W., and Zeraisky, A.G. (1997). *Anf*: a novel class of vertebrate homeobox genes expressed at the anterior end of the main embryonic axis. *Gene* *200*, 25-34.
- Kim, A.H., and Bonni, A. (2007). Thinking within the D box: initial identification of Cdh1-APC substrates in the nervous system. *Mol Cell Neurosci* *34*, 281-287.
- Kioussi, C., Briata, P., Baek, S.H., Rose, D.W., Hamblet, N.S., Herman, T., Ohgi, K.A., Lin, C., Gleiberman, A., Wang, J., *et al.* (2002). Identification of a Wnt/Dvl/beta-Catenin --> Pitx2 pathway mediating cell-type-specific proliferation during development. *Cell* *111*, 673-685.
- Kissinger, C.R., Liu, B.S., Martin-Blanco, E., Kornberg, T.B., and Pabo, C.O. (1990). Crystal structure of an engrailed homeodomain-DNA complex at 2.8 Å resolution: a framework for understanding homeodomain-DNA interactions. *Cell* *63*, 579-590.

- Knoetgen, H., Viebahn, C., and Kessel, M. (1999). Head induction in the chick by primitive endoderm of mammalian, but not avian origin. *Development* *126*, 815-825.
- Konishi, Y., Stegmuller, J., Matsuda, T., Bonni, S., and Bonni, A. (2004). Cdh1-APC controls axonal growth and patterning in the mammalian brain. *Science* *303*, 1026-1030.
- Kornberg, T.B. (1993). Understanding the homeodomain. *J Biol Chem* *268*, 26813-26816.
- Kraft, C., Herzog, F., Gieffers, C., Mechtler, K., Hagting, A., Pines, J., and Peters, J.M. (2003). Mitotic regulation of the human anaphase-promoting complex by phosphorylation. *EMBO J* *22*, 6598-6609.
- Kraft, C., Vodermaier, H.C., Maurer-Stroh, S., Eisenhaber, F., and Peters, J.M. (2005). The WD40 propeller domain of Cdh1 functions as a destruction box receptor for APC/C substrates. *Mol Cell* *18*, 543-553.
- Kyriakis, J.M., and Avruch, J. (2001). Mammalian mitogen-activated protein kinase signal transduction pathways activated by stress and inflammation. *Physiol Rev* *81*, 807-869.
- Lasorella, A., Stegmuller, J., Guardavaccaro, D., Liu, G., Carro, M.S., Rothschild, G., de la Torre-Ubieta, L., Pagano, M., Bonni, A., and Iavarone, A. (2006). Degradation of Id2 by the anaphase-promoting complex couples cell cycle exit and axonal growth. *Nature* *442*, 471-474.
- Lawrence, C.W. (2002). Cellular roles of DNA polymerase zeta and Rev1 protein. *DNA Repair (Amst)* *1*, 425-435.
- Lawrence, C.W., Das, G., and Christensen, R.B. (1985). REV7, a new gene concerned with UV mutagenesis in yeast. *Mol Gen Genet* *200*, 80-85.
- Lehmann, A.R. (2006). Translesion synthesis in mammalian cells. *Exp Cell Res* *312*, 2673-2676.
- Li, S., Crenshaw, E.B., 3rd, Rawson, E.J., Simmons, D.M., Swanson, L.W., and Rosenfeld, M.G. (1990). Dwarf locus mutants lacking three pituitary cell types result from mutations in the POU-domain gene pit-1. *Nature* *347*, 528-533.
- Li, X., and Heyer, W.D. (2008). Homologous recombination in DNA repair and DNA damage tolerance. *Cell Res* *18*, 99-113.
- Li, Y., Gorbea, C., Mahaffey, D., Rechsteiner, M., and Benezra, R. (1997). MAD2 associates with the cyclosome/anaphase-promoting complex and inhibits its activity. *Proc Natl Acad Sci U S A* *94*, 12431-12436.
- Li, Z., Zhang, H., McManus, T.P., McCormick, J.J., Lawrence, C.W., and Maher, V.M. (2002). hREV3 is essential for error-prone translesion synthesis past UV or benzo[a]pyrene diol epoxide-induced DNA lesions in human fibroblasts. *Mutat Res* *510*, 71-80.
- Lin, W., Wu, X., and Wang, Z. (1999). A full-length cDNA of hREV3 is predicted to encode DNA polymerase zeta for damage-induced mutagenesis in humans. *Mutat Res* *433*, 89-98.
- Littlepage, L.E., and Ruderman, J.V. (2002). Identification of a new APC/C recognition domain, the A box, which is required for the Cdh1-dependent destruction of the kinase Aurora-A during mitotic exit. *Genes Dev* *16*, 2274-2285.
- Liu, P., Jenkins, N.A., and Copeland, N.G. (2003). A highly efficient recombineering-based method for generating conditional knockout mutations. *Genome Res* *13*, 476-484.

- Lobrich, M., and Jeggo, P.A. (2007). The impact of a negligent G2/M checkpoint on genomic instability and cancer induction. *Nat Rev Cancer* 7, 861-869.
- Mantovani, G., Asteria, C., Pellegrini, C., Bosari, S., Alberti, L., Bondioni, S., Peverelli, E., Spada, A., and Beck-Peccoz, P. (2006). HESX1 expression in human normal pituitaries and pituitary adenomas. *Mol Cell Endocrinol* 247, 135-139.
- Marangos, P., Verschuren, E.W., Chen, R., Jackson, P.K., and Carroll, J. (2007). Prophase I arrest and progression to metaphase I in mouse oocytes are controlled by Emi1-dependent regulation of APC(Cdh1). *J Cell Biol* 176, 65-75.
- Martinez-Barbera, J.P., Rodriguez, T.A., and Beddington, R.S. (2000). The homeobox gene *Hesx1* is required in the anterior neural ectoderm for normal forebrain formation. *Dev Biol* 223, 422-430.
- Martynova, N., Eroshkin, F., Ermakova, G., Bayramov, A., Gray, J., Grainger, R., and Zارايسки, A. (2004). Patterning the forebrain: *FoxA4a/Pintallavis* and *Xvent2* determine the posterior limit of *Xanf1* expression in the neural plate. *Development* 131, 2329-2338.
- Martynova, N.Y., Eroshkin, F.M., Ermolina, L.V., Ermakova, G.V., Korotaeva, A.L., Smurova, K.M., Gyoeva, F.K., and Zارايسки, A.G. (2008). The LIM-domain protein *Zyxin* binds the homeodomain factor *Xanf1/Hesx1* and modulates its activity in the anterior neural plate of *Xenopus laevis* embryo. *Dev Dyn* 237, 736-749.
- Masuda, Y., Ohmae, M., Masuda, K., and Kamiya, K. (2003). Structure and enzymatic properties of a stable complex of the human REV1 and REV7 proteins. *J Biol Chem* 278, 12356-12360.
- McCulloch, S.D., and Kunkel, T.A. (2008). The fidelity of DNA synthesis by eukaryotic replicative and translesion synthesis polymerases. *Cell Res* 18, 148-161.
- McNally, K., Neal, J.A., McManus, T.P., McCormick, J.J., and Maher, V.M. (2008). hRev7, putative subunit of hPolzeta, plays a critical role in survival, induction of mutations, and progression through S-phase, of UV((254nm))-irradiated human fibroblasts. *DNA Repair (Amst)*.
- Mülhardt, C. (2004). *Der Experimentator: Molekularbiologie/Genomics*, 4th edn (Spektrum, Akad. Verl.).
- Murakumo, Y. (2002). The property of DNA polymerase zeta: REV7 is a putative protein involved in translesion DNA synthesis and cell cycle control. *Mutat Res* 510, 37-44.
- Murakumo, Y., Ogura, Y., Ishii, H., Numata, S., Ichihara, M., Croce, C.M., Fishel, R., and Takahashi, M. (2001). Interactions in the error-prone postreplication repair proteins hREV1, hREV3, and hREV7. *J Biol Chem* 276, 35644-35651.
- Murakumo, Y., Roth, T., Ishii, H., Rasio, D., Numata, S., Croce, C.M., and Fishel, R. (2000). A human REV7 homolog that interacts with the polymerase zeta catalytic subunit hREV3 and the spindle assembly checkpoint protein hMAD2. *J Biol Chem* 275, 4391-4397.
- Muyrers, J.P., Zhang, Y., and Stewart, A.F. (2001). Techniques: Recombinogenic engineering--new options for cloning and manipulating DNA. *Trends Biochem Sci* 26, 325-331.
- Nagy, A., Gertsenstein, M., Vintersten, K., and Behringer, R. (2003). *Manipulating the Mouse Embryo: A Laboratory Manual*. In Cold Spring Harbor Laboratory Press.

- Nasonkin, I.O., Ward, R.D., Raetzman, L.T., Seasholtz, A.F., Saunders, T.L., Gillespie, P.J., and Camper, S.A. (2004). Pituitary hypoplasia and respiratory distress syndrome in Prop1 knockout mice. *Hum Mol Genet* *13*, 2727-2735.
- Nelson, J.R., Lawrence, C.W., and Hinkle, D.C. (1996). Thymine-thymine dimer bypass by yeast DNA polymerase zeta. *Science* *272*, 1646-1649.
- Nelson, K.K., Schlondorff, J., and Blobel, C.P. (1999). Evidence for an interaction of the metalloprotease-disintegrin tumour necrosis factor alpha convertase (TACE) with mitotic arrest deficient 2 (MAD2), and of the metalloprotease-disintegrin MDC9 with a novel MAD2-related protein, MAD2beta. *Biochem J* *343 Pt 3*, 673-680.
- Okada, T., Sonoda, E., Yoshimura, M., Kawano, Y., Saya, H., Kohzaki, M., and Takeda, S. (2005). Multiple roles of vertebrate REV genes in DNA repair and recombination. *Mol Cell Biol* *25*, 6103-6111.
- Olson, L.E., Tollkuhn, J., Scafoglio, C., Kronen, A., Zhang, J., Ohgi, K.A., Wu, W., Taketo, M.M., Kemler, R., Grosschedl, R., *et al.* (2006). Homeodomain-mediated beta-catenin-dependent switching events dictate cell-lineage determination. *Cell* *125*, 593-605.
- Osoegawa, K., Tateno, M., Woon, P.Y., Frengen, E., Mammoser, A.G., Catanese, J.J., Hayashizaki, Y., and de Jong, P.J. (2000). Bacterial artificial chromosome libraries for mouse sequencing and functional analysis. *Genome Res* *10*, 116-128.
- Paroush, Z., Finley, R.L., Jr., Kidd, T., Wainwright, S.M., Ingham, P.W., Brent, R., and Ish-Horowicz, D. (1994). Groucho is required for Drosophila neurogenesis, segmentation, and sex determination and interacts directly with hairy-related bHLH proteins. *Cell* *79*, 805-815.
- Paull, T.T., Rogakou, E.P., Yamazaki, V., Kirchgessner, C.U., Gellert, M., and Bonner, W.M. (2000). A critical role for histone H2AX in recruitment of repair factors to nuclear foci after DNA damage. *Curr Biol* *10*, 886-895.
- Peters, J.M. (2002). The anaphase-promoting complex: proteolysis in mitosis and beyond. *Mol Cell* *9*, 931-943.
- Peters, J.M. (2006). The anaphase promoting complex/cyclosome: a machine designed to destroy. *Nat Rev Mol Cell Biol* *7*, 644-656.
- Pfleger, C.M., and Kirschner, M.W. (2000). The KEN box: an APC recognition signal distinct from the D box targeted by Cdh1. *Genes Dev* *14*, 655-665.
- Pfleger, C.M., Salic, A., Lee, E., and Kirschner, M.W. (2001). Inhibition of Cdh1-APC by the MAD2-related protein MAD2L2: a novel mechanism for regulating Cdh1. *Genes Dev* *15*, 1759-1764.
- Pickart, C.M. (2001). Mechanisms underlying ubiquitination. *Annu Rev Biochem* *70*, 503-533.
- Pilarski, S. (2004). Interaction partners of the homeoprotein Hesx1. In Max-Planck-Institute for Biophysical Chemistry, Dept Molecular Cell Biology, Research Group Developmental Biology (Göttingen, Georg August University Göttingen), pp. 59.
- Pravtcheva, D.D., and Wise, T.L. (1996). A transgene-induced mitotic arrest mutation in the mouse allelic with Oligosyndactylism. *Genetics* *144*, 1747-1756.

- Prinz, S., Hwang, E.S., Visintin, R., and Amon, A. (1998). The regulation of Cdc20 proteolysis reveals a role for APC components Cdc23 and Cdc27 during S phase and early mitosis. *Curr Biol* 8, 750-760.
- Quirk, J., and Brown, P. (2002). Hesx1 homeodomain protein represses transcription as a monomer and antagonises transactivation of specific sites as a homodimer. *J Mol Endocrinol* 28, 193-205.
- Raetzman, L.T., Ward, R., and Camper, S.A. (2002). Lhx4 and Prop1 are required for cell survival and expansion of the pituitary primordia. *Development* 129, 4229-4239.
- Rattray, A.J., Shafer, B.K., McGill, C.B., and Strathern, J.N. (2002). The roles of REV3 and RAD57 in double-strand-break-repair-induced mutagenesis of *Saccharomyces cerevisiae*. *Genetics* 162, 1063-1077.
- Reimann, J.D., Gardner, B.E., Margottin-Goguet, F., and Jackson, P.K. (2001). Emi1 regulates the anaphase-promoting complex by a different mechanism than Mad2 proteins. *Genes Dev* 15, 3278-3285.
- Reis, A., Levasseur, M., Chang, H.Y., Elliott, D.J., and Jones, K.T. (2006). The CRY box: a second APCcdh1-dependent degron in mammalian cdc20. *EMBO Rep* 7, 1040-1045.
- Reis, A., Madgwick, S., Chang, H.Y., Nabti, I., Levasseur, M., and Jones, K.T. (2007). Prometaphase APCcdh1 activity prevents non-disjunction in mammalian oocytes. *Nat Cell Biol* 9, 1192-1198.
- Reynaud, R., Saveanu, A., Barlier, A., Enjalbert, A., and Brue, T. (2004). Pituitary hormone deficiencies due to transcription factor gene alterations. *Growth Horm IGF Res* 14, 442-448.
- Rizzoti, K., and Lovell-Badge, R. (2005). Early development of the pituitary gland: induction and shaping of Rathke's pouch. *Rev Endocr Metab Disord* 6, 161-172.
- Robertson, G., Bilenky, M., Lin, K., He, A., Yuen, W., Dagginar, M., Varhol, R., Teague, K., Griffith, O.L., Zhang, X., *et al.* (2006). cisRED: a database system for genome-scale computational discovery of regulatory elements. *Nucleic Acids Res* 34, D68-73.
- Rogakou, E.P., Pilch, D.R., Orr, A.H., Ivanova, V.S., and Bonner, W.M. (1998). DNA double-stranded breaks induce histone H2AX phosphorylation on serine 139. *J Biol Chem* 273, 5858-5868.
- Rudner, A.D., and Murray, A.W. (2000). Phosphorylation by Cdc28 activates the Cdc20-dependent activity of the anaphase-promoting complex. *J Cell Biol* 149, 1377-1390.
- Saiki, R.K., Gelfand, D.H., Stoffel, S., Scharf, S.J., Higuchi, R., Horn, G.T., Mullis, K.B., and Erlich, H.A. (1988). Primer-directed enzymatic amplification of DNA with a thermostable DNA polymerase. *Science* 239, 487-491.
- Sajedi, E., Gaston-Massuet, C., Andoniadou, C.L., Signore, M., Hurd, P.J., Dattani, M., and Martinez-Barbera, J.P. (2007). DNMT1 interacts with the developmental transcriptional repressor HESX1. *Biochim Biophys Acta*.
- Sakamoto, A., Lan, V.T., Hase, Y., Shikazono, N., Matsunaga, T., and Tanaka, A. (2003). Disruption of the AtREV3 gene causes hypersensitivity to ultraviolet B light and gamma-rays in *Arabidopsis*: implication of the presence of a translesion synthesis mechanism in plants. *Plant Cell* 15, 2042-2057.

- Sauer, B. (1998). Inducible gene targeting in mice using the Cre/lox system. *Methods* 14, 381-392.
- Sauer, B., and Henderson, N. (1989). Cre-stimulated recombination at loxP-containing DNA sequences placed into the mammalian genome. *Nucleic Acids Res* 17, 147-161.
- Schiestl, R.H., and Gietz, R.D. (1989). High efficiency transformation of intact yeast cells using single stranded nucleic acids as a carrier. *Curr Genet* 16, 339-346.
- Schwenk, F., Baron, U., and Rajewsky, K. (1995). A cre-transgenic mouse strain for the ubiquitous deletion of loxP-flanked gene segments including deletion in germ cells. *Nucleic Acids Res* 23, 5080-5081.
- Scully, K.M., and Rosenfeld, M.G. (2002). Pituitary development: regulatory codes in mammalian organogenesis. *Science* 295, 2231-2235.
- Seet, B.T., Dikic, I., Zhou, M.M., and Pawson, T. (2006). Reading protein modifications with interaction domains. *Nat Rev Mol Cell Biol* 7, 473-483.
- Sheng, H.Z., Zhadanov, A.B., Mosinger, B., Jr., Fujii, T., Bertuzzi, S., Grinberg, A., Lee, E.J., Huang, S.P., Mahon, K.A., and Westphal, H. (1996). Specification of pituitary cell lineages by the LIM homeobox gene Lhx3. *Science* 272, 1004-1007.
- Sgrist, S.J., and Lehner, C.F. (1997). *Drosophila* fizzy-related down-regulates mitotic cyclins and is required for cell proliferation arrest and entry into endocycles. *Cell* 90, 671-681.
- Simmons, D.M., Voss, J.W., Ingraham, H.A., Holloway, J.M., Broide, R.S., Rosenfeld, M.G., and Swanson, L.W. (1990). Pituitary cell phenotypes involve cell-specific Pit-1 mRNA translation and synergistic interactions with other classes of transcription factors. *Genes Dev* 4, 695-711.
- Smith, S.T., and Jaynes, J.B. (1996). A conserved region of engrailed, shared among all engrailed, Nk1-, Nk2- and msh-class homeoproteins, mediates active transcriptional repression in vivo. *Development* 122, 3141-3150.
- Sobrier, M.L., Maghnie, M., Vie-Luton, M.P., Secco, A., di Iorgi, N., Lorini, R., and Amselem, S. (2006). Novel HESX1 mutations associated with a life-threatening neonatal phenotype, pituitary aplasia, but normally located posterior pituitary and no optic nerve abnormalities. *J Clin Endocrinol Metab* 91, 4528-4536.
- Sobrier, M.L., Netchine, I., Heinrichs, C., Thibaud, N., Vie-Luton, M.P., Van Vliet, G., and Amselem, S. (2005). Alu-element insertion in the homeodomain of HESX1 and aplasia of the anterior pituitary. *Hum Mutat* 25, 503.
- Sornson, M.W., Wu, W., Dasen, J.S., Flynn, S.E., Norman, D.J., O'Connell, S.M., Gukovsky, I., Carriere, C., Ryan, A.K., Miller, A.P., *et al.* (1996). Pituitary lineage determination by the Prophet of Pit-1 homeodomain factor defective in Ames dwarfism. *Nature* 384, 327-333.
- Spieler, D., Baumer, N., Stebler, J., Kopranner, M., Reichman-Fried, M., Teichmann, U., Raz, E., Kessel, M., and Wittler, L. (2004). Involvement of Pax6 and Otx2 in the forebrain-specific regulation of the vertebrate homeobox gene ANF/Hesx1. *Dev Biol* 269, 567-579.
- Stegmuller, J., Huynh, M.A., Yuan, Z., Konishi, Y., and Bonni, A. (2008). TGFbeta-Smad2 signaling regulates the Cdh1-APC/SnoN pathway of axonal morphogenesis. *J Neurosci* 28, 1961-1969.

- Stegmuller, J., Konishi, Y., Huynh, M.A., Yuan, Z., Dibacco, S., and Bonni, A. (2006). Cell-intrinsic regulation of axonal morphogenesis by the Cdh1-APC target SnoN. *Neuron* *50*, 389-400.
- Stelter, P., and Ulrich, H.D. (2003). Control of spontaneous and damage-induced mutagenesis by SUMO and ubiquitin conjugation. *Nature* *425*, 188-191.
- Sudakin, V., Chan, G.K., and Yen, T.J. (2001). Checkpoint inhibition of the APC/C in HeLa cells is mediated by a complex of BUBR1, BUB3, CDC20, and MAD2. *J Cell Biol* *154*, 925-936.
- Suh, H., Gage, P.J., Drouin, J., and Camper, S.A. (2002). Pitx2 is required at multiple stages of pituitary organogenesis: pituitary primordium formation and cell specification. *Development* *129*, 329-337.
- Susa, T., Nakayama, M., Kitahara, K., Kimoto, F., Kato, T., and Kato, Y. (2007). Homeodomain transcription factor Hesx1/Rpx occupies Prop-1 activation sites in porcine follicle stimulating hormone (FSH) beta subunit promoter. *Biochem Biophys Res Commun* *357*, 712-717.
- Szeto, D.P., Rodriguez-Esteban, C., Ryan, A.K., O'Connell, S.M., Liu, F., Kioussi, C., Gleiberman, A.S., Izpisua-Belmonte, J.C., and Rosenfeld, M.G. (1999). Role of the Bicoid-related homeodomain factor Pitx1 in specifying hindlimb morphogenesis and pituitary development. *Genes Dev* *13*, 484-494.
- Tajima, T., Hattorri, T., Nakajima, T., Okuhara, K., Sato, K., Abe, S., Nakae, J., and Fujieda, K. (2003). Sporadic heterozygous frameshift mutation of HESX1 causing pituitary and optic nerve hypoplasia and combined pituitary hormone deficiency in a Japanese patient. *J Clin Endocrinol Metab* *88*, 45-50.
- Takahashi, S., Sakamoto, A., Sato, S., Kato, T., Tabata, S., and Tanaka, A. (2005). Roles of Arabidopsis AtREV1 and AtREV7 in translesion synthesis. *Plant Physiol* *138*, 870-881.
- Takao, N., Kato, H., Mori, R., Morrison, C., Sonada, E., Sun, X., Shimizu, H., Yoshioka, K., Takeda, S., and Yamamoto, K. (1999). Disruption of ATM in p53-null cells causes multiple functional abnormalities in cellular response to ionizing radiation. *Oncogene* *18*, 7002-7009.
- Thomas, P., and Beddington, R. (1996). Anterior primitive endoderm may be responsible for patterning the anterior neural plate in the mouse embryo. *Curr Biol* *6*, 1487-1496.
- Thomas, P.Q., Dattani, M.T., Brickman, J.M., McNay, D., Warne, G., Zacharin, M., Cameron, F., Hurst, J., Woods, K., Dunger, D., *et al.* (2001). Heterozygous HESX1 mutations associated with isolated congenital pituitary hypoplasia and septo-optic dysplasia. *Hum Mol Genet* *10*, 39-45.
- Thomas, P.Q., Johnson, B.V., Rathjen, J., and Rathjen, P.D. (1995). Sequence, genomic organization, and expression of the novel homeobox gene Hesx1. *J Biol Chem* *270*, 3869-3875.
- Thomas, P.Q., and Rathjen, P.D. (1992). HES-1, a novel homeobox gene expressed by murine embryonic stem cells, identifies a new class of homeobox genes. *Nucleic Acids Res* *20*, 5840.
- Thornton, B.R., and Toczyski, D.P. (2006). Precise destruction: an emerging picture of the APC. *Genes Dev* *20*, 3069-3078.

- Thrower, J.S., Hoffman, L., Rechsteiner, M., and Pickart, C.M. (2000). Recognition of the polyubiquitin proteolytic signal. *EMBO J* 19, 94-102.
- Todaro, G.J., and Green, H. (1963). Quantitative studies of the growth of mouse embryo cells in culture and their development into established lines. *J Cell Biol* 17, 299-313.
- Tolkunova, E.N., Fujioka, M., Kobayashi, M., Deka, D., and Jaynes, J.B. (1998). Two distinct types of repression domain in engrailed: one interacts with the groucho corepressor and is preferentially active on integrated target genes. *Mol Cell Biol* 18, 2804-2814.
- van den Hurk, W.H., Martens, G.J., Geurts van Kessel, A., and van Groningen, J.J. (2004). Isolation and characterization of the *Xenopus laevis* orthologs of the human papillary renal cell carcinoma-associated genes PRCC and MAD2L2 (MAD2B). *Cytogenet Genome Res* 106, 68-73.
- van Roessel, P., Elliott, D.A., Robinson, I.M., Prokop, A., and Brand, A.H. (2004). Independent regulation of synaptic size and activity by the anaphase-promoting complex. *Cell* 119, 707-718.
- Van Sloun, P.P., Romeijn, R.J., and Eeken, J.C. (1999). Molecular cloning, expression and chromosomal localisation of the mouse Rev3l gene, encoding the catalytic subunit of polymerase zeta. *Mutat Res* 433, 109-116.
- Vidal, M. (1997). The Reverse Two-Hybrid System in The Two-Hybrid System. (Bartel, P. and Fields, S., eds.). Oxford University Press, New York, 109.
- Vilenchik, M.M., and Knudson, A.G. (2003). Endogenous DNA double-strand breaks: production, fidelity of repair, and induction of cancer. *Proc Natl Acad Sci U S A* 100, 12871-12876.
- Wan, Y., and Kirschner, M.W. (2001). Identification of multiple CDH1 homologues in vertebrates conferring different substrate specificities. *Proc Natl Acad Sci U S A* 98, 13066-13071.
- Warming, S., Costantino, N., Court, D.L., Jenkins, N.A., and Copeland, N.G. (2005). Simple and highly efficient BAC recombineering using galK selection. *Nucleic Acids Res* 33, e36.
- Wei, W., Ayad, N.G., Wan, Y., Zhang, G.J., Kirschner, M.W., and Kaelin, W.G., Jr. (2004). Degradation of the SCF component Skp2 in cell-cycle phase G1 by the anaphase-promoting complex. *Nature* 428, 194-198.
- Weterings, E., and Chen, D.J. (2008). The endless tale of non-homologous end-joining. *Cell Res* 18, 114-124.
- Wilson, D., Sheng, G., Lecuit, T., Dostatni, N., and Desplan, C. (1993). Cooperative dimerization of paired class homeo domains on DNA. *Genes Dev* 7, 2120-2134.
- Wilson, D.S., Guenther, B., Desplan, C., and Kuriyan, J. (1995). High resolution crystal structure of a paired (Pax) class cooperative homeodomain dimer on DNA. *Cell* 82, 709-719.
- Wirth, K.G., Ricci, R., Gimenez-Abian, J.F., Taghybeeglu, S., Kudo, N.R., Jochum, W., Vasseur-Cognet, M., and Nasmyth, K. (2004). Loss of the anaphase-promoting complex in quiescent cells causes unscheduled hepatocyte proliferation. *Genes Dev* 18, 88-98.

- Wittschieben, J., Shivji, M.K., Lalani, E., Jacobs, M.A., Marini, F., Gearhart, P.J., Rosewell, I., Stamp, G., and Wood, R.D. (2000). Disruption of the developmentally regulated Rev3 gene causes embryonic lethality. *Curr Biol* *10*, 1217-1220.
- Wittschieben, J.P., Reshmi, S.C., Gollin, S.M., and Wood, R.D. (2006). Loss of DNA polymerase zeta causes chromosomal instability in mammalian cells. *Cancer Res* *66*, 134-142.
- Wu, G., Glickstein, S., Liu, W., Fujita, T., Li, W., Yang, Q., Duvoisin, R., and Wan, Y. (2007). The anaphase-promoting complex coordinates initiation of lens differentiation. *Mol Biol Cell* *18*, 1018-1029.
- Yang, X.J. (2005). Multisite protein modification and intramolecular signaling. *Oncogene* *24*, 1653-1662.
- Ying, B., and Wold, W.S. (2003). Adenovirus ADP protein (E3-11.6K), which is required for efficient cell lysis and virus release, interacts with human MAD2B. *Virology* *313*, 224-234.
- Zander, L., and Bemark, M. (2004). Immortalized mouse cell lines that lack a functional Rev3 gene are hypersensitive to UV irradiation and cisplatin treatment. *DNA Repair (Amst)* *3*, 743-752.
- Zaraisky, A.G., Ecochard, V., Kazanskaya, O.V., Lukyanov, S.A., Fesenko, I.V., and Duprat, A.M. (1995). The homeobox-containing gene XANF-1 may control development of the Spemann organizer. *Development* *121*, 3839-3847.
- Zaraisky, A.G., Lukyanov, S.A., Vasiliev, O.L., Smirnov, Y.V., Belyavsky, A.V., and Kazanskaya, O.V. (1992). A novel homeobox gene expressed in the anterior neural plate of the *Xenopus* embryo. *Dev Biol* *152*, 373-382.
- Zhang, L., Yang, S.H., and Sharrocks, A.D. (2007). Rev7/MAD2B links c-Jun N-terminal protein kinase pathway signaling to activation of the transcription factor Elk-1. *Mol Cell Biol* *27*, 2861-2869.
- Zhou, Y., Ching, Y.P., Ng, R.W., and Jin, D.Y. (2002). The APC regulator CDH1 is essential for the progression of embryonic cell cycles in *Xenopus*. *Biochem Biophys Res Commun* *294*, 120-126.
- Zhu, X., Gleiberman, A.S., and Rosenfeld, M.G. (2007). Molecular physiology of pituitary development: signaling and transcriptional networks. *Physiol Rev* *87*, 933-963.
- Zhu, X., Lin, C.R., Prefontaine, G.G., Tollkuhn, J., and Rosenfeld, M.G. (2005). Genetic control of pituitary development and hypopituitarism. *Curr Opin Genet Dev* *15*, 332-340.

CURRICULUM VITAE

Personal Information

Name: Sven Pilarski

Date of birth: April 4th 1978

Place of birth: Wolfsburg

Nationality: German

Education

- Since 2004 Max Planck Institute for Biophysical Chemistry Göttingen
PhD thesis in Prof. Dr. Michael Kessel's laboratory
Dept. Molecular Cell Biology/Research Group Developmental Biology
- 2003-2004 Max Planck Institute for Biophysical Chemistry Göttingen
MSc thesis in Prof. Dr. Michael Kessel's laboratory
Dept. Molecular Cell Biology/Research Group Developmental Biology
- 2002-2003 Georg August University Göttingen
MSc/PhD Program "Molecular Biology"
International Max Planck Research School
- 1999-2002 Georg August University Göttingen
Biology

Internships & Additional Education

- 07-09/2001 Harvard Medical School, Dept. of Genetics, Boston/MA, USA
Developmental Biology in Prof. Clifford J. Tabin, Ph.D.'s laboratory
- 2000-2002 DeveloGen AG, Obesity Research Group, Göttingen
Experimental Genetics in Dr. Günter Brönner's laboratory

Scholarships

- 2007-2008 Scholarship of the Max Planck Society
- 2004-2007 Georg Christoph Lichtenberg PhD-Stipend of the State Lower Saxony
- 2002-2003 Scholarship of the International Max Planck Research School

Contact Details

Department Molecular Cell Biology
Max Planck Institute for Biophysical Chemistry
Am Fassberg 11
37077 Göttingen, Germany

Phone: + 49 551 2011752

E-mail: spilars@gwdg.de